Investigation of binding of Bacteriophage and *Staphylococcus aureus* using Magnetoelastic Biosensor

By

Nitilaksha P. Hiremath

A thesis submitted to the Graduate Faculty of
Auburn University
in partial fulfillment of the
requirements for the Degree of
Master of Science

Auburn, Alabama
May 06, 2013

Keywords: Bacteriophage 12600, Phage characterization, Magnetoelastic, *Staphylococcus aureus*, Uniform distribution, Biosensors

Approved by

Bryan A. Chin, Chair, Professor, Materials Engineering, Auburn University
Vitaly Vodyanoy, Professor, College of Veterinary Medicine, Auburn University
Zhong-Yang Cheng, Professor, Materials Engineering, Auburn University

Abstract

Consumption of bacteria-contaminated food products results in illness, hospitalization and even deaths and researchers have been making efforts in finding a way for early detection of pathogenic bacteria, such as *Staphylococcus aureus*, with low-cost, highly specific devices. However, traditional methods, such as culture-based and PCR-based assays, not only are expensive but also take hours-to-days to detect and identify the bacteria present in the contaminated food. Hence, there is a need for low-cost, rapid analytical devices in conjunction with highly specific biomolecular-recognition elements for detection and identification of food borne pathogens.

This thesis presents the development and characterization of a lytic phage-based magnetoelastic (ME) biosensor for the detection of *Staphylococcus aureus*. ME biosensors are mass sensitive devices composed of a ME material as the transducer platform and phage-based biomolecular-recognition element for specific target species detection. A lytic bacteriophage 12600, with high binding affinity for the *Staphylococcus aureus* bacterium, was immobilized on gold-coated ME biosensors via physical adsorption with various phage concentrations and immobilization times. To maximize bacteria capture on a ME biosensor, optimization of mean free length and uniform distribution of the biomolecular-recognition element is necessary. The maximum surface density of the phage physically bound on the sensor surface was calculated with the assistance of SEM images for five different concentrations, ranging from 10^8 pfu/mL to 10^{12} pfu/mL, as a function of immobilization time. In addition, the mean free length

(MFL) between successive bound phages was calculated for the surfaces exposed to the two highest concentrations of phage, 10^{11} pfu/mL and 10^{12} pfu/mL, and compared with the size of the bacterium. Experiments were conducted to confirm the maximum bacteria capture between the two highest surface densities of phage immobilized sensors. The maximum bacteria capture was achieved with 10^{11} pfu/mL phage concentration, surface density of 1.68×10^7 phage particles/mm^2 of sensor surface and MFL of ≈ 0.92 μm.

In addition, from the bacteriophage-characterized biosensors, the specificity and sensitivity of the lytic phage immobilized ME biosensors to detect *Staphylococcus aureus* in the presence of high concentration of masking bacteria was carried out. The sensors were exposed to different types of bacteria such as *Salmonella typhimurium, E. coli O157:H7* and *Listeria monocytogenes* to determine the specificity of biomolecular-recognition element towards *S. aureus*. The effect of the presence of one masking bacteria (*L. monocytogenes*), two masking bacteria (*L. monocytogenes and E. coli*) and three masking bacteria (*L. monocytogenes, E. coli* and *S. typhimurium*) in a mixture with *S. aureus* upon the response of the ME biosensor was studied. In response, the sensors had the similar trends; however the sensitivity and frequency differences were slightly lower for the masked mixtures.

Acknowledgments

First of all, I would like to thank Lord Ganesha, Lord Veerabhadreshwara, and Goddess Saraswati for giving me this wonderful life surrounded by some wonderful people whose influence has made me a better human being.

My sincere and heartfelt gratitude is due to Dr Bryan Chin for his expert advice and guidance all the time I needed. The timely discussions with him were mind provoking and his influence on me was not only in acquiring scientific knowledge but also as a person.

I also received greatest support from my committee members, Dr Vitaly Vodyanoy, Dr Z.-Y. Cheng, and I would like to express my heartfelt gratitude and thank them wholeheartedly. I sincerely thank Dr Vitaly Vodyanoy for the valuable discussions on my thesis and results.

I would like to thank late L.C Mathison, Dr Rajesh Guntupalli, Shin Horikawa, Dr. Kanchana Weerakoon, Dr. M-K Park, Dr Suiqiong Li, and Yating Chai for all timely discussions and motivations.

I would like to thank my friends Sachin Jambovane, Seema Jambovane, Gautham Jeppu, Pratheek Hejmady, Patrick Bass, Naved Siddiqui, Santosh Kulkarni, Harish Rao, Abhilash Kittanna, Vijay Sheshadri, Sanjay Kulkarni, Adarsh Jain, and Amit Jain for all the constant motivation, encouragement and support.

Finally I thank my nearest and dearest ones, my father, Dr Phalaxayya R. Hiremath, my mother, Sharada P. Hiremath, my brothers, Rachayya P. Hiremath and

Kshitij P. Hiremath, for all the unconditional love and affection, motivation and encouragement, support, sacrifice, patience and confidence in me.

Table of Contents

List of Tables

List of Figures

List of Abbreviations

BMR	Biomolecular-recognition element
MFL	Mean free length
BSA	Bovine serum albumin
NPB	Number of phage bindings
CDC	Center for disease control
QCM	Quartz crystal microbalance
SPR	Surface Plasmon resonance
ME	Magnetoelastic
PZ	Piezoelectric

CHAPTER 1

INTRODUCTION

1.1 Background

1.1.1 Food borne illness

Food borne illness, commonly known as food poisoning, affects 1 in 6 Americans every year due to consumption of contaminated food products. There are different microbes or organisms that contaminate food products that are responsible for different types of food borne infections. In addition food borne illness can also be caused by harmful chemicals, gases etc. There are as many as 250 food borne infections that have been noted. Most of these are caused by contamination due to microorganisms and bacteria. There is no typical symptom(s) of food borne illness, however, the initial symptoms are common such as vomiting, diarrhea, nausea and in the severe condition the infection might lead to death (CDC 2011).

The most commonly known food borne illnesses are caused due to bacterial contamination such as *Staphylococcus aureus, Listeria monocytogenes, Escherichia coli O157,* and *Salmonella typhimurium*. These contaminants can spread through various routes such as food, drinking water, plants, swimming water, etc and controlling them at the source is difficult. Contamination of food products might occur at various levels of processing, such as, production, packaging, transportation or storage. Bacterial contamination has increased with the increase in mass population migration from one

region to another, which reasons back to the human behavior, hygiene, etc. Food also gets contaminated during the raising of healthy animals. The pathogens that are already present in the animals do not harm animals but the humans that consume the food. Similarly vegetables and fruits can get contaminated when they are washed with contaminated water. Water gets contaminated due to animal manure or seepage of water channels with underground drains. Other sea food products are contaminated with the bacteria and viruses that are already present in the sea water, water contamination again caused by the dumping of human waste. Furthermore, the food gets contaminated even after cooking on high heat, i.e. by cooked food coming in contact with the raw food or due to handling and transportation. A few examples of the most commonly found food borne illness are *Staphylococcal* Food Poisoning, Listeriosis, and Salmonellosis (CDC 2011).

Staphylococcal Food Poisoning

It is a condition where a gastrointestinal illness occurs and is caused by eating foods contaminated with toxins produced by *Staphylococcus aureus.* In direct contamination of food especially in food industries, people who carry *S. aureus* can contaminate if they don't wash hands frequently. The *S. aureus* bacterium can also be found in unpasteurized milk and cheese products because of its stability in salt environment. *S. aureus* can grow in foods like ham and multiplies in food to produce toxins that can cause food poisoning and the toxins are resistant to heat and cannot be destroyed during cooking.

Most commonly found foods that are contaminated by *S. aureus* bacterium are those that do not require cooking such as sliced meat, puddings, pastries and sandwiches.

The foods may not smell bad or look spoiled when containing the toxins. The symptoms of Staphylococcal Food Poisoning are nausea, retching, vomiting, stomach cramps, and diarrhea. The illness does not spread and it typically lasts for a day, but sometimes it can last up to three days. In some small population of patients the illness may be more severe (CDC 2012b).

Listeriosis

Listeria monocytogenes is the causative organism of Listeriosis and primarily affects older adults, pregnant women, newborns, and adults with weakened immune systems. The symptoms of listeriosis are fever and muscle aches, sometimes preceded by diarrhea or other gastrointestinal symptoms. Pregnant women typically experience only a mild, flu-like illness. Other people experience fever and muscle aches, headache, stiff neck, confusion, loss of balance, and convulsions.

Listeriosis can affect in different ways depending on the type of infection. Manifestations of listeriosis are host-dependent. In older adults and persons with low immunity, septicemia and meningitis are the most commonly found clinical observations. Pregnant women may experience a mild, flu-like illness followed by fetal loss or bacteremia and meningitis in their newborns. Immuno-competent persons may experience acute febrile gastroenteritis or no symptoms (CDC 2012a).

Salmonellosis

Salmonellosis is caused by bacteria called *Salmonella*. Typical symptoms include diarrhea, fever, and abdominal cramps 12 to 72 hours after infection. In the event of severe infection, the patient needs to be hospitalized. The reason for the cause of

Salmonellosis is again the unhygienic food processing, not cleaning the vegetables and meat properly (CDC 2012c).

In addition many reports recently have warned of new drug-resistant strains of bacteria. One such strain is Methicillin-resistant *Staphylococcus aureus* (MRSA) (Barie 1998; Byun 1997; Duan *et al*. 2011; Giamarellou *et al*. 1981; Knopf 1997). The resistance of MRSA to a wide range of antibiotics has been documented in several reports (Broughan *et al*. 2011; Chakraborty *et al*. 2011; Durgaryan 2010; Shittu *et al*. 2011). *S. aureus* generates extremely contagious chemical compounds and proteins, including different types of enterotoxins and shock syndrome toxin (Arbuthnott 1990. ; Jarraud *et al*. 2001; Lina *et al*. 1997). For food poisoning, as low as 1 μg of enterotoxin is required, and this amount can be generated by a mere 10^5 cfu/g concentration of *S. aureus* bacteria. Early detection of MRSA is one of the best preventive measures to overcome severe sickness and potential loss of life from this antibiotic resistant bacterium. There are various types of biosensors available for the detection of pathogenic bacteria.

1.1.2 Transducer Platforms

A biosensor is defined as a device that incorporates a biomolecular-recognition element and a transducer element for the detection of a target species of interest. The transducer needs to be capable of transferring information about the specific interaction between the target and the biomolecular-recognition element into measurable signals with high sensitivity. The biomolecular-recognition element is an integral part of any biosensor technology. The biomolecular-recognition element is responsible for the selectivity, sensitivity and thermal stability of a biosensor.

The food industry is the highly concerned stratum about the spread of pathogenic bacteria. Failure to detect particular pathogenic bacteria has proved to be fatal. The following sections describe the various approaches that are most commonly accepted to detect and identify pathogenic bacteria. Biosensors have become a very important tool in modern day life. A biosensor has two important components, a biomolecular-recognition element and a transducer element. The transducer is a part of the biosensor which helps to convert the detection of bacteria into a measurable signal. There are a number of physical and chemical properties detected, (mass, temperature, electrical properties, and optical properties) to allow for different transduction formats as shown in **Figure 1.1**.

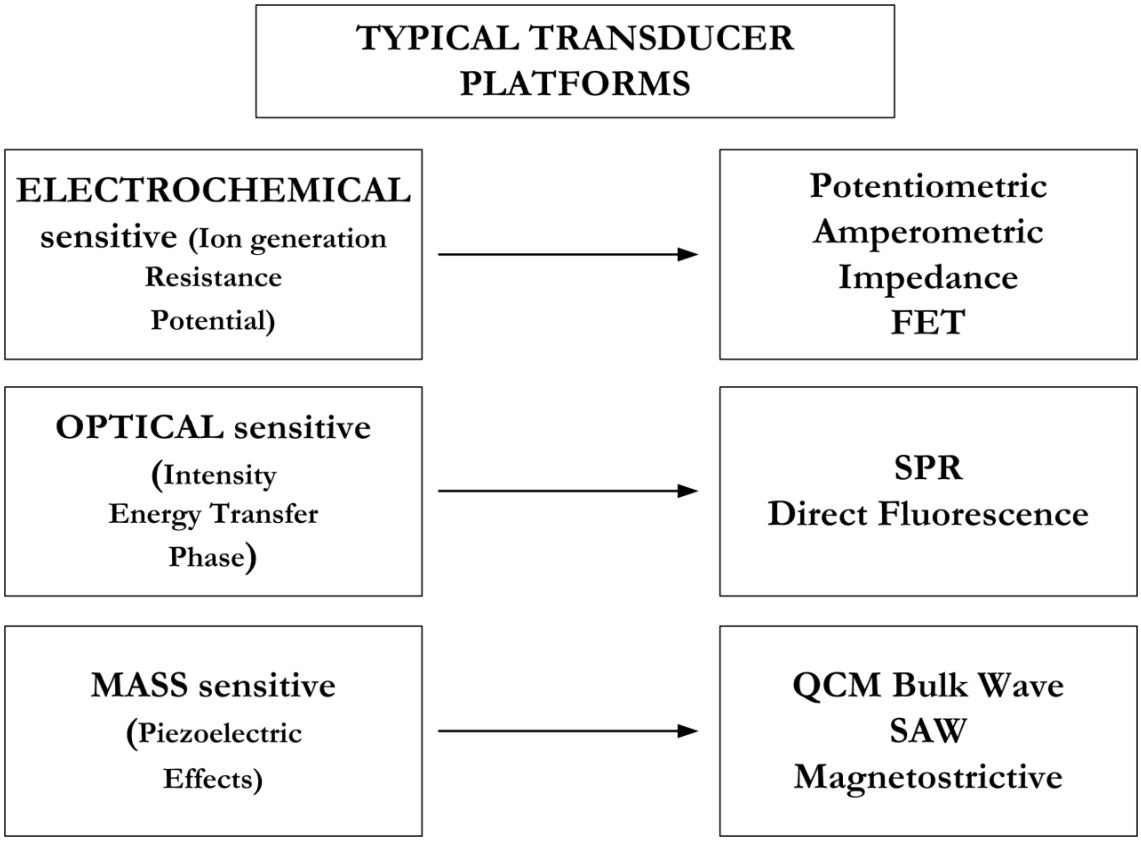

Figure 1.1 *Schematic of various transducer platforms used in biosensors technology.*

The three basic transduction types: electrochemical, optical and mass sensitive are reviewed here, with emphasis on the advantages and disadvantages to each, and recent advances toward optimizing biosensor performance (Griffin 2009; Ramasamy 2010).

Electrochemical Sensors

Electrochemical transduction is one of the most popularly found detection methods in biosensor technology used to detect and identify pathogenic bacteria. The greatest advantage of electrochemical transduction is that it can be used to operate in colloidal media and in complex matrices. A schematic representation of operation of an electrochemical biosensor is as depicted in **Figure 1.2**.

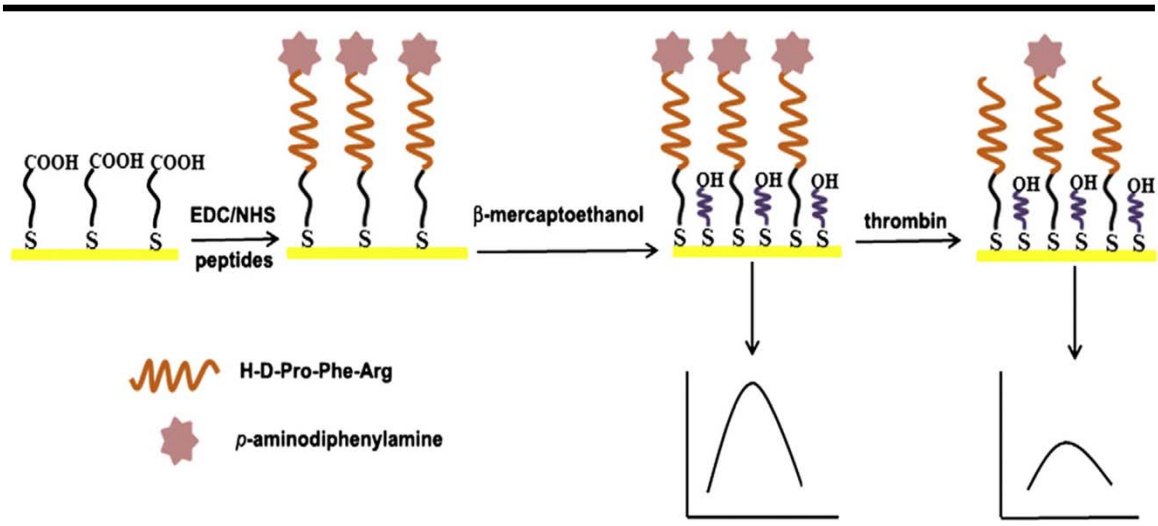

Figure 1.2 *Schematic of an electrochemical biosensor with gold electrode exposed to MAA (mercaptoacetic acid) to form a self-assembled (SA) monolayer of carboxyl groups. SA carboxyl group monolayer electrode is exposed to EDC and NHS there by activating carboxyl groups; followed by exposure to peptide solution. The system is then exposed to ethanolamine to reduce the reactivity of succinimidyl groups and blocking the bare gold*

surface with b-mercaptoethanol. The electrode is exposed for the detection of thrombin (Ji Ji et al, 2009).

The detection systems are inexpensive and can be made to be portable. Electrochemical-based sensing can be divided into four major categories: potentiometric, amperometric, impedance, and FET. Potentiometric sensors, as the name says, work on a change in potential, caused by the production of an electro active species that is measured by an ion selective electrode as the biomolecular-recognition process.

The most commonly used biomolecular-recognition element in electrochemical biosensors is enzyme. In an amperometric sensor system, a change in current is measured as a detection signal which corresponds to the type of analyte. In amperometric based detection systems, the sensor potential is adjusted to a value where the analyte generates a current. Electrochemical sensors based on impedance measurement are used to detect variations in the sensor surface properties; the change in the resistance to flow of an alternating current is measured in terms of change in voltage or current. Impedimetric transduction has been used to identify various types of food borne pathogenic bacteria. Metabolic changes (e.g., growth and metabolism) have been shown to correspond to an increase or decrease in impedance (Ramasamy 2010; Vo-Dinh *et al*. 1987).

In the improved versions of electrochemical biosensors, FETs (field effect transistors) and ECL (electrochemiluminescence) are used. Due to miniaturization of potentiometric sensors by employing FETs, researchers are able to increase sensitivity. ECL, having the combined advantages of chemiluminescence (high sensitivity and low background) with electrochemical transduction, has limited selectivity and sensitivity when compared to their optical counterparts (Lazcka 2007)**.**

Optical Sensors

Optical biosensors have been studied extensively for pathogenic bacteria detection due to their high sensitivity and selectivity. Optical-based detection systems include different subclasses depending on absorption, reflection, refraction, dispersion, infrared, Raman, chemiluminescence, fluorescence, and phosphorescence. However, a suitable spectrometer to record the spectrochemical properties of the analyte is necessary for all the above subclasses. The most commonly used optical detection techniques are SPR (surface plasmon resonance) and fluorescence because of their introduction of high sensitivity. Optical techniques incorporating fiber optics, laser, prism and waveguides have also been employed for pathogen detection (Mello and Kubota 2002; Ramasamy 2010)**.** Direct fluorescence techniques that are employed for bacterial identification use the natural fluorescent components of the bacterium present. The bacteria detected by direct methods must produce or contain some suitable fluorophore.

Slots and Reynolds *et al.* identified the species by the fluorescence of cells under an ultraviolet lamp of *Bacteroides* (these are genus of gram-negative bacillus bacteria and are non-endospore forming anaerobes) by direct fluorescence method. Some species of *Bacteroides* were found not to fluoresce, whereas others emitted fluorescence of characteristic colors. In the direct fluorescence method, a mixture of fluorescent metabolic products is detected. Direct detection using the fluorescence of cells, can be made very simple and inexpensive. However, the major disadvantage of direct detection is that not all bacterial cells can be detected; only those bacteria which contain or produce some fluorescent pigment may be detected. Therefore, the utility of this approach becomes very limited (Rossi and Warner, 1985). SPR biosensors (Cooper, 2003) measure

changes in RI (refractive index) caused by structural alterations in the proximity of a thin film gold surface. A typical operation and schematic representation of the SPR instrument is as shown in **Figure 1.3**.

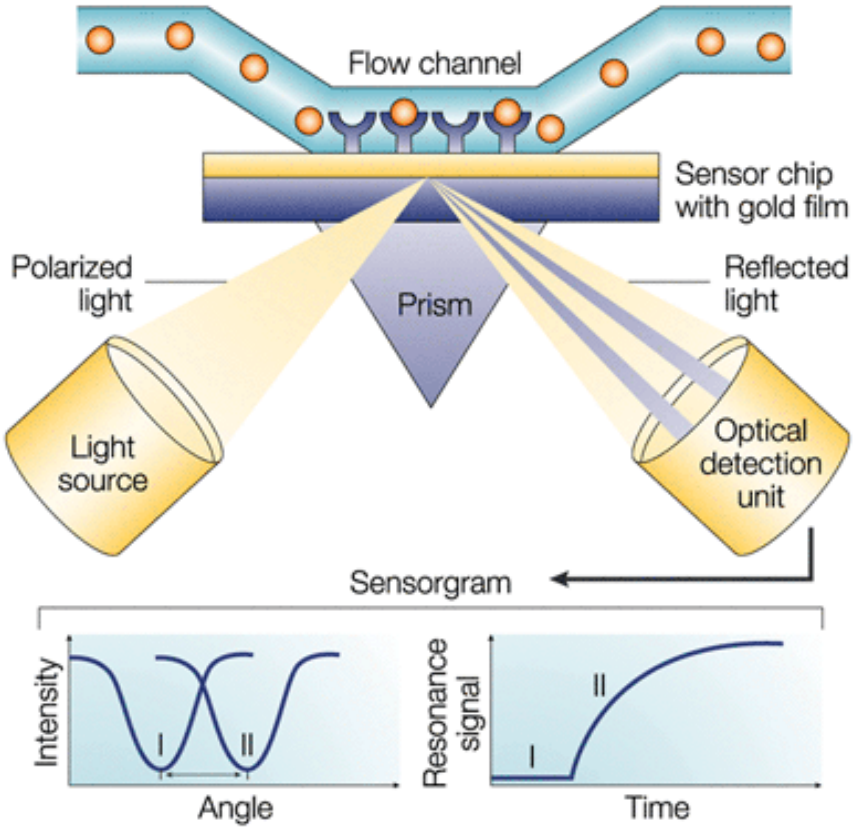

Figure 1.3 *Schematic diagram of a biosensor utilizing surface plasmon resonance (SPR) transduction. SPR detects changes in the RI near the surface layer of a sensor chip. The SPR angle shifts (from I to II in the lower left-hand diagram) when biomolecules bind to the surface and hence changes the mass of the surface layer. This change in resonant angle could be monitored in real time as shown in the plot of resonance signal versus time [Matthew A. Cooper et al, 2002].*

SPR is capable of detecting minor changes in RI due to cells bound to the biomolecular-recognition element on the transducer which corresponds to the measurement of change of angle of reflected light with respect to change in the density of

medium on the surface. A glass plate sputtered by a thin film of gold is irradiated from the backside by p-polarized light (from a laser) via a hemispherical prism, and the reflectivity is measured as a function of the angle of incidence. SPR is a very powerful technique because of the fact that it can be used to study the reaction kinetics of antibody-antigens and to determine affinity constants. However due to expensive equipments, complexity of operation and large size, the technique is not widely used (Taylor *et al*., 2005; Oh *et al*., 2005a) (Mello and Kubota 2002; Ramasamy 2010).

Mass Sensors

One type of mass transducer is the piezoelectric transducer. Change in mass due to target and biomolecular-recognition element interactions may be detected by piezoelectric transduction. Piezoelectric transduction is carried out due to an electrical charge imbalance due to a change in mass attached to the sensor surface. This mass change, which is proportional to a biomolecular-recognition binding interaction, causes an increase in the mass on the piezoelectric device. The main advantage of piezoelectric transduction (i.e., mass sensor) is the ability to perform label-free measurements of the binding events in conjunction to real-time analysis of binding kinetics (Griffin 2009; Ramasamy 2010).

Quartz Crystal Microbalance Sensors

The most commonly employed mass sensitive transducer is the quartz crystal microbalance (QCM), which relies on a bulk wave effect. A QCM device is made up of a quartz disk plated with electrodes (Griffin 2009). When the QCM is subjected to alternating electric field, an acoustic wave propagates through the device. The change in mass associated with target-biomolecular-recognition element interactions decreases the

resonant frequency which is directly proportional to the mass of the target attached on the QCM sensor surface. A typical operation and schematic representation of a piezoelectric transducer used in biosensor application is as shown in **Figure 1.4**, (Hirao *et al* 2012).

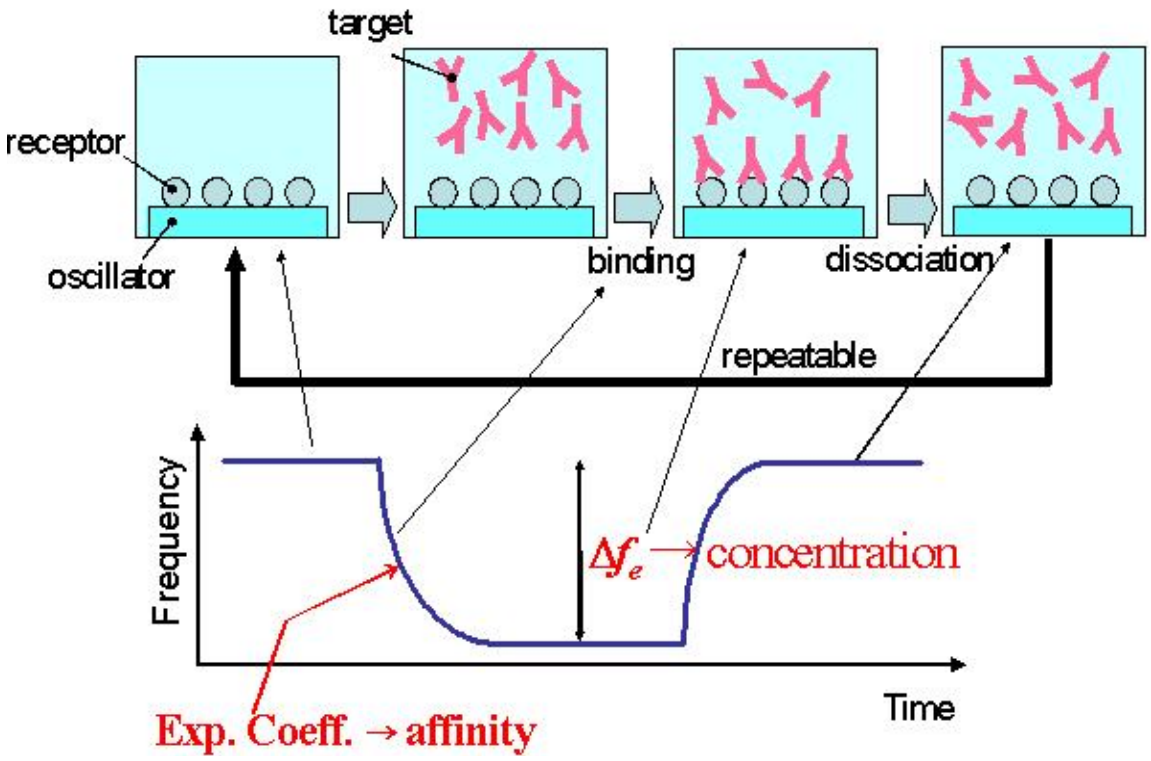

Figure 1.4 *Schematic diagram of a biosensor based on piezoelectric transduction. From the figure it is clear that when the oscillator with the receptor is resonating the resonance is highest to the respective condition. However when the oscillator comes in contact with the target analyte, the receptor binds with the target analyte, there is reduction in resonant frequency. The reduction in resonant frequency is directly corresponding to amount of analyte bound to the receptors. When the analytes are dissociated from the receptors the resonant frequency increases thereby reaching the initial resonant frequency correlating to the detection of analyte in the presence of specific receptors, [Hirao et al, 2012].*

This transduction method can be employed using a wide variety of target-biomolecular-recognition element interactions (e.g., antibody, aptamer, and imprinted polymer); for a measurable change in signal the mass change should be large enough. A major disadvantage of PZ sensors is the long incubation time of the bacteria, numerous washing and drying steps, and the problem of regeneration of the crystal surface. Other disadvantages include lack of specificity, sensitivity, and interference of liquid media (Grate 1993).

Surface Acoustic Wave Sensors

Mass-change can also be measured by alternative piezoelectric transducer devices for target-biomolecular-recognition element interactions that have some added advantages over bulk wave sensing. Surface acoustic wave (SAW) devices exhibit enhanced sensitivity compared to bulk wave devices. SAW devices transmit along a single crystal face, with the transducer acting as both transmitter and a receiver having the electrodes located on the same side of the crystal. SAW devices can directly detect changes in mass due to binding interactions between the immobilized biomolecular-recognition element and target and exhibit increased sensitivity when compared to bulk wave devices. However most biological detection is done in liquids. Liquids significantly dampen the acoustic waves, limiting the SAW's usage for biosensing applications. There are many reports of improvements using dual channel devices, and special coated electrode systems allowing for non-contact SAW devices, for biological solution interfaces. However, reliability of such devices for biosensor applications is under improvement especially in terms of sensitivity and for specific microbial analyses (Grate 1993).

Magnetostrictive Sensors

The principle of magnetostriction was discovered by James Joule in 1840. Recently, Magnetoelastic biosensor (ME) platforms are gaining attention in chemical and biological sensing. ME materials are amorphous ferromagnetic alloys that usually include a combination of iron, nickel, molybdenum and boron. These materials work on the principle of magnetostriction, wherein the material experiences changes in its dimensions in presence of a magnetic field. Upon application of a magnetic field, the randomly oriented magnetic domains in the material tend to align in the direction of the applied field. The alignment of the magnetic domains in the ME material results in a change in the sensor's dimensions. By applying a time varying magnetic field, the ME materials can efficiently convert the applied magnetic energy into mechanical oscillations. The characteristic fundamental resonant frequency of these oscillations is dependent on the physical properties (elastic modulus, density and Poisson's ratio) and the dimensions of the material. Both the actuation of the sensor and the detection of the response of the sensor can be measured using changes in the impedance of a non-contact solenoid pick-up coil. ME biosensors are actuated by the application of an AC magnetic field that causes the sensors to oscillate mechanically. When the frequency of the applied field is in resonant with the natural frequency of the sensor, the conversion of electrical energy to elastic energy is the largest. For a thin, planar, ribbon shaped sensor of length L, vibrating in its basal plane, the fundamental resonant frequency of longitudinal oscillations is given by (Liang *et al*. 2007).

$$f_n = \frac{1}{2L}\sqrt{\frac{E}{\rho(1-\sigma)}} \qquad 1.1$$

Where f_n is resonant frequency of the sensor, ρ is density of the sensor material, E is elastic modulus of the sensor, σ is Poisson's ratio and L is length of the sensor. The ME biosensors can be coated with various biomolecular-recognition elements to target analytes. A change in resonant frequency is observed when the target binds to the ME sensor which can be measured rapidly and accurately. The ME biosensors is very inexpensive and hence they may be used as disposable sensors. ME biosensor measurement is by magnetic flux; hence, no direct connections are needed between the sensor and monitoring electronic equipment making possible a variety of in situ and in vivo monitoring applications (Li *et al*. 2010). Recently, ME biosensors have been fabricated using immobilized bacteriophage as the biomolecular-recognition element for real-time in vitro detection of *S. aureus.*

METGLAS® 2628MB

Ferromagnetic materials generally are Fe, Ni, and Co metals or their alloys. Ferromagnetic materials have been considered to be good candidates for ME biosensors sensors because of their soft magnetic properties (low remanence and coercive field) in general. Moreover, ferromagnetic material can be made into amorphous (non-crystalline) metallic alloys by high speed spinning and cooling of a liquid alloy. For example, METGLAS® 2826 MB, consisting of Fe, Ni, Mo, and B, is a typical amorphous ferromagnetic material having the advantages of nearly magnetic isotropic structure, considerable high permeability, low coercivity, and low hysteresis loss. METGLAS® 2826 MB can be used as a ME sensor platform and hence long ribbon is diced to small free standing beams and coated with chromium and gold using E-beam deposition.

There are many methods of transduction platforms; electrochemical, optical, and mass sensitive transductions are few of them (Kress-Rogers, E 1998, Turner, A.P.F.; Karube, I.; Wilson, G.S. 1987). PZ materials, quartz-crystal microbalance systems (QCM), microcantilever devices, have all been used as transducer platforms for biosensors (Aberl *et al*., 1994; Pathirana *et al*., 2000; Olsen *et al*., 2003). However, because of inherent physical contact with the sensors, the lack of specificity and interference by the liquid medium the performance of these sensors has not met expectations. In this study, ME material as a transducer platform is investigated. The principal advantages of ME transducers are the absence of physical wire contacts to the sensor, enabling in-situ wireless measurements.

1.1.3 Biomolecular-Recognition Element

The biomolecular-recognition element is the heart of a biosensor. Ideally the function of a biomolecular-recognition element, say A, is that it should capture the bacterium, say B, and that the biomolecular-recognition element A is specific only to bacterium B. Furthermore the biomolecular-recognition element A should only capture bacteria B even after exposure to a mixture of bacteria B, C, and D. However in reality this is difficult to achieve and researchers continue to search for highly specific biomolecular-recognition elements for each pathogenic bacterium that is present in nature. In this paper a highly specific lytic bacteriophage 12600 is used to detect *S. aureus* (Balasubramanian *et al*. 2007; Guntupalli *et al*. 2008). The bacteriophage or phage is a kind of virus that infects its host bacterium at highly specific sites. There are different types of phage that exist in nature and some are genetically engineered to obtain specific bacteria detection.

A lytic phage is inert metabolically when it is extracellular in nature (virions); however, when it comes in contact with a bacterial cell, it attacks the cell, injects genetic material (DNA or RNA) replicates using bacterial genetic material and eventually destroys the bacteria due to infection. As there are replicated virions available they try to find new host bacteria and the cycle continues known as the lytic cycle. This function of lysis of the bacteria for replication is an advantage for the detection of specific bacteria as the phage attacks only the bacteria that can be used for its own replication. In this study the bacteriophage 12600 highly specific to *Staphylococcus aureus* is used. **Figure 1.5** shows scanning electron micrographs of the structure of the phage and *S. aureus* captured on an ME biosensor. A schematic of the biosensor is also shown in **Figure 1.5**.

1.2 Binding Definition and Concept

Binding in terms of biological science relates to a biological entity getting attached or captured to another biological entity due to affinity for each other. For biosensors, the higher binding of bacteria is expected to improve the sensitivity of the biosensor. For higher binding of bacteria to the biosensor, uniform distribution and an optimized density of the biomolecular-recognition element on the sensor surface is also necessary. To achieve optimum density of the biomolecular-recognition element in conjunction with uniform distribution, optimization of immobilization time and concentration of biomolecular-recognition element solution to the biosensor is important. Therefore optimum surface density of the biomolecular-recognition element with uniform distribution is necessary for maximum bacteria capture. For maximum bacteria capture, mean free length between the successive phage binding sites was calculated and compared to the size of the bacteria. To confirm calculation, confirmatory experiments

were conducted between the two higher phage concentrations respective to maximum binding and uniform distribution of phage on the sensor for the detection of *S. aureus*.

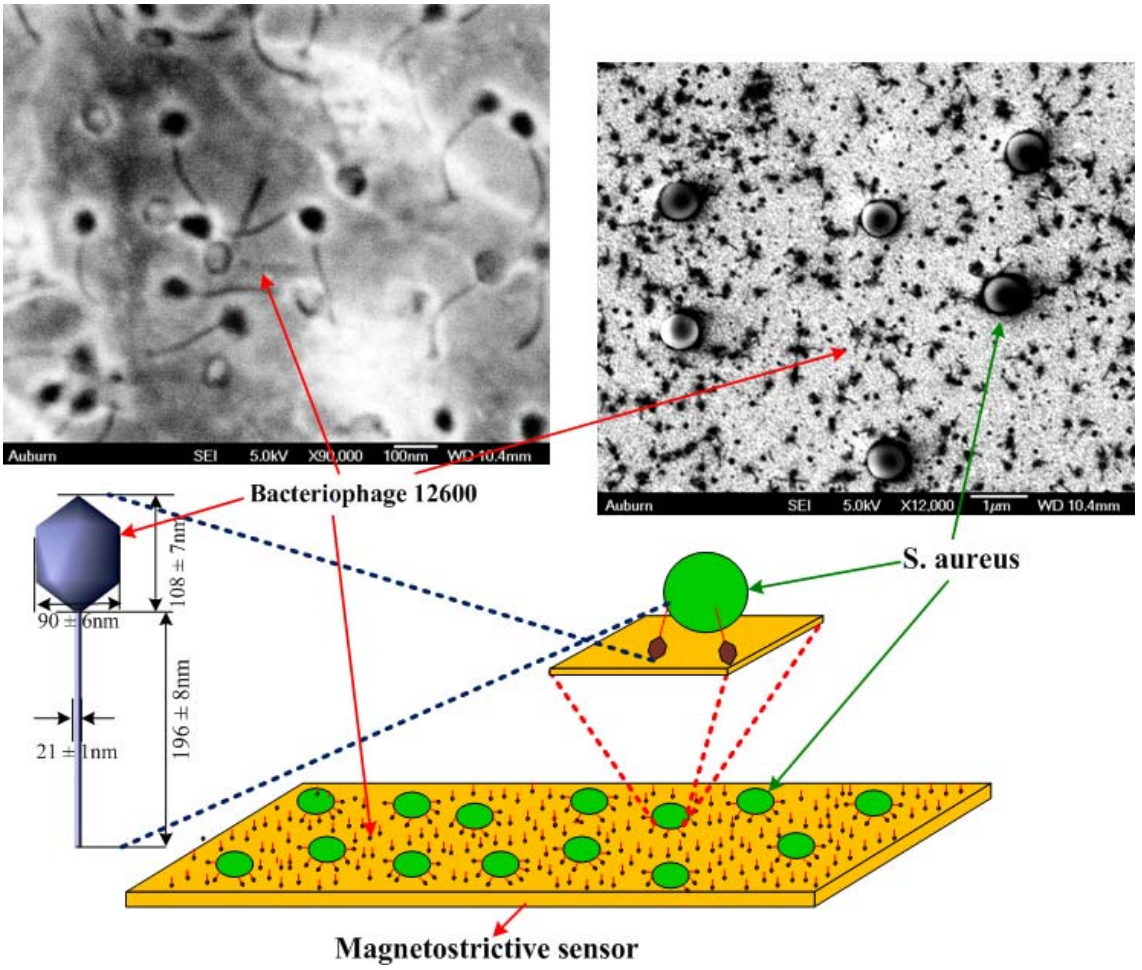

Figure 1.5 *Schematic of phage and S. aureus bound onto the sensor surface with respective SEM images. It is clear from the SEM images that the schematic drawn corresponds to the verification observed in SEM images.*

1.2.1 Binding of Bacteriophage and Bacteria

The binding of bacteriophage on the sensor surface is through physical adsorption. However the capture of bacteria by the bacteriophage is due to protein affinity between the bacteria and the phage. Since the bacteriophage 12600 is specific to a broad range of the *S. aureus* bacteria while capturing of other bacteria is very low. We

found that there was a strong binding between phage 12600 and *S. aureus* than compared to other bacteria.

1.2.2 Hill Plot

Hill plots help to understand the binding ability of a system, wherein a single molecule binds two or more of a second molecule such as,

$$A + nB \leftrightarrow AB_n \tag{1.2}$$

Hill plot calculations were constructed to understand the binding and dissociation constant of the phage 12600 and *S. aureus.* The Hill plot slope provides information on the binding while the, K_D, dissociation constant is calculated from the relation

$$K_D = \frac{[A][B]^n}{[AB]_n} \tag{1.3}$$

1.3 Objective of Research

The objective of this research was to optimize and determine the procedure required to produce the highest bacterial binding to the ME biosensor surface of *S. aureus* using lytic phage 12600 as biomolecular-recognition element. This procedure is divided into three steps.

1. Fabrication and characterization of biosensor platform

   Fabricating 1 mm resonators using the METGLAS® 2628MB strips by dicing in the dicing saw machine DAD 3220 DISCO (Kiru, Japan)

2. Phage characterization of the biosensors

   Following resonator fabrication, the biosensors are characterized as a function of the lytic phage 12600 concentration (ranging from 10^8 to 10^{12} pfu/mL) and

immobilization times (10, 30, 90, 270, 810, 2430 min). **Figure 1.6** shows the summary of experimental steps.

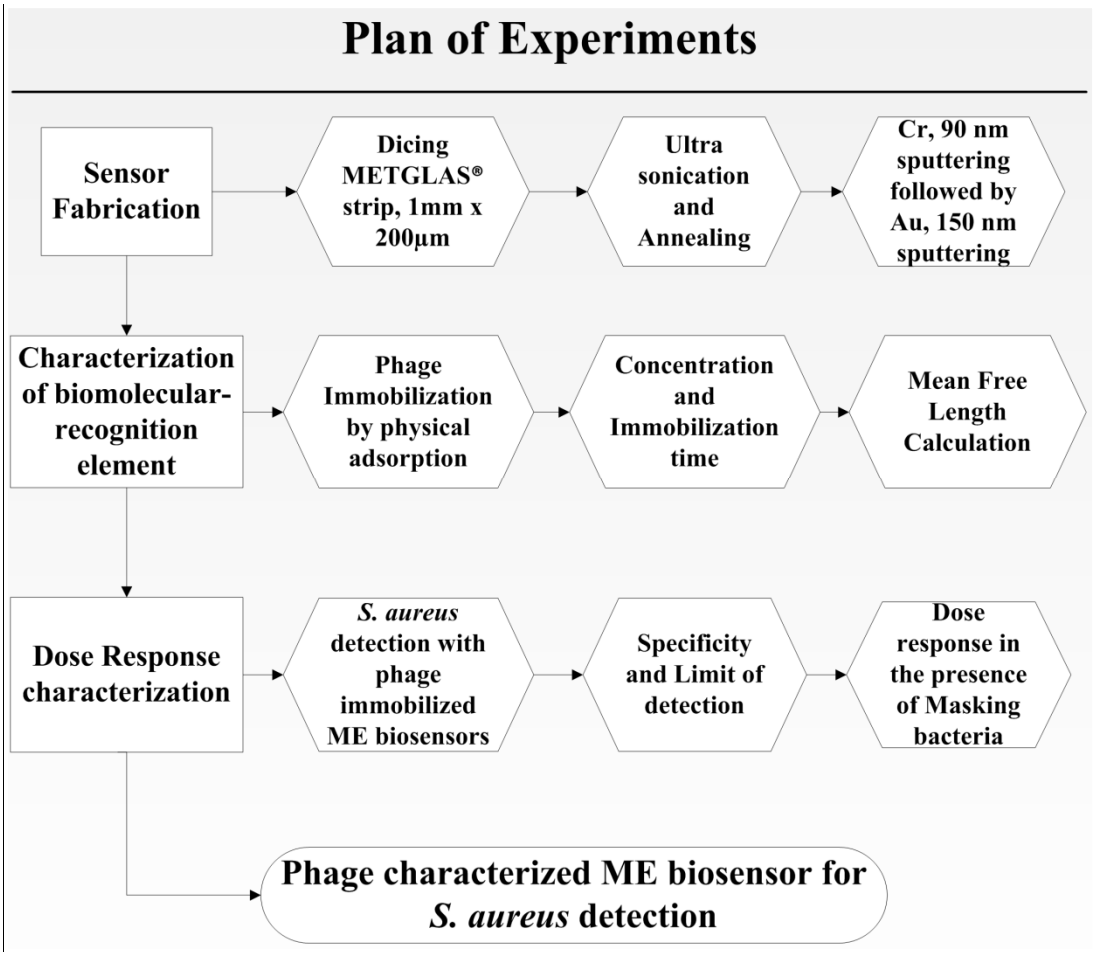

Figure 1.6 *Plan of experiments*

Deducing the number of phage bindings as a function of immobilization time and concentration of the phage suspension, with the SEM images followed by estimation of optimal concentration and immobilization times with the mean free length calculations were carried out. This followed by study of selectivity of the phage immobilized sensors to various bacteria and studying the dose response characteristics of phage immobilized biosensors in the presence of high concentration of masking bacteria.

CHAPTER 2

LITERATURE REVIEW

2.1 Biomolecular–Recognition Elements

Biomolecular-recognition elements, being the sole factor of specificity for biosensor technologies, help in capturing the target analyte of interest. There are many kinds of biomolecular-recognition elements, as many as the different target analytes that have been studied so far for biosensors. However there are five major categories of biomolecular-recognition elements such as antibody/antigen, enzymes, nucleic acids/DNA, cellular structures/cells (Cellular systems, Non-enzymatic proteins) and biomimetic structures.

2.1.1 Antibody/Antigen

Antibodies are considered to be highly versatile biomolecules that can be designed or developed against any kind of target analyte. This characteristic nature of antibodies makes them selective and specific. It is a complex biomolecule made up of amino acids with orderly arrangement. The organisms develop a kind of protein, antibody, which can bind with a foreign body, antigen, which can be harmful to the organism. The interaction is more analogous to a lock and key arrangement. **Figure 2.1** shows the schematic of antibody/antigen interaction on a piezoelectric transducer.

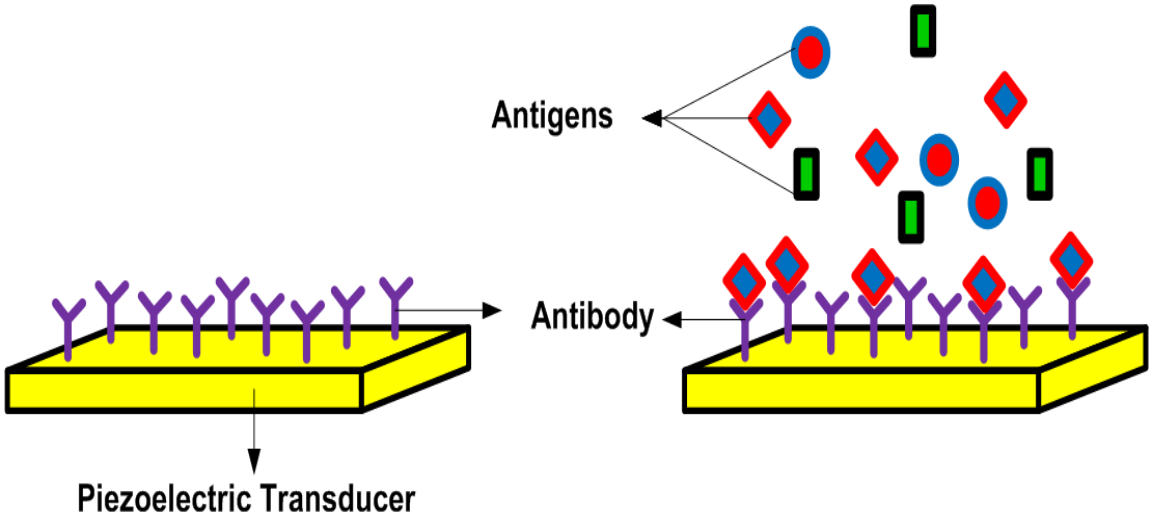

Figure 2.1 *Schematic of antibody – antigen interaction on a piezoelectric transducer material. An antigen specific antibody is coated on the piezoelectric transducer. When the transducer coated with the antibody comes in contact with the antigen in a mixture of other antigens, the transducer could detect the specific antigen.*

Because of their specificity, antibodies are used in immunosensors where only the specific analyte of interest, the antigen, fits into the antibody binding site. Typical reaction of antibody (Ab)-antigen (Ag) reaction can be given by the equation as shown below and K being the affinity constant.

$$Ab + Ag = (Ab{\cdot}Ag)_{complex} \tag{2.1}$$

$$K = \frac{[Ag \cdot Ab]}{[Ag][Ab]} \tag{2.2}$$

Unknown antibodies are normally identified by incorporating labeling. Labeling of antibodies is done by using radioisotopes, enzymes, RBCs (red blood cells), fluorescent probes, chemiluminescent probes or metal tags. However in biosensor

technologies enzymes are mostly used to label the antibodies. The advantages of using antibodies in biosensors as selective biomolecular-recognition elements are

1. Highly selective and have ability to differentiate between strains.
2. Highly sensitive.
3. They have a very strong binding.

However the major disadvantage of the antibodies is that there is no catalytic activity of the enzymes, and hence antibodies should be used only in a labeled format.

There are various formats of labeling the antibodies, such as radioimmunoassay (RIA) using radioactive labels, the most widely used immunoassay method. Radioimmunoassays are used in different fields such as, pharmacology, clinical chemistry, forensic science, environmental monitoring, molecular epidemiology, etc. However due to expensive instrumentation, limited shelf life of radioisotopes, and potential harmful biological effects of radioactive materials on the environment, radioimmunoassays have limited use. Vast research has been carried out since the 1980's to find a replacement for the RIA.

Antibodies have become the most commonly used biomolecular-recognition elements due to their availability and use in the medical industry. There are two types of biomolecular interactions, direct and in-direct. In a direct interaction format, the immobilized target molecule reacts with a ligand molecule or vice-versa. In immunosensors *in-situ* incubation (exposure to the target molecule) is done followed by direct measurement of a naturally fluorescent analyte (T *et al*. 1991). However for non-fluorescent targets, the *in situ* incubation is carried out by a fluorophor-labeled antibody thereby producing a fluorescence signal which is directly proportional to the number of

bound target molecules. An increase in sensitivity can be achieved by increasing the number of antibody immobilized.

In case of the indirect format the unlabeled analyte competes with the labeled analyte for a limited number of biomolecular-recognition element binding sites. Assay sensitivity can be increased by decreasing the amounts of immobilized reagent. Ligler and coworkers reported the use of two different fluorescent dyes, labeling of captured antibodies with a dye and the antigen with a different dye in order to characterize the fluorescence based antibody biosensors (Campbell *et al*. 1999a). Both the dyes are excited at the same wavelength and their resultant emission spectrum from the captured antibodies is used to normalize the signal from the tagged antigen.

Heller and coworkers developed a sandwich-type separationless amperometric immunoassay which excluded washing steps (Kröger *et al*. 1999). The assay was carried out on a carbon electrode on which avidin and choline oxidase was co-immobilized in the presence of conducting redox hydrogel. When the antigen binds to the sensor, a complementary peroxidase labeled antibody is bound to the antigen thereby creating an electrical contact between the redox hydrogel and the peroxidase (Kröger *et al*. 1999). Vo-Dinh and coworkers developed submicron fiberoptic antibody-based biosensors to understand the biochemistry in a single cell (Alarie JP 1996; Cullum *et al*. 2000; Vo-Dinh T ; Vo-Dinh T 1986). These nanometer scale fiberoptic biosensors use a monoclonal antibody for benzo[a]pyrene tetrol (BPT), a metabolite of the carcinogen benzo[a]pyrene, as the biomolecular-recognition elements that are associated with exposure to polycyclic aromatic hydrocarbons.

Light is excited into the fiber and the resulting brief field of light at the tip of the fiber is used to excite any of the BPT molecules that have bound to the antibody. The fluorescent light is then collected through a microscope. Absolute detection limits for BPT of *ca.* 300 zeptomol (10^{-21} moles) have been reported (Alarie JP 1996). These nanosensors allow the probing of cellular and subcellular environments (Cullum *et al*. 2000; Vo-Dinh T).

2.1.2 Enzymes

An enzyme is a large, complex molecule made up of proteins and usually associated with a metal atom as a prosthetic group. The mode of operation of enzymes that are used in biosensors technology are due to either oxidation or reduction and often detected with electrochemical transduction methods. **Figure 2.2** shows an overview on the working mechanism of enzyme based biosensors.

The typical catalytic activity of an enzyme is as shown in the equation 2.3.

$$S + E \underset{k_{-1}}{\overset{k_1}{\longleftrightarrow}} ES \xrightarrow{k_2} E + P \qquad 2.3$$

Where S is substrate, E is enzyme, ES is enzyme substrate complex and P is product. In reactions involving biocatalytic recognition mechanisms, the amplification of the signal is carried out by a reaction catalyzed by biocatalysts. Some enzymes use their amino acid residues for activity while others require an additional chemical component called a **cofactor**, such as inorganic ions (Fe^{2+}, Mg^{2+}, Mn^{2+}, Zn^{2+}) or a more complex organic or metalloorganic molecule called a **coenzyme**.

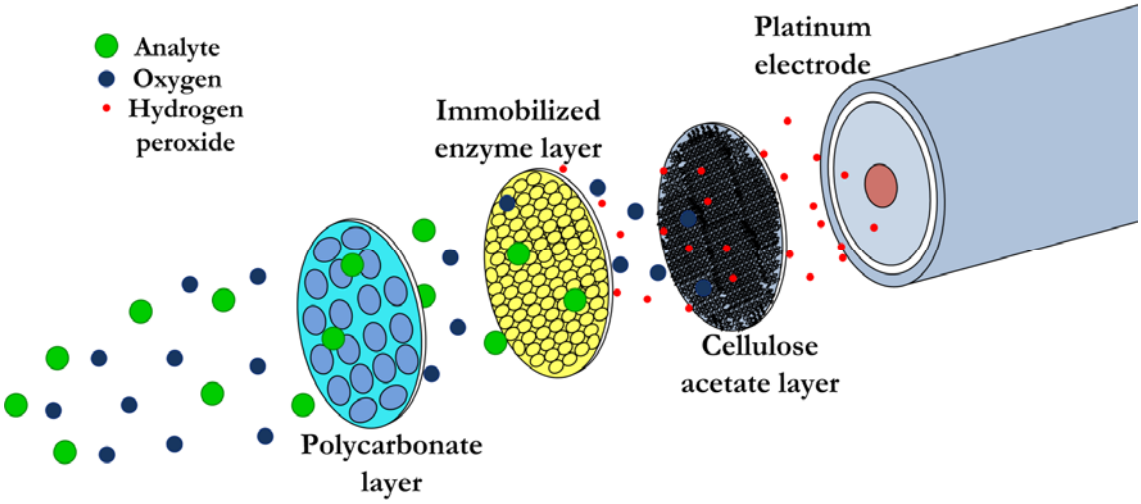

Figure 2.2 *A general overview of enzyme based electrochemical biosensor is shown in the schematic. An enzyme specific for the substrate of interest is immobilized between two membrane layers, polycarbonate and cellulose acetate. The substrate is oxidized as it enters the enzyme layer, producing hydrogen peroxide, which passes through cellulose acetate to a platinum electrode where the hydrogen peroxide is oxidized. The resulting current is proportional to the concentration of the substrate, [inspired by Vladimir et al, 1998].*

The sensitivity of an enzyme based sensor may be enhanced due to catalytic activity of the enzymes. The catalytic activity of enzymes depends upon the integrity of their native protein; however, if an enzyme is denatured, dissociated into amino acids, its catalytic activity is destroyed.

Enzyme-coupled receptors are also used to modify the recognition mechanisms where a ligand binds at the receptor site (D 1998). Gauglitz and coworkers immobilized enzymes on an array of optical fibers, for simultaneous detection of penicillin and ampicillin (Polster *et al*. 1995). Due to hydrolysis by penicillinase resulting in a pH change, the biosensors tend to act as an indirect technique to detect penicillin and

ampicillin. Kopelman and coworkers described the development and use of a micrometer-sized, fiber-optic biosensor for the detection of glucose (Rosenzweig and Kopelman 1996). Because of the biosensors being 100 times smaller than the existing glucose optodes, a new trend in nanosensor technology was set (Barker *et al*. 1998).

These biosensors are based on the enzymatic reaction of glucose oxidase that catalyzes the oxidation of glucose and oxygen into gluconic acid and hydrogen peroxide. Tris (1, 10-henanthroline) ruthenium chloride acts as a receptor site for oxygen measurement and is immobilized into an acrylamide polymer with the glucose oxidase; Photopolymerization is carried out to attach the polymer to the optical fiber. A comparison of the response of glucose sensors created on different size fibers was made, and it was found that the micrometer size sensors have response times at least 25 times faster (only 2 s) than the larger fibers. In addition, these sensors are reported to have absolute detection limits of ca. 10^{-15} mol and an absolute sensitivity of 5 to 6 orders of magnitude greater than current glucose optodes (Rosenzweig and Kopelman 1996).

The advantages of enzyme based biosensors are:

1. The enzymes bind to the substrate and are highly selective
2. The catalytic activity of the enzymes make them sensitive and reasonably fast acting
3. They are widely used as a biomolecular-recognition element in biosensor technologies.

The disadvantages of the enzyme based biosensors are:

1. They are expensive and extracting, isolating and purifying from the source is a very tedious and expensive process.

2. The activity of the enzymes is often lost when they are immobilized on a transducer element.
3. There is loss of activity observed after a short period of time.

2.1.3 Nucleic Acids

Another type of biomolecular-recognition element involves the use of hybridized deoxyribonucleic acid (DNA) or ribonucleic acid (RNA), which are the building blocks of life. Nucleic acids also behave similarly to antibodies where a specific base-paring of strands between the immobilized DNA and the target leads to a specific genetic code. In the last decade, nucleic acids have received increasing interest as receptor sites for biosensor and biochip technologies (Bardea *et al*. 1999; Erdem *et al*. 1999; Marrazza *et al*. 1999; Niemeyer *et al*. 1999; Sawata *et al*. 1999; Wang *et al*. 1998). The DNA probes are used to detect diseases that are genetically infected, such as cancer and viral infections. Similar to antibodies the labeling of the DNA is necessary and DNA labeling can be carried out by radioactive, photometric, electroactive etc. A schematic of biosensors immobilized with DNA as biomolecular- recognition element is as shown in **Figure 2.3** (J. Tamayo y M. Calleja, *et al*). The specificity of the DNA as a biomolecular-recognition element in DNA biosensors is due to the coexistence of adenine: thymine (A: T) and cytosine: guanosine (C: G) pairing, often referred to as genosensors. A probe is often labeled with an optically detectable molecule for a complementary known base pair sequence of DNA. By unwinding the double-stranded DNA into single strands, adding the probe, and then annealing the strands, the labeled probe will hybridize to its complementary sequence on the target molecule.

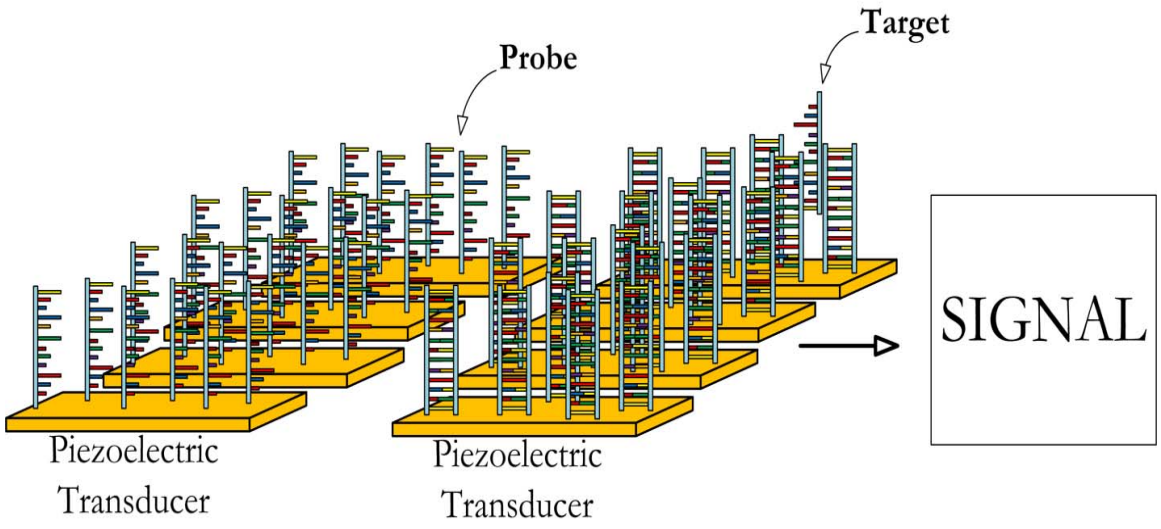

Figure 2.3 *Schematic of the biosensors immobilized with DNA as biomolecular-recognition element. The PZ transducer is immobilized with the DNA strand as probe as shown in the figure. When the biosensor is exposed to the target DNA strand the probe strand binds with the target strand and is detected due to reduction in frequency. [Inspired by J. Tamayo y M. Calleja, et al.]*

Grabley and coworkers used DNA biosensors for the monitoring of DNA-ligand interactions (Piehler *et al*. 1997). The irreversible bonding of DNA fragments to LMW (low molecular weight) ligands was observed real-time by employing SPR as the transducer platform.

Yevdokimov and coworkers developed sandwich-type biosensors based on liquid-crystalline dispersions generated from DNA-polycation complexes (Skuridin *et al*. 1996). These sandwich biosensors are shown to be useful for detection of compounds that affect the ability of specific DNA crosslinkers, i.e. polycationic molecules, to bind between adjacent DNA molecules. Karube and coworkers have shown that peptide nucleic acid-can be used as a biomolecular-recognition element (Sawata *et al*. 1999). The peptide

nucleic acid is an artificial oligo-amide which strongly binds to complimentary oligonucleotide sequences. This technique was capable of monitoring the target DNA over a concentration range of 40–160 nM, corresponding to an absolute detection limit of 7.5 picomol. Vo-Dinh and coworkers have developed a new type of DNA gene probe based on surface-enhanced Raman scattering (SERS) detection, which has both sensitivity and selectivity through label multiplexing due to inherent narrow bandwidths of Raman peaks (Isola *et al*. 1998; Vo-Dinh *et al*. 1994).

2.1.4 Cellular Structures/Cells

Cellular structures and cells comprise a broad category of biomolecular-recognition elements that have been continuously improved and used in the development of biosensors and biochips (Anzai et al. 1999; Barker et al. 1999; Blake et al. 1999; Campbell et al. 1999b; Cosnier et al. 1999; Franchina et al. 1999; Garjonyte and Malinauskas 1999; Gooding JJ 1999; Gooding et al. 1999; Hall et al. 1999; Hara-Kuge et al. 1999; Houshmand et al. 1999; Hu et al. 1999; Huang et al. 1999; Kim et al. 1999; Lebrón and Bjorkman 1999; Lee and Huh 2007; Nelson et al. 1999; Pancrazio et al. 1998; Patolsky et al. 1999; Pemberton et al. 1999; Piehler et al. 1999; Roos et al. 1999; Sergeyeva et al. 1999; Serra et al. 1999; Shih and Huang 1999; SS et al. 1999; Vo-Dinh et al. 1998; YS et al. 1999; Zhang et al. 1998; Zhao et al. 1998). A schematic of the Ligands used as biomolecular-recognition element on the biosensor is as shown in **Figure 2.4** (Anne-Catherine Huet., *et al*, 2010). These bioreceptors are either employed as an entire cell/microorganism or a specific cellular component, such as DNA, enzymes or other tissue material that is capable of binding specifically to certain target species on the

biosensor surface. Microorganism based biosensors are commonly employed in brewing, pharmaceutical industries, food manufacturing and waste water treatment plants, etc.

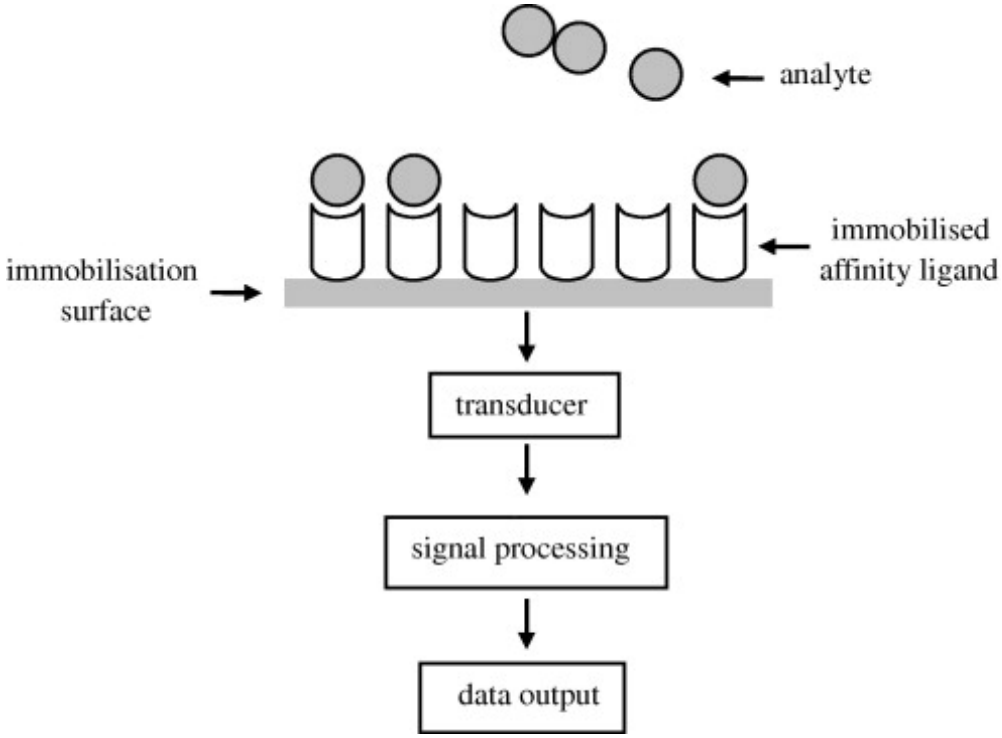

Figure 2.4 *A schematic of the Ligands used as biomolecular-recognition element on the biosensor [Anne-Catherine Huet., et al. 2010]*

The major advantage of using cells or its components as the biomolecular-recognition element is that very low amounts of target analyte can be detected because of signal amplification and the biosensors that are developed with these bioreceptors rely on their catalytic or pseudocatalytic properties.

a) Cellular Systems

Microorganisms, such as bacterial cells, viruses, phages, plant cells etc, are also used as biomolecular-recognition elements that allow a wide variety of targets to be analyzed. Certain kinds of bacteria and fungi are used as toxicity indicators or for the measurement of specific substances. Whole mammalian tissue slices or *in vitro* cultured

mammalian cells, plant tissues, are also used in plant-based biosensors because they contain different types of enzymes and possess enzymatic pathways for detection (D 1998). Arthrobacter nicotianae-based microbial biosensor, developed Bilitewski and coworkers, was used to monitor short-chain fatty acids in milk (Heim *et al*. 1999). By monitoring the oxygen consumption of the Arthrobacter nicotianae electrochemically, its respiratory activity is monitored indirectly correlating to fatty acid consumption. Short-chain fatty acids of length 4 to 12 carbons were detected in milk using butyric acid as the recognition element.

b) Non-Enzymatic Proteins

Often proteins, such as enzymes, that are found within cells serve the purpose of bioreception for intracellular reactions that take place in the cell or in another part of the cell. These proteins can be used for transport of a chemical from one place to another, such as a carrier protein. By immobilizing these proteins on various types of transducer elements, many researchers have constructed biosensors based on non-enzymatic protein biorecognition. Cusanovich and coworkers developed micro and nano-biosensors for nitric oxide that are not affected by most external factors (Barker *et al*. 1998). A fluorescent excited cytochrome c from the hemoprotein was immobilized by two different polymerization techniques, polymerization in an acrylamide gel and reversible binding using a gold colloid-based attachment. James *et al* demonstrated the use of a protein biomolecular-recognition element for the detection of liposaccharide endotoxin, the causative agent in clinical syndrome known as sepsis, killing more than 100,000 annually (James *et al*. 1996). Vogel and coworkers have demonstrated the use of lipopeptides, containing an antigenic peptide segment of VP1 (a capsid protein of the

picornavirus that causes foot-and mouth diseases in cattle), as a biomolecular-recognition element for biosensors (Boncheva *et al*. 1996). The protein, characterized with circular dichroism, was verified to retain the same structure as in its free form upon self-assembly onto a solid surface. Based on SPR measurements, it was found that the protein was still fully accessible for antibody binding. This technique could provide an effective means to develop biomimetic ligands for binding to cell surfaces.

2.1.5 Biomimetic Receptors

A biomimetic receptor is a designed and engineered biomolecular-recognition element that mimics the biological agents, such as genetically engineered molecules, artificial membrane fabrication and molecular imprinting; a typical biomimetic receptor (Boncheva *et al*. 1996; Cornell *et al*. 1997; Costello *et al*. 1998; Costello *et al*. 1999; Cotton *et al*. 1999; Girard-Egrot *et al*. 1998; Göpel and Heiduschka 1995; James *et al*. 1996; Kriz *et al*. 1996; Ramsden 1998; Ramström and Ansell 1998; Situmorang *et al*. 1999; Song and Swanson 1999; Wollenberger *et al*. 1998; Yano and Karube 1999; Zhang *et al*. 1999) is as shown in **Figure 2.5**. Biosilica is synthesized on the inert matrices functionalized with a reactive polymer that subsequently chemisorb nitrilotriacetic acid (NTA), a required binder for His-tagged recombinant silicatein. Silicatein immobilized onto this matrix using NTA-His tag linkage is used to synthesize nanoparticulate biosilica, biotitania, and biozirconia from monomeric precursors. In the presence of crosslinkers the analyte molecules are mixed with monomers in a molecular imprinting technique. After polymerization, organic solvents are employed to extract the analyte molecules from the powdered polymer resulting in the formation of molecular holes that

mimic the size of the analyte. With the help of recombinant techniques a wide variety of binding sites with desired properties can be synthesized using chemical means.

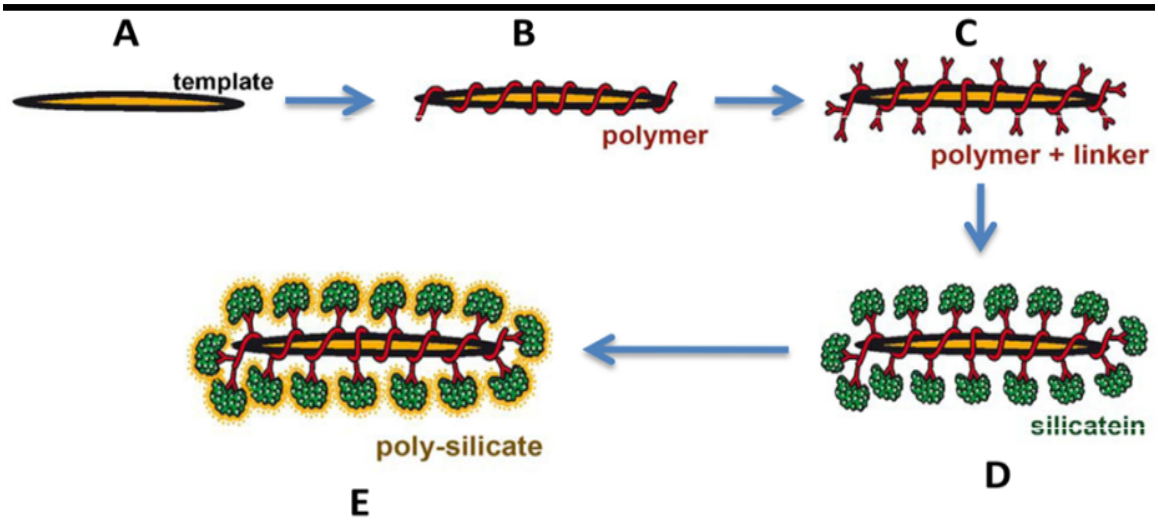

Figure 2.5 *Schematic of usage of a biomimetic receptor on the biosensor. Biosilica is synthesized on the inert matrices functionalized with a reactive polymer that subsequently chemisorb nitrilotriacetic acid (NTA), a required binder for His-tagged recombinant silicatein. Silicatein immobilized onto this matrix using NTA-His tag linkage is used to synthesize nanoparticulate biosilica, biotitania, and biozirconia from monomeric precursors. [Applied Microbiology and Biotechnology, volume 83, number 3, 408. Copyright © 2009, Springer-Verlag]*

Hellinga and coworkers have demonstrated the use of a genetically engineered single-chain antibody fragment specific to phosphorylcholine (Piervincenzi *et al*. 1998). The peptide sequence is fused, using protein engineering methods, in a way that imitates the binding properties of biotin to the carboxy terminus of the phosphorylcholine-binding fragment of IgA. This genetically engineered molecule bound to a streptavidin monolayer is monitored by total internal reflection fluorescence of a fluorescently labeled phosphorylcholine analog.

In another study, Stevens and coworkers developed an artificial membrane by imparting gangliosides in diacetylenic lipids-matrix (5–10% of which were derived in the presence of sialic acid) (Charych *et al*. 1996). The lipids experience self-assemblage into Langmuir- Blodgett layers; followed by photopolymerization through UV irradiation into polydiacetylene membranes. When cholera toxins come in contact with the membrane, the color changes (from natural blue to red) and absorption measurements are monitored for toxin concentration. A molecularly imprinted polymer membrane, on a platinum wire using agarose, was constructed on an electrochemical-based biosensor for the detection of morphine (Kriz and Mosbach 1995; Mayes *et al*. 1999). The resulting imprinted polymer was used to specifically bind morphine to the electrode. After the morphine was bound, electro-inactive codeine was used to wash the electrode thereby releasing some of the bound morphine. Oxidation at the electrode correlated with the measurement of the concentration of morphine. One of the greatest advantages of the molecularly imprinted polymer is that it can withstand harsh environments such as autoclave conditions or chemicals that would denature a protein.

CHAPTER 3

EXPERIMENTAL METHODOLOGY

Introduction:

This chapter covers the experimental setup of the study on bacteriophage-immobilized ME biosensors for *Staphylococcus aureus* detection. In the beginning of the chapter a brief overview of the sensor fabrication is discussed followed by the phage immobilization. The phage immobilized sensors are characterized for BSA blocking and resonant frequency measurement is carried out. After the resonant frequency, f1, is measured, the phage immobilized sensors are exposed to bacteria solution and resonant frequency is measured, f2, the difference in resonant frequency, (f1 – f2)= Δf, is correlated with SEM imaging of sensors to verify bacterial binding to the biosensor surface. This chapter also covers the brief experimental procedure for the bacteria capture with phage concentration optimized sensors, BSA blocking optimization, specificity and limit of detection, mean free length (MFL) estimation, Hill plot analyses and theory of measurement.

3.1 Sensor Fabrication

The METGLAS® 2826MB alloy was originally obtained from Honeywell International (Conway, SC) in the form of a long roll, ≈ 20 m. For our resonator application, this material is relatively inexpensive and has large magnetostriction with high ME coupling coefficient, making it an efficient converter of magnetic to elastic

energies. Resonators of the size 1000 µm × 200 µm × 28 µm were diced using a standard microelectronics fabrication dicing saw, DAD 3220 Disco Automatic Dicing Machine, (DISCO, Japan). After dicing, the resonator strips were ultrasonically cleaned in acetone, three times, 60 min each and once in methanol for 45 min to get rid of acetone. Annealing was carried out at 218 ºC for 3 hours, followed by furnace cooling. The annealed sensors were then placed carefully, with the help of tweezers, on a magnetic strip and then E-beam (electron beam evaporation technique) deposited with chromium, 90 nm, followed by gold, 150 nm, on both the faces. The gold surface helps in phage immobilization and Cr interlayer improves gold adherence.

3.2 Phage Structure and Phage Immobilization

The bacteriophage 12600 used in this research was prepared and provided by College of Veterinary Medicine, Auburn University, AL. The bacteriophage (3×10^{12} pfu/mL) were derived from the *S. aureus* ATCC 12600 strain (Balasubramanian *et al*.' 2007a). The structure and physical dimensions of the phage is depicted in **Figure 1.5**. SEM analysis, using a JEOL 7000F SEM machine showed the bacteriophage possessed slightly oval to hexagonal heads [(90 ± 6 nm) × (108 ± 7 nm)] with tails measuring 196 ± 8 nm in length and 21 ± 1 nm in diameter. These dimensions coincide well with those found for staphylococcal phage in the literature.

The bacteriophage was immobilized on the sensor surface by physical adsorption. The phage suspensions acquired were serially diluted from stock solution using Deionized (DI) water; C1 to C5, (10^8 to 10^{12} pfu/mL). The sensors were exposed to phage; for six time intervals, T1 to T6 (10, 30, 90, 270, 810, 2430 min), by rotating in 330 µL vials and then two times washed with DI water to remove any unbound phage

from the sensor surface. The sensors were then exposed to osmium tetroxide (OsO_4), after phage immobilization, for 45 min. OsO_4 helps to retain the biological structures intact and deactivate microorganism. SEM analyses of phage immobilized sensors were conducted and graphs were plotted depicting the number of phage bindings per sensor (NPB/sensor) versus exposure time, as shown in **Figure 4.4** and **4.5.**

3.3 BSA Blocking

The phage immobilized sensors were modified by BSA, to reduce non specific binding of bacteria on to the sensor. The phage immobilized sensors were exposed to BSA at concentrations of 0.1 mg/mL, 1 mg/mL, and 10 mg/mL (B1, B2 and B3) followed by bacteria capture. SEM analysis was carried out to determine what concentration of BSA would block the sensor surface to reduce the non specific binding.

3.4 Resonant Frequency Measurement and Setup

The resonant frequency of the sensor was measured using a solenoid coil as shown in **Figure 3.1**. A solenoid coil wound on a 2 mm inner diameter glass was used to measure responses of the sensor. The sensor was placed in the center of the coil; an AC current applied to the solenoid generates an AC magnetic field. The AC magnetic field induces the sensor to oscillate. In the presence of AC magnetic field, an external DC magnetic field was used to bias the ME sensor. A maximum conversion of mechanical energy to magnetic energy takes place at the mechanical resonant frequency of the sensor. The **Figure 3.1** shows the sensor placed in the capillary tube for the resonant frequency measurement. The DC magnetic field bias is used as shown in the figure.

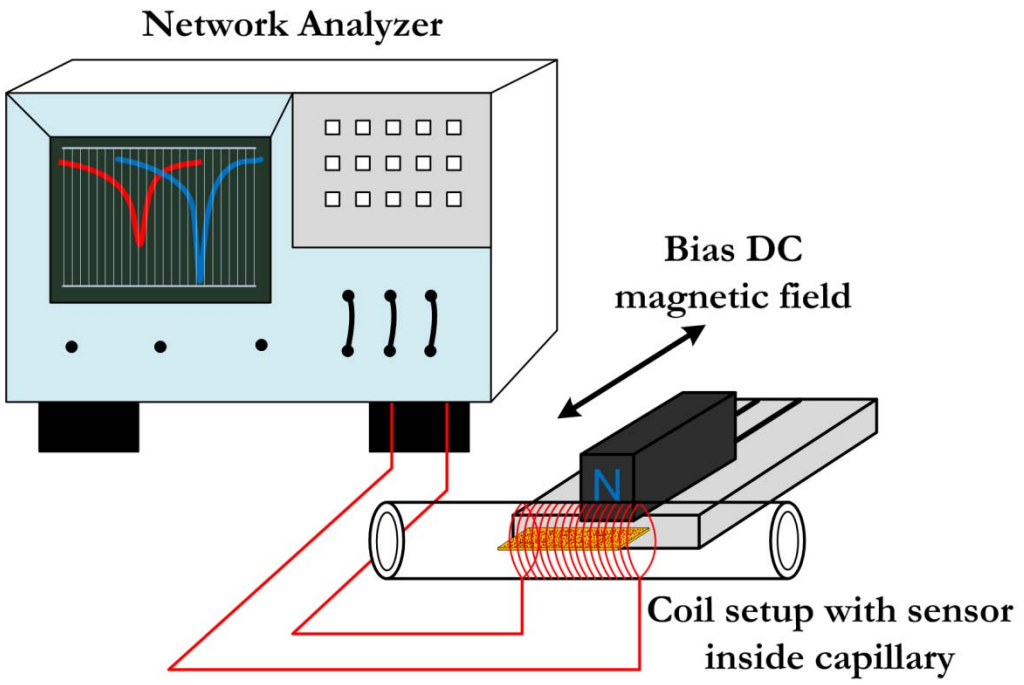

Figure 3.1 *A schematic of ME biosensor resonant frequency measurement setup.*

3.5 Bacteria Suspensions

The *Staphylococcus aureus, E. coli O157:H7, Listeria monocytogenes,* and *Salmonella typhimurium* used in this work were prepared and provided by Dr. James M. Barbaree's lab in the department of Biological Sciences at Auburn University, Auburn, AL. One colony of bacteria from a master plate was inoculated into NZY (Casein Hydrolysate (10g), Yeast extract (5g), NaCl (5g), $MgCl_2$ (2g)) broth and incubated at 37 ºC for 12 hours. After incubation, the culture was mixed gently for homogenous distribution and then transferred into sterile tubes followed by centrifugation. The concentrations of bacteria obtained from Dr. Barbaree's lab were suspension of 5×10^8 cfu/mL. The bacterial suspensions were serially diluted with DI water ranging from 5×10^1 cfu/mL to 5×10^8 cfu/mL. prior to every dilution; the solution was mixed using a vortex mixer to ensure homogenous distribution in the solution.

3.6 Scanning Electron Microscope (SEM) imaging

The biosensors were analyzed at various stages of experiments, using scanning electron microscope (SEM). SEM analyses provided visual verification of 12600 phage and *S. aureus* cells bound to the sensor surface. The sensors, after experimentation, were attached to aluminum stubs with the double sided carbon adhesive tape. The sensors placed on the aluminum stubs were allowed to dry in air for 25 min. Then they were placed in the Petri dish containing a small volume (20 μL) of Osmium tetraoxide (OsO_4) for 45 min. Osmium tetraoxide keeps the biological structures intact and deactivates the microorganisms. A JEOL-7000F Field Emission Scanning Electron Microscope was used for imaging. The images were taken at an accelerating voltage of 5 kV with a working distance of 10 mm, aperture of 3 and probe current of 54 μA.

SEM images of the sensor surface at desired magnification were recorded in electronic format using JEOL-Imaging software. The phage concentration and immobilization time were estimated by counting the number of phage bindings on the sensor surface by analyzing images of six areas and averaging. These results were then used to obtain the total number of phage bindings on the sensor surface. The sample preparation technique limited the imaging to only one side of the sensor. The number of phage bindings to either side of the sensor platform was assumed to be the same. Hence, the total number of phage bindings on the sensor surface was calculated as two times of that obtained for one side of the sensor.

3.7 Estimation of Bound Phage Based On SEM analysis

SEM images were taken at six different regions on the sensor surface. The number of phage attached on the sensor surface was counted manually for each of the

photographs taken (to reduce error). The average number of bound phage per unit area was calculated. The resulting number was multiplied by the entire surface area of the sensor to obtain the total number of bound phage. Each photograph was divided into eighty equal sections as shown in **Figure 4.2 and 4.3**. The number of phage in each of these sections was counted. The total number was calculated as shown:

$$\sum \textbf{(80 squares) = Total no. of phage binding} \qquad 3.1$$

3.8 Mean Free Length Calculations

The mean free length (MFL) between the successive phage bound sites was calculated by marking ten horizontal lines on the SEM images of C4 and C5 concentration phage immobilized sensors, at 30 min immobilization time. The average distance between the successive phage bound sites along the line drawn were calculated as shown in **Figures 4. 6 and 4. 7** followed by tables 1and 2. The MFL of C4 (≈ 0.9 μm, is closely comparable to the *S. aureus* bacteria size ≈ 0.8 to 1 μm). In contrast C5 (≈ 0.45 μm) was significantly smaller than the size of the bacteria. Using these facts, we suggested that the C4 sensors could capture more bacteria than C5 sensors. To verify this idea the C4 and C5 sensors were exposed to *S. aureus* (5×10^8 cfu/mL) and the change in resonant frequency measured.

3.9 Testing Procedure

3.9.1 Bacteria Capture

To capture bacteria, BSA blocked phage sensors were immersed in 330 μL vials with various concentrations of bacteria ranging from 5×10^1 cfu/mL to 5×10^8 cfu/mL. The resonant frequency of the sensor before and after exposure to the bacteria was

measured and the change in the resonant frequency was plotted as a function of the number of captures bacteria (**Figure 4.15)** determining by SEM imaging (**Figure 4.16).**

3.9.2 BSA Optimization

For optimum sensor performance the sensor free surface is covered with BSA to reduce nonspecific binding. The BSA blocking experiments are conducted with three concentrations, 0.1 mg/mL, 1 mg/mL and 10 mg/mL. It was observed that 1 mg/mL of BSA concentration was sufficient to block the free surface on the sensor to avoid nonspecific binding as shown in **Figure 4.12**.

3.9.3 Specificity

The specificity of the biosensor was studied by exposing the biosensor to pathogens other than *S. aureus*. The affinity of the biosensor to other pathogens was compared with the biosensor's affinity to *S. aureus*. Three gram-negative pathogens (*S. aureus*, *S. typhimurium* and *E. coli*) and one gram-positive pathogen (*L. monocytogenes*) were used in this test. The biosensors were exposed to each of the pathogens individually. After exposure to bacteria the SEM imaging, as shown in **Figure 4.14**, of the sensors were carried out. The number of pathogens attached to the biosensor was calculated using the methods described in section 3.7.

To evaluate the specificity of the phage immobilized sensors, the sensors were incubated in a 330 μL of the four different bacteria (*S. aureus, L. monocytogenes, E. coli,* and *S. typhimurium*) for 30 min and the SEM analyses was carried out. The data were plotted for number of bacteria versus type of bacteria as shown in **Figure 4.13.**

3.9.4 Limit of Detection

Dose response of the biosensor was studied by monitoring the resonant frequency of the biosensor, upon exposure to different concentrations of *S. aureus*. The different concentrations (5×10^1 cfu/mL through 5×10^8 cfu/mL) were prepared by successive dilutions of the as-received *S. aureus* (5×10^8 cfu/mL). Each successive dilution reduced the concentration of *S. aureus* by a factor of 10. The phage immobilized biosensors were placed in 330 µL vials and rotated on the rocking instrument at 6 rpm. The biosensor was placed in the center of a solenoid coil wound around a glass tube. Resonant frequency measurement was carried out for each biosensor, before and after bacteria capture. The difference in frequency shift, **Figure 4.15**, was correlated to the amount of bacteria captured by the biosensor with the assistance of SEM images as shown in **Figure 4.16**. Control sensors (devoid of phage) were used to quantify that the bacteria capture was not because of the non-specific binding.

3.9.5 Hill Plot

A Hill plot was constructed from the number of phage binding/sensor curves to study the kinetics of the *S. aureus*-phage binding. This plot was also used to determine the apparent dissociation constant and binding valency. The *S. aureus* binding to the phage immobilized on the sensor's surface can be expressed as a reversible reaction:

$$nSA + phage \leftrightarrow SA_n \cdot phage \qquad 3.2$$

where $1/n$ represents binding valency of the *S. aureus* attaching to the phage immobilized on the sensor surface. The relationship between association (K_A) and the dissociation (K_D) constant for the eq 3.2 is as follows:

$$K_A = \frac{[phage][SA]^n}{[phage \cdot SA_n]} = \frac{1}{K_D} \quad 3.3$$

The association of bacteria to the phage is primarily because of the movement of bacteria in solution and its interaction with the immobilized phage. The dissociation is governed by the strength with which bacteria binds to the immobilized phage on the sensor surface. The calculations to determine the values of dissociation constant (K_D) and binding valency ($1/n$) were done by constructing a Hill plot. The value of K_D can be determined as the reciprocal of the ordinate intercept. The binding valency is determined as the reciprocal of the slope of the hill plots. The binding valency is the number of phage binding sites that interact with *S. aureus*.

$$K_D \text{ (apparent)} = K_D^{1/n} \quad 3.4$$

The Hill plots were traditionally used to study kinetics of reactions, where the reactant and the product concentrations were expressed using molar concentrations. However, in this method the concentration of *S. aureus* has the units of cfu/mL. The use of K_D (apparent) takes into account the scaling factor due to the use of different units for the concentrations of the analyte. The K_D (apparent) is defined as the concentration at which half of the available binding sites are occupied. Hence, a stronger *S. aureus*-phage binding is indicated by lower values for K_D (apparent). The Hill plot was constructed by plotting log X versus the log [***S. aureus***], where X is given as

$$X = \frac{Y}{(1-Y)} \quad 3.5$$

And

$$Y = \frac{A}{B} \quad 3.6$$

Here A denotes the number of phage binding of each concentration of bacteriophage 12600 to the biosensor. B denotes the maximum number of phage binding achieved before the biosensor has reached saturation. B was calculated from the Hill Plot curves of the NPB/ sensor vs. immobilization times curve obtained for the biosensor. The values of the apparent dissociation constant and binding valency are as shown in **Figure 4.10** and **4.11**, were calculated from the NPB/ sensor vs. immobilization time curves and NPB/ sensor vs. concentration of phage curves.

3.10 Theory of Measurement

ME resonators are activated by the application of a time-varying magnetic field. This field results in mechanical oscillations of the resonator. If the frequency of oscillation is in resonant with the natural frequency of the sensor, there is maximum conversion of magnetic energy to elastic energy. These oscillations in the longitudinal direction can be described by (Landau and Lifshitz 1975)

$$\boldsymbol{\rho_s \frac{\partial^2 u_y}{\partial t^2} = \frac{E}{2(1-\sigma^2)} \frac{\partial^2 u_y}{\partial y^2}} \qquad 3.7$$

The solution to this first order differential equation yields the resonant frequency as

$$\boldsymbol{f_n = \frac{n}{2L} \sqrt{\frac{E}{\rho(1-\sigma)}}} \qquad 3.8$$

Where f_n is resonant frequency of the sensor, ρ is density of the sensor material, E is elastic modulus of the sensor, σ is Poisson's ratio, L is length of the sensor, and n is mode of oscillation.

The above equation is for the n^{th} mode of oscillation. By substituting n=1, the relation for the resonant frequency will be:

$$f_1 = \frac{1}{2L}\sqrt{\frac{E}{\rho(1-\sigma)}} \quad 3.9$$

In equation (3.9), if E, σ, and L are constants (for a particular material at constant temperature and pressure) then,

$$\Rightarrow f_0 \propto \sqrt{\frac{1}{M}} \quad 3.10$$

$$\Rightarrow \frac{\Delta f}{\Delta m} = -\frac{f_0}{2M} \quad 3.11$$

Here, ($\Delta m << M$)

Where, M is mass of the sensor, Δm is mass attached on the sensor surface, Δ*f* is change in resonant frequency. The above equation (3.11) gives the relationship between the mass that is uniformly attached to the sensor surface and the resulting shift in the resonant frequency of the ME sensor. Therefore any non-ME mass attached to the sensor dampens the longitudinal oscillations forcing the resonant frequency to shift to a lower value. A spectrum of AC frequencies is acquired by scanning through the range of frequencies. Furthermore, from equation (3.11), the sensitivity of the sensor could be increased by reducing the initial mass (M) of the sensor, and which profoundly depends on the reduction of width and length (Liang *et al*. 2007).

CHAPTER 4

RESULTS AND DISCUSSION

4.1 Introduction

This chapter begins with a characterization of the phage 12600 distribution on the resonator's surface. Concentration of phage, in solution, and immobilization time of the resonator in the phage solution are variables; that will determine the final characteristics of the phage morphology and density on the resonator's surface. Phage-characterization of the resonators also includes mean free length calculations to estimate and correlate the maximum bacteria capture, and experimental results to confirm hypothesis.

Specificity of the phage immobilized sensors is studied by exposing the sensors to other masking bacteria such as *L. monocytogenes, E. coli,* and *S. typhimurium*. Resonant frequency changes response and SEM analysis confirms that 12600 phage immobilized biosensors are highly specific to *S. aureus*.

An experimental study is carried out to determine the limit of detection of *S. aureus* using ME biosensors. In this set of experiments, phage-characterized biosensors, with respect to concentration and immobilization time of phage solution, are used and the biosensors responses are measured as a function of exposure to increasing concentration of *S. aureus* suspended in deionized (DI) water. The limit of detection of *S. aureus* in the presence of a high concentration of masking bacteria was also studied.

4.2 Phage-Characterization

The bacteriophage 12600 used in this research was prepared and provided by the College of Veterinary Medicine, Auburn University, AL. The bacteriophage used (3×10^{12} pfu/mL) were derived from the *S. aureus* ATCC 12600 strains (Balasubramanian *et al*. 2007). The phage suspension acquired were serially diluted from stock suspension using DI water, C1 to C5 (10^8, 10^9, 10^{10}, 10^{11} and 10^{12} pfu/mL). The sensors were exposed to phage; for six time intervals, T1 to T6 (10, 30. 90, 270, 810, 2430 min), by rotating in 330 µL vials on a rocking instrument at 6 rpm. The biosensors were then washed with DI water for two times to remove any unbound phage from the sensor surface.

The sensors were then exposed to osmium tetroxide (OsO_4), after phage immobilization, for 45 min. OsO_4 helps to retain the biological structures intact and kill the activity of the microorganisms. SEM analyses of phage immobilized sensors were conducted; **Figure 4.1** summarizes the results for all phage binding conditions investigated. Enlarged images of each phage binding condition are shown in appendix A. From the SEM images it is explicitly clear that at lower concentration (10^8 to 10^{11} pfu/mL) of phage immobilization, as immobilization time increased the NPB/sensor also increased. However, at the highest concentration, 10^{12} pfu/mL, the NPB/sensor decreased. The probable reason for this decrease is because of washing step after immobilization step. During washing the loosely bound phage clump might have washed away resulting in reduction of NPB/sensor. After the SEM analyses of the phage immobilized biosensors were completed, the places on the biosensor surface where phage had bound where counted by hand to reduce errors. An average of six regions was taken

on each sensor for a total of 90 sensors measurements, assuming phage binding was uniform throughout the sensor surface. Each SEM picture was divided into eighty equal sections, a grid, for counting the phage binding spots (**Figure 4.2** and **4.3)**. The number of phage bound in each of these grids was counted. Typical SEM image of phage-immobilized sensor counted is as shown in **Figures 4.2 and 4.3.** After SEM analyses a graph was plotted for number of phage bindings per sensor (NPB/sensor) versus exposure time, as shown in **Figure 4.4** and **4.5.** From **Figure 4.4** it is clear that the concentration gets saturated from 10^{11} pfu/mL for all the time slots.

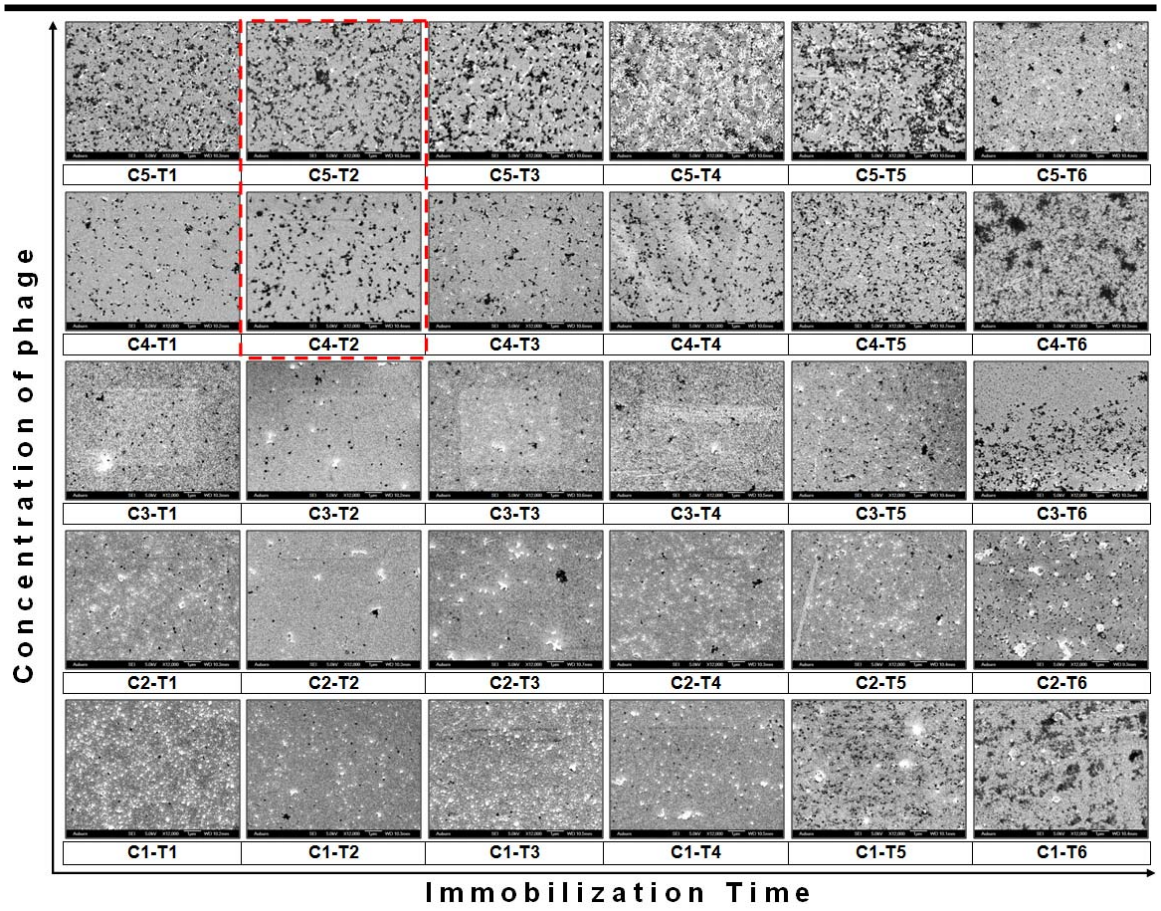

Figure 4.1 *A summary of SEM images showing the phage distribution on the sensor surface with respect to phage concentration versus immobilization time. The highlighted images are the C4-T2 and C5-T2, which were studied the most because of uniform*

distribution and higher surface density of phage on the sensor surface. The black dots on the images are the phage bound to the sensor.

Hence in this study concentrations 10^{11} and 10^{12} pfu/mL was studied the most. After the concentration of phage immobilization was fixed, immobilization time was another variable that needed to be studied. Hence for optimum phage distribution with higher surface density, a graph for NPB/sensor vs immobilization time was plotted, with the assistance of SEM images, and was understood that the uniformly distributed and maximum phage binding was achieved at T2 (30 min) for both 10^{11} and 10^{12} pfu/mL phage concentration. The graphs for NPB/sensor vs concentration of phage and NPB/sensor vs immobilization time is as shown in **Figures 4.4** and **4.5** respectively.

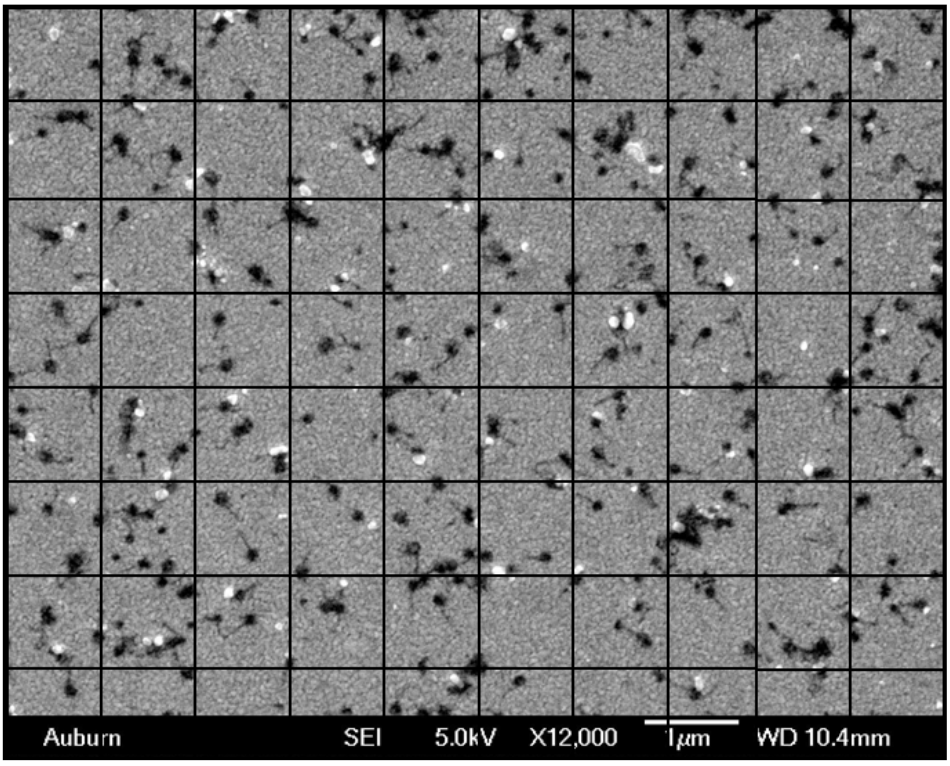

Figure 4.2 *SEM image divided into eighty sections to count phage density; conditions 10^{11} pfu/mL phage immobilized sensor at T2 (30 min) immobilization time.*

In **Figure 4.2** and **4.3**, it is clear that the phage bindings is counted in each grid added to together to get the total phage binding respective to the area of SEM image. Similarly six to eight images were analyzed for 90 sensors and an average was deduced assuming uniform binding throughout the sensor surface.

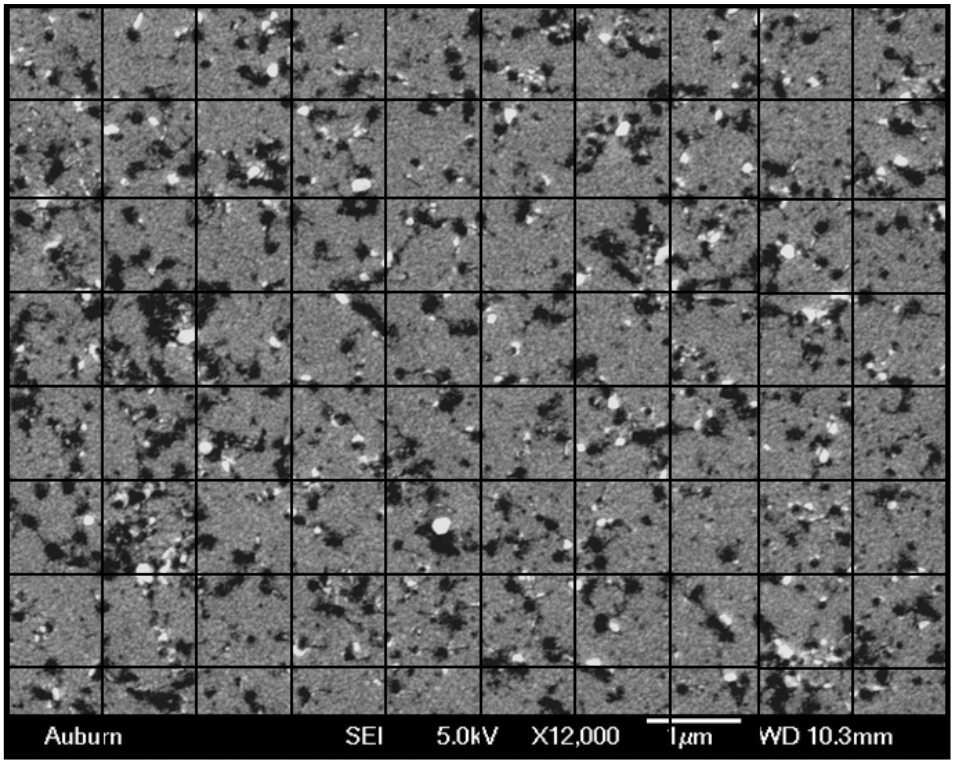

Figure 4.3 *SEM image divided into eighty parts to count phage density; conditions 10^{12} pfu/mL phage immobilized sensor at T2 (30 min) immobilization time.*

From the SEM images and the graphs, **Figures 4.1, 4.4 and 4.5**, the combinations of concentration and time that lead to the highest phage density are C4-T2 and C5-T2. From the graph, the surface density of phage on the sensor surface increased as the concentration of the phage increased with immobilization time.

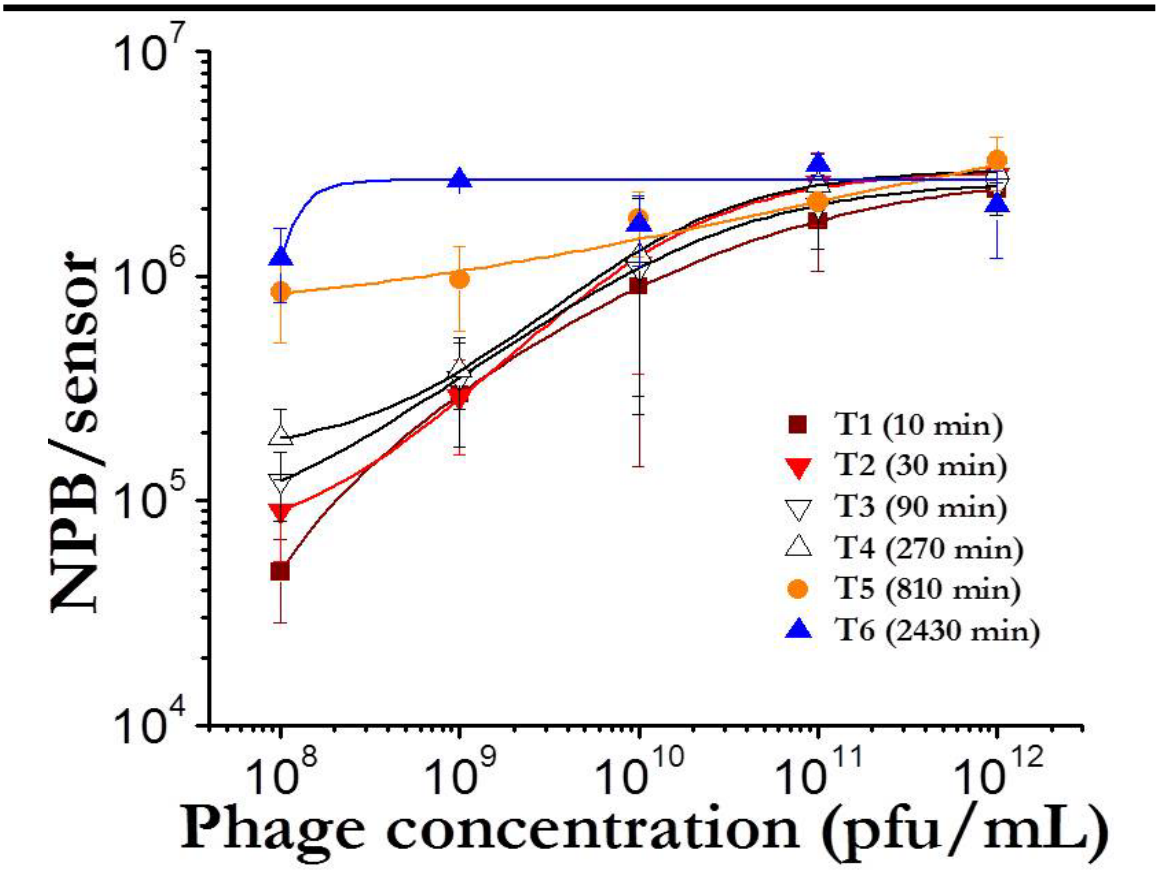

Figure 4.4 *Data of maximum surface density of phage with respect to phage concentration.*

From **figure 4.4**, it is clear that from 10^{11} pfu/mL concentration phage, NPB/ sensor is saturating with respect to immobilization times and hence in this research 10^{11} pfu/mL and 10^{12} pfu/mL concentration phage immobilized sensors were studied the most. However, at lower concentrations the maximum phage binding required higher immobilization time. Consequently, which did not serve the purpose of having a highly specific phage based biosensor for rapid detection. At time T2 (30 min) exposure, there is almost equal binding of phage between 10^{11} pfu/mL and 10^{12} pfu/mL phage concentration. Furthermore, from **figure 4.5**, we can see that there is difference in binding of phage between 10^{11} pfu/mL and 10^{12} pfu/mL phage concentration.

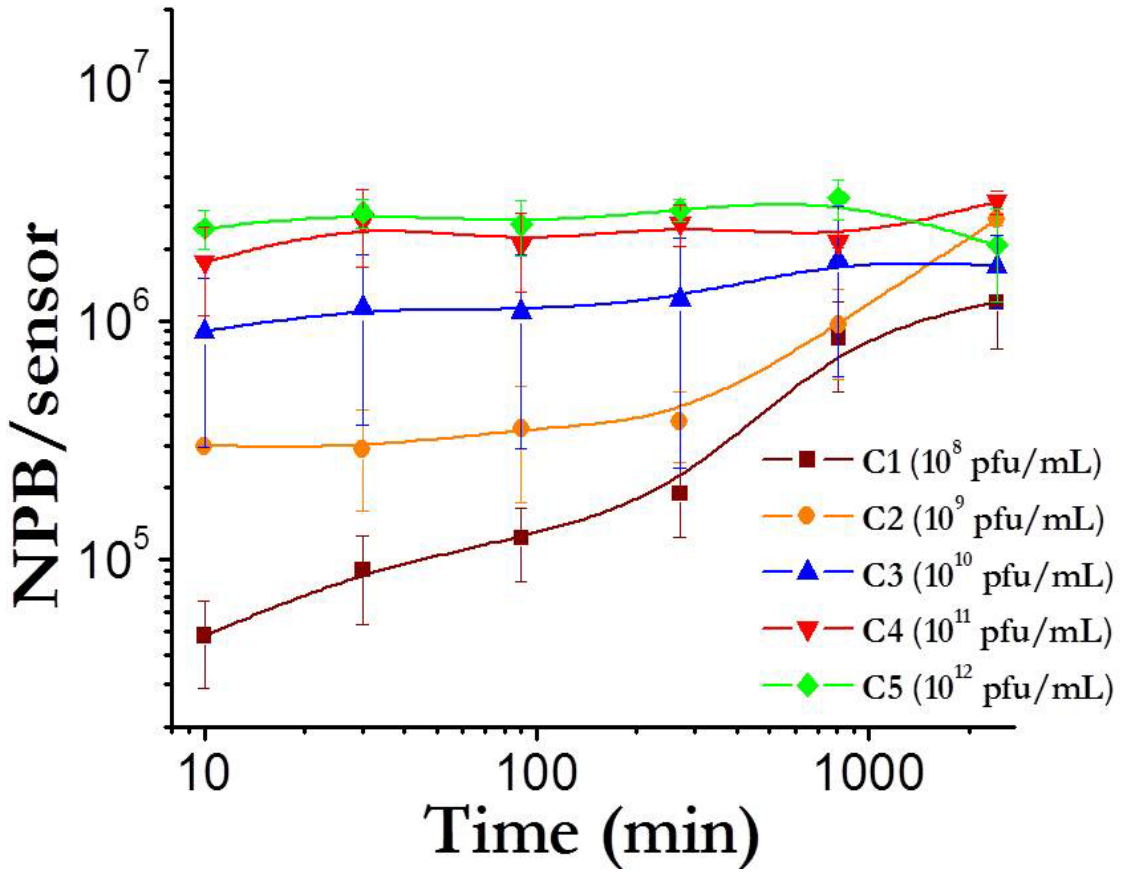

Figure 4.5 *Data of maximum surface density of phage with respect to immobilization time. For uniform distribution conditions C4-T2 and C5-T2 were studied most.*

At higher times of exposure the phage started to agglomerate resulting in phage clumps on the sensor surface. Also at T3 and T6 with C5 concentration, it is hypothesized that phage clumps may have washed away during the washing step resulting in a reduction of number of phage bindings. Since we are looking for the phage binding that is uniformly distributed on the biosensor for maximum bacteria capture, the maximum binding of phage was achieved at T2 immobilization time for concentrations C4 and C5. SEM images, **Figure 4.1**, show the phage binding of increasing concentration versus immobilization time. At C4-T2 and C5-T2, the phage binding is uniformly distributed with relatively high surface density.

4.3 Mean Free Length (MFL) Estimation

The mean free length (MFL) between successive phage binding sites was calculated by marking ten horizontal lines on the SEM images of C4 and C5 concentration phage immobilized biosensors, at T2 immobilization time. The average distance between the closest neighbor phage binding sites was calculated as shown in **Figures 4.6** and **4.7.** The MFL of C4 (≈ 0.9 μm, almost comparable to the *S. aureus* bacteria size ≈ 0.8 to 1 μm) and C5 (≈ 0.45 μm, half of the bacteria size) sensors were compared with the size of the bacteria and it was estimated that the C4 sensors could capture more bacteria than the C5 sensors.

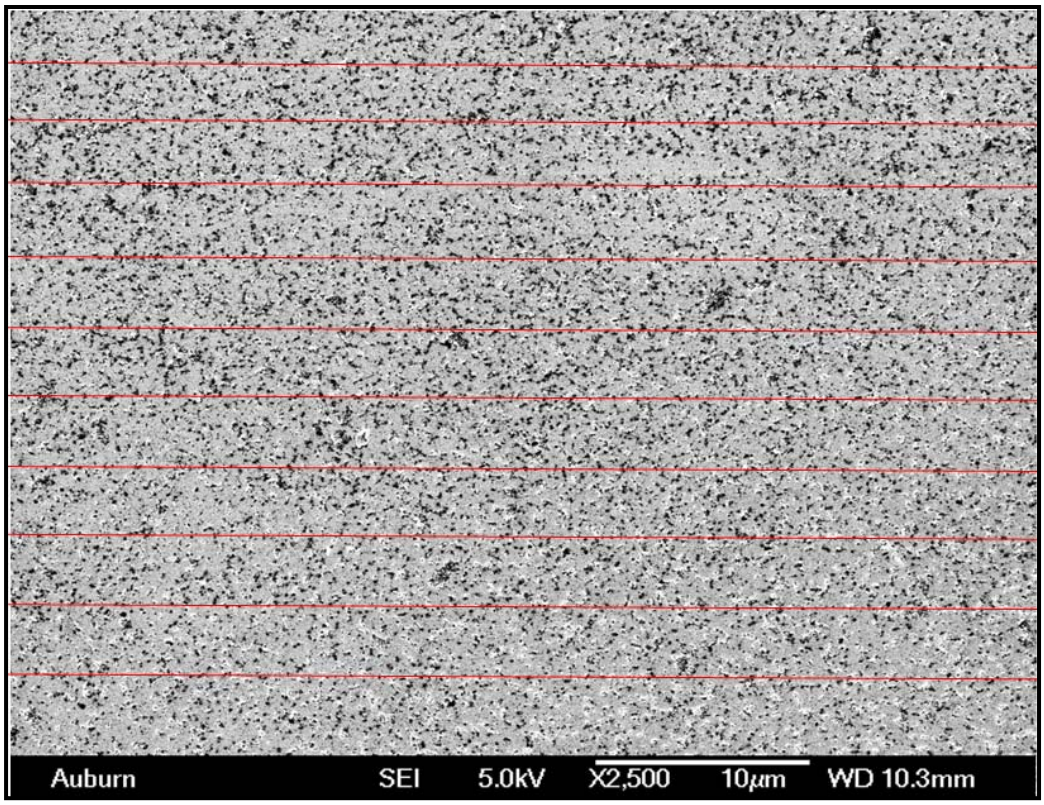

Figure 4.6 *10^{12} pfu/mL concentration phage immobilized sensor at T2 (30min) immobilization time, MFL= 0.45μm.*

Table 1 *MFL calculations: 10^{12} pfu/mL phage immobilized sensor at T2 (30min) immobilization time.*

Line No.	Total L (cm)	No. of phage	Measured Distance between phage (cm)	Scaled Distance between phage (μm)
1	26.8	97	0.276	0.493
2	26.3	105	0.250	0.447
3	26	107	0.243	0.434
4	25.9	103	0.251	0.449
5	26.7	114	0.234	0.418
6	26.2	94	0.279	0.498
7	26.3	104	0.253	0.452
8	26.4	112	0.236	0.421
9	25.8	101	0.255	0.456
10	26.5	99	0.268	0.478
			Avg =	0.455 μm

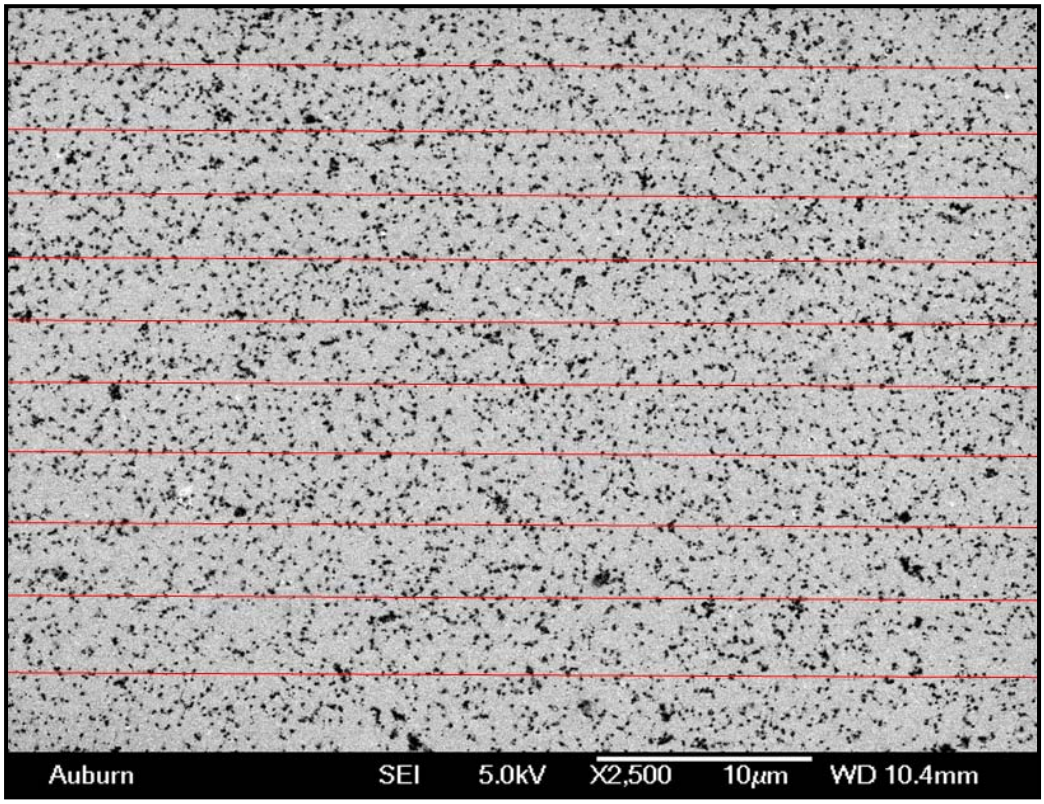

Figure 4.7 *10^{11} pfu/mL concentration phage immobilized sensor at T2 (30min) immobilization time, MFL= 0.9μm.*

Table 2 *MFL calculations: 10^{11} pfu/mL phage immobilized sensor at T2 (30min) immobilization time.*

Line No.	Total L (cm)	No. of phage	Measured Distance between phage (cm)	Scaled Distance between phage (μm)
1	26	49	0.531	0.948
2	26.7	58	0.460	0.822
3	26.5	50	0.530	0.946
4	24.7	51	0.484	0.865
5	26.8	44	0.609	1.088
6	25.9	53	0.489	0.873
7	26.3	52	0.506	0.903
8	26.1	53	0.492	0.879
9	26.9	49	0.549	0.980
10	26.3	54	0.487	0.870
			Avg =	0.917 μm

To confirm the calculated result, experiments were conducted by exposing the C4 and C5 sensors to *S. aureus* (5×10^8 cfu/mL) and the change in resonant frequency was measured, as shown in **Figure 4.8 and 4.9.** From figure 4.8 it is clear that the 10^{11} pfu/mL phage immobilized sensor had captured more bacteria and had corresponding frequency shift of ≈ 3500 Hz. Likewise from figure 4.9 it is clear that 10^{12} pfu/mL phage immobilized sensor had captured lesser bacteria and had corresponding frequency shift of ≈ 2250 Hz. Even though the biosensor was immobilized with highest concentration (10^{12} pfu/mL) of phage solution it did not help in capturing more bacteria. An understanding here required is that, consider a platform with a wavy surface and a ball is thrown on this surface; **Case 1**: if the wavy surface curvature is of comparable size with at least 35% > (an assumption) of curvature of the ball then the chances of ball sitting in the wavy platform are high. **Case 2**: if the wavy surface curvature is smaller in size compared to the curvature of the ball then the chances of ball sitting in the wavy platform are less. A similar situation has happened here while capturing bacteria. Wavy surface platform being phage immobilized sensors and *S. aureus* bacteria being the ball.

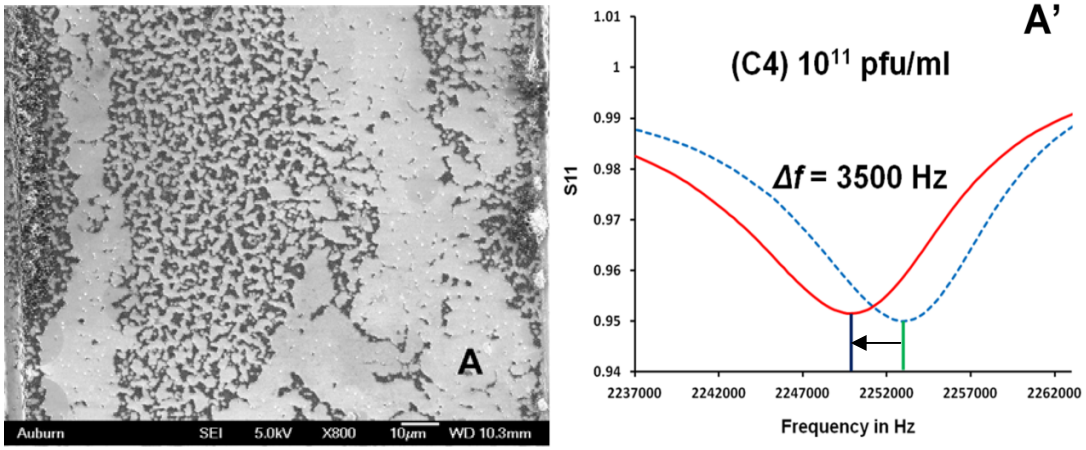

Figure 4.8 *(A) Showing the typical SEM image of 10^{11} pfu/mL (C4) phage immobilized sensor captured bacteria and (A') Showing the typical frequency shift data of 10^{11} pfu/mL phage immobilized biosensor, dashed blue curve is before bacteria capture and solid red curve is after bacteria capture.*

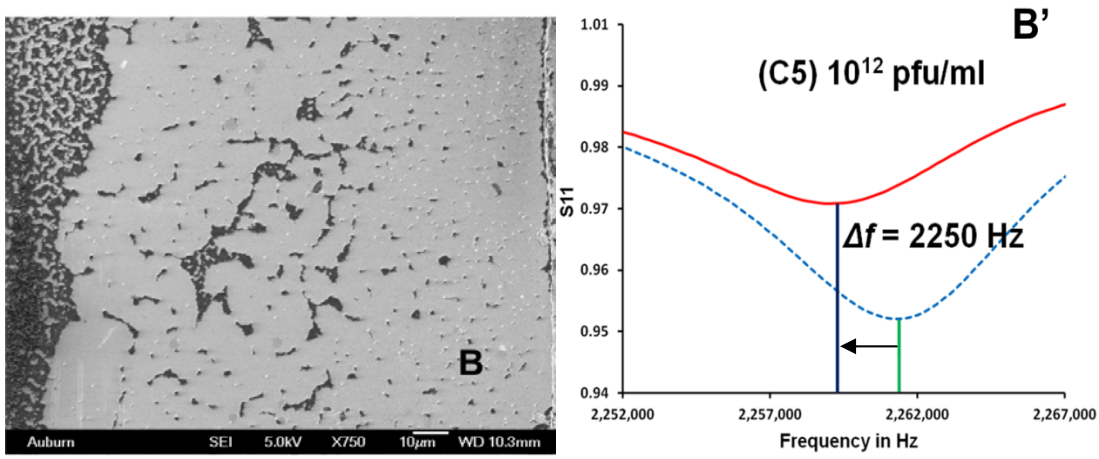

Figure 4.9 *(B) showing the typical SEM image of 10^{12} pfu/mL (C5) phage immobilized sensor captured bacteria and (B') Showing the typical frequency shift data of 10^{12} pfu/mL phage immobilized biosensor, dashed blue curve is before bacteria capture and solid red curve is after bacteria capture.*

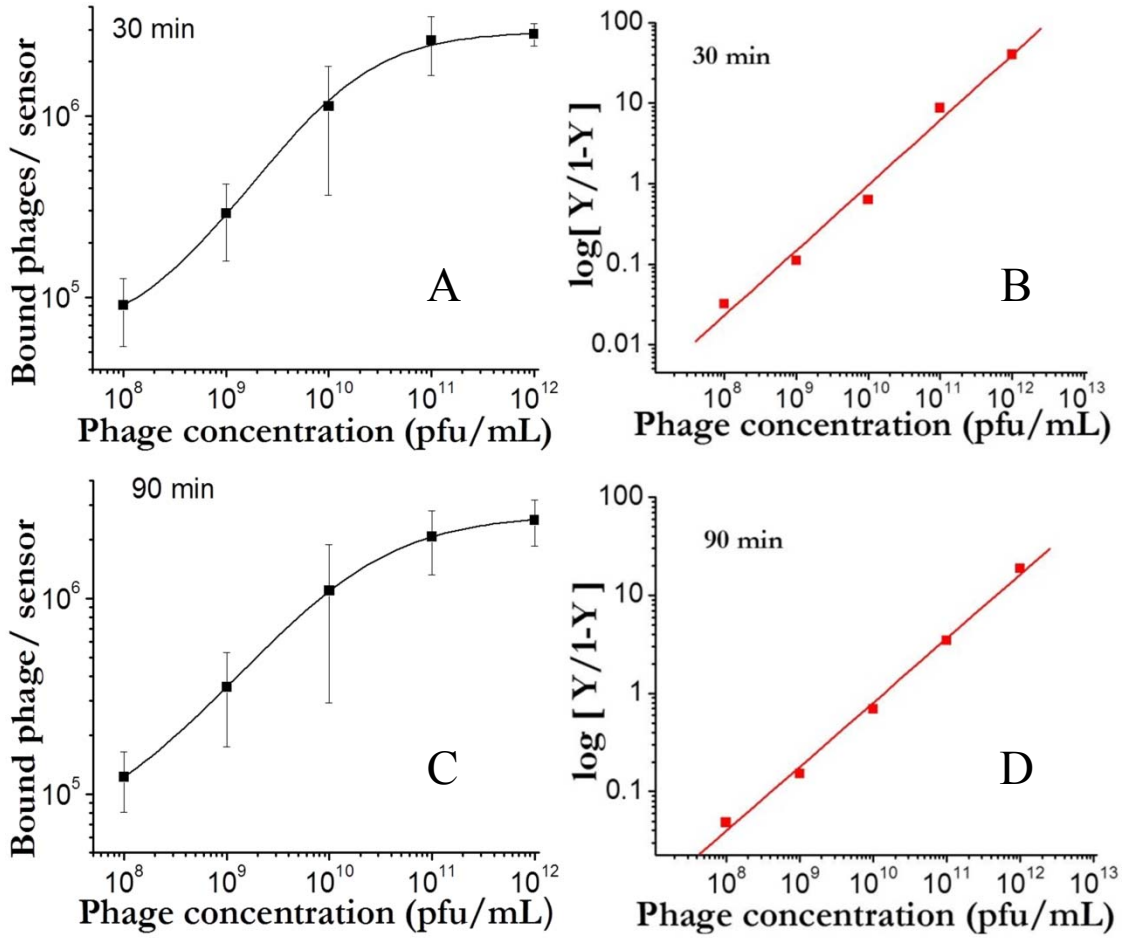

Figure 4.10 *A and C shows the phage binding on the biosensor with respect to concentration of phage for 30 min and 90 min immobilization time followed by B and D respective Hill Plots. Similarly the phage binding curves for 10, 270, 810, 2430 min were constructed and respective hill plots were derived and a plot for Hill coefficient vs time and K_D (dissociation constant) vs time was constructed as shown in* ***Figure 4.11****.*

In addition the 10^{12} pfu/mL phage concentration preparation is very hard, expensive and time consuming. Even though we could use the 10^{12} pfu/mL concentration recycling of phage solution was not possible since there would be difference in phage binding surface density on the sensor surface between the first cycle and the subsequent cycle.

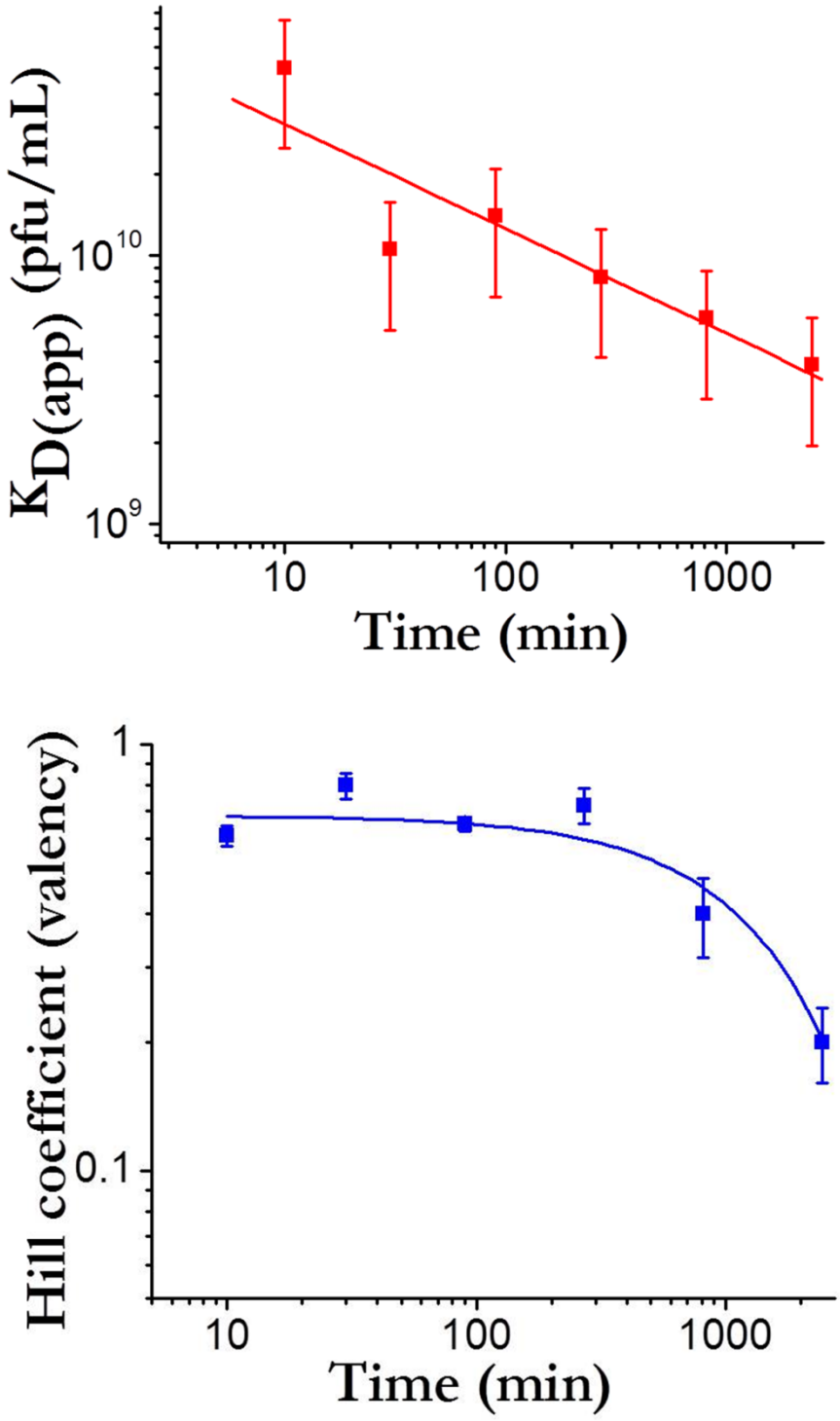

Figure 4.11 *Plot showing the Hill coefficient of phage binding on the biosensor surface, it is clear from the plot that higher Hill coefficient represents the stronger binding of phage and bacteria.*

4.4 BSA Blocking Experiments

Reduction of non-specific binding is a very important part of the development of working biosensors. A good blocking should only reduce non specific binding with minimum effect on the specific binding that is being sought.

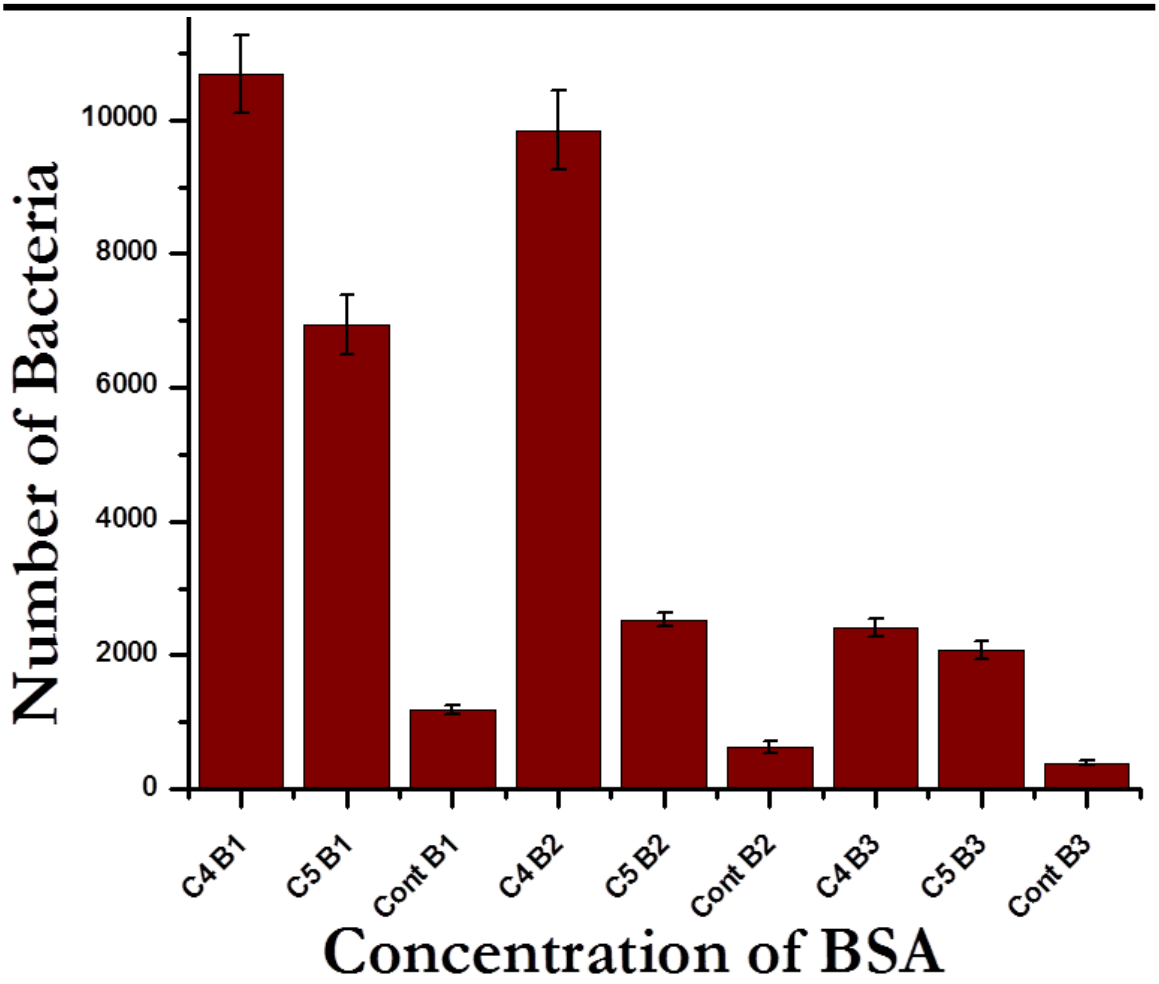

Figure 4.12 *Data of BSA blocking experiment. C4 B1 represents the 10^{11} pfu/mL phage immobilized sensors blocked with 0.1 mg/mL BSA concentration, C5 B1 represents the 10^{12} pfu/mL phage immobilized sensors blocked with 0.1 mg/mL BSA concentration, C4 B2 represents the 10^{11} pfu/mL phage immobilized sensors blocked with 1 mg/mL BSA concentration, C5 B2 represents the 10^{12} pfu/mL phage immobilized sensors blocked with 1 mg/mL BSA concentration, C4 B3 represents the 10^{11} pfu/mL phage immobilized*

sensors blocked with 10 mg/mL BSA concentration, C5 B3 represents the 10^{12} pfu/mL phage immobilized sensors blocked with 10 mg/mL BSA concentration. 'Cont' are all control sensors devoid of phage. From figure it is clear that there is considerable reduction in bacteria capture due to blocking of phage immobilized sensors with 1mg/mL BSA concentration. Furthermore it is clear that between C4 and C5 concentration phage immobilized sensors, C4 phage immobilized sensors has captured more bacteria even after BSA blocking.

Specifically, for the detection of *S. aureus* using ME biosensors, a good blocking step should provide maximum binding on measurement sensors that are coated with bacteriophage 12600 and, at the same time, minimum binding on control sensors that are devoid of bacteriophage 12600. In this research, Bovine Serum Albumin (BSA) was used for blocking and the experiments were conducted by exposing the phage optimized sensors to BSA for concentrations 0.1 mg/mL (B1), 1 mg/mL (B2), 10 mg/mL (B3). It was found that the optimum concentration for blocking was about 1mg/mL, as shown in **Figure 4.12**.

4.5 Specificity

In evaluating the performance of a sensor it is essential to establish the specificity and sensitivity of the biomolecular-recognition element to the target pathogen. As a preliminary study we compared the binding and the response of the biosensor to *S. aureus*, *E. coli, L. monocytogenes* and *S. typhimurium* individually. The phage immobilized sensors were exposed to each of the species with a concentration of 5×10^8 cfu/mL for 30 min. The total number of bacteria on the biosensor surface for different

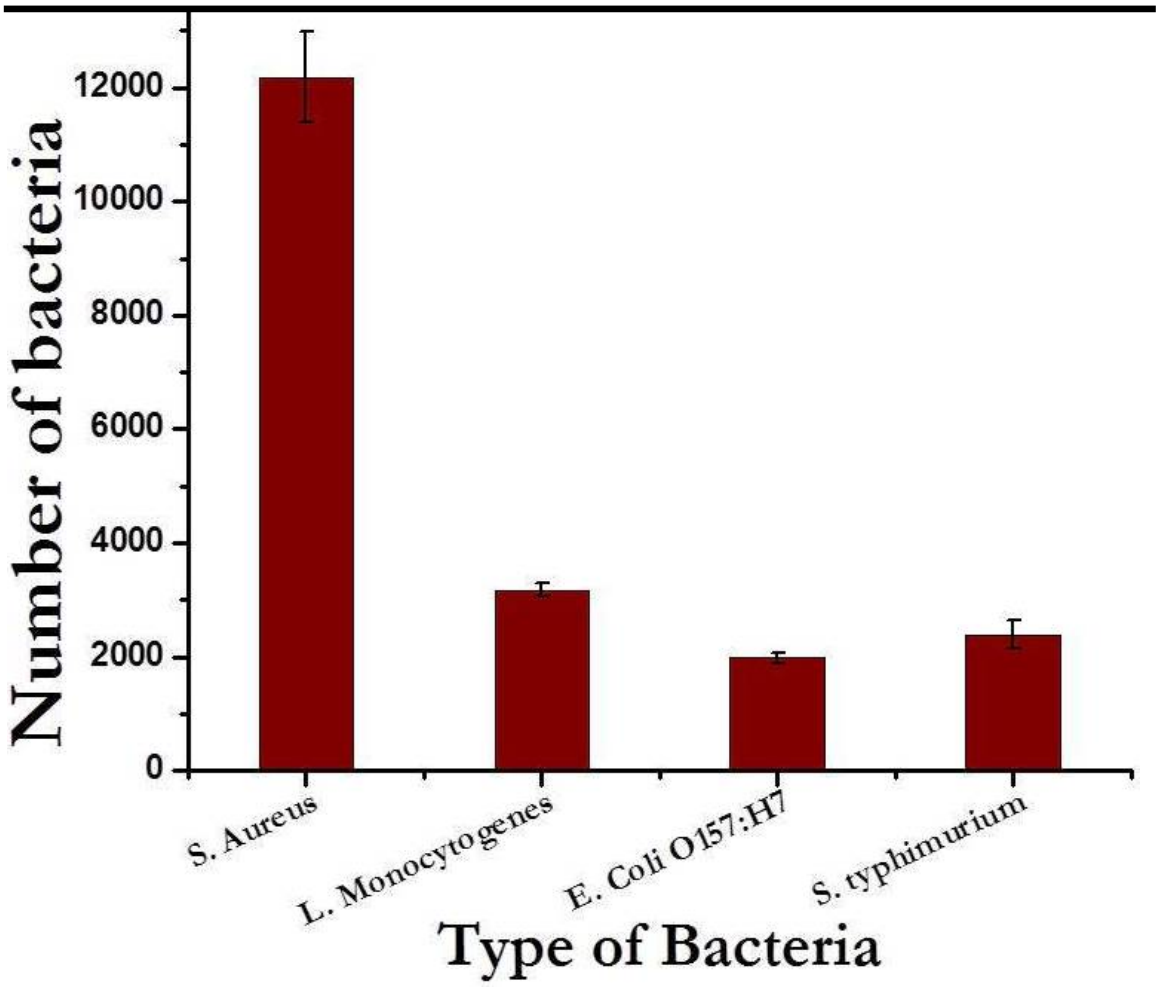

Figure 4.13 *Specificity of phage 12600 immobilized sensors exposed to various bacteria. The graph was deduced by counting the number of bacteria in the respective SEM images of biosensors exposed to various bacteria.*

bacteria with respect to the specificity of the bacteriophage 12600 are as shown in **Figure 4.13**. In a report by Guntupalli *et al*. a similar result was observed wherein they used a real-time optical detection assay. The bacteriophage 12600 showed a significantly higher binding affinity to *S. aureus* as compared to the other species. SEM of the biosensors was used to obtain a visual verification of the frequency responses obtained from the sensors

and to observe the differences in binding affinity of the immobilized phage to different species.

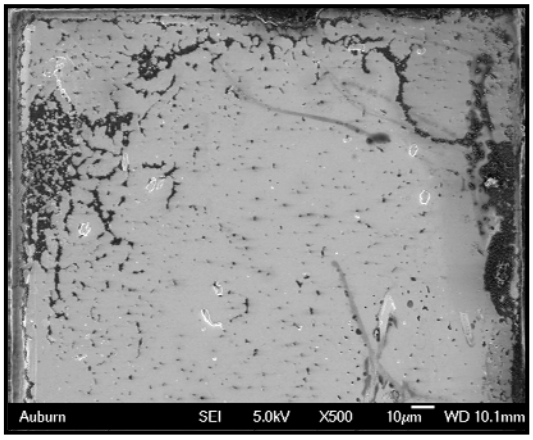

Staphylococcus aureus

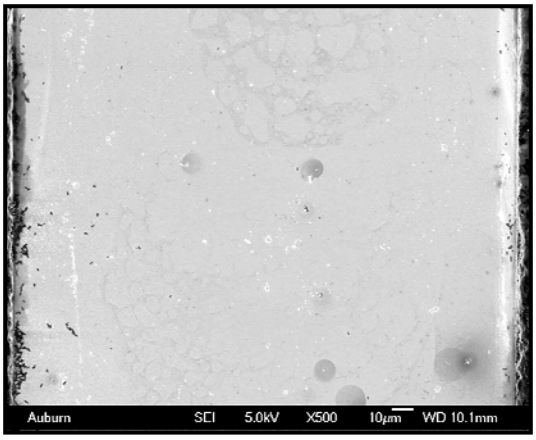

Salmonella typhimurium

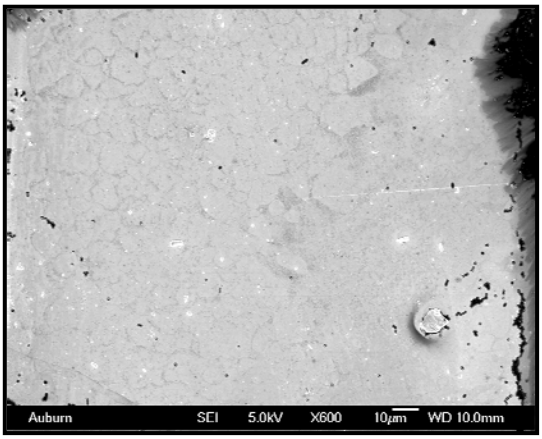

E Coli O157: H7

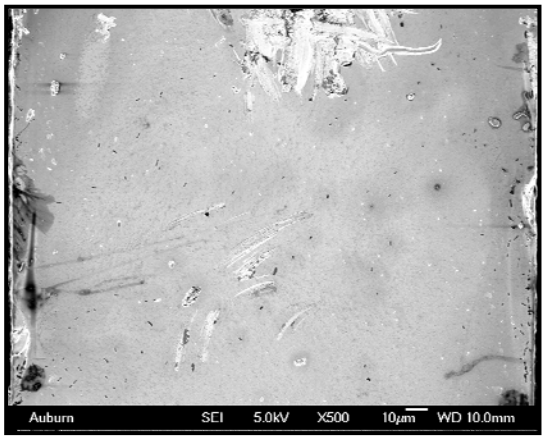

Lysteria monocytogenes

Figure 4.14 *Specificity experiment SEM images. It is clear from the SEM images that S. aureus binding is higher than other bacteria. This demonstrates that the phage12600 is highly specific to S. aureus.*

The SEM images of typical binding of bacteria to the sensors after exposure to each of the chosen species are shown in **Figure 4.14**. It is clear from the images that the *S. aureus* binding in comparison to the other bacteria is greater and is evident that phage 12600 is highly specific to *S. aureus*.

4.6 Limit of Detection

The dose response of ME biosensors to different concentrations of *S. aureus* suspensions was studied. The dose response tests were carried out using procedures

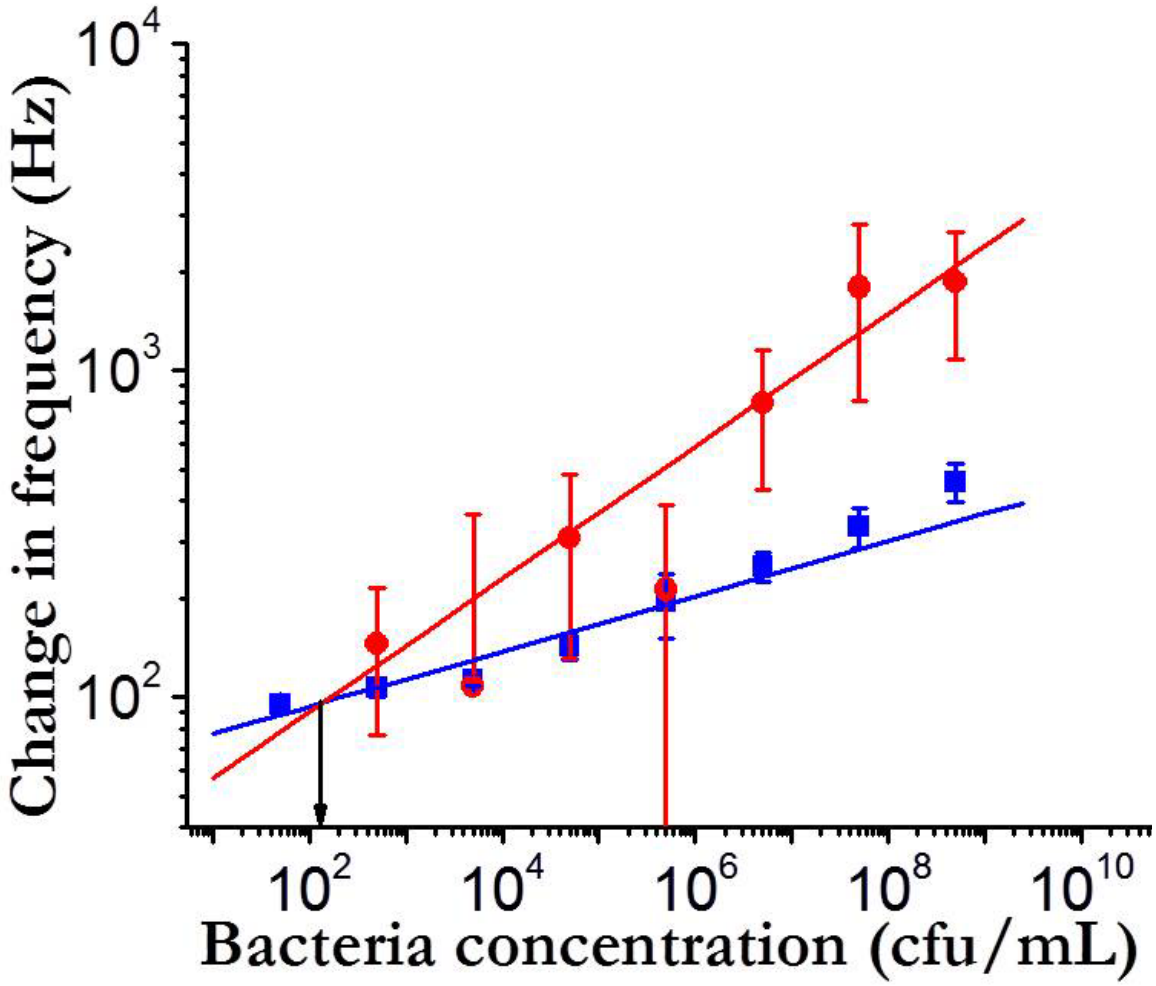

Figure 4.15 *Limit of detection data with LOD = 110 ± 30 cfu/mL and 140 Hz of frequency shift. Full circles resembing the measurement sensors($y=63.56x^{0.0843}$ $R^2= 0.95414$) and full squares control sensors($y=35.375x^{0.2035}$ $R^2= 0.96968$).*

described in section 3.9.4. **Figure 4.15** shows a typical resonant frequency response as a function of concentration for a biosensor (L = 1 mm) exposed to different concentrations of bacterial suspensions. The biosensor's resonant frequency was recorded before and

after bacteria capture. There was no change in the resonant frequency upon exposure to the lowest concentrations (5×10^1 cfu/mL) of *S. aureus*. The first measurable decrease in the resonant frequency occurred when the biosensor was exposed to a concentration of 5×10^2 cfu/mL of *S. aureus*. The resonant frequency decreased with the introduction of each successive concentration (5×10^3 cfu/mL through 5×10^8 cfu/mL) of *S. aureus*. The control sensor was devoid of any phage on the sensor surface blocked with BSA (1mg/mL) and had a negligible change in its frequency even upon exposure to very high concentrations (5×10^8 cfu/mL) of bacteria. In order to confirm the results obtained from frequency shifts, SEM imaging was carried out. The SEM images of limit of detection are as shown in **Figure 4.16**. The negligible change in resonant frequency of the control sensor was further confirmed by the nominal binding observed in the SEM image.

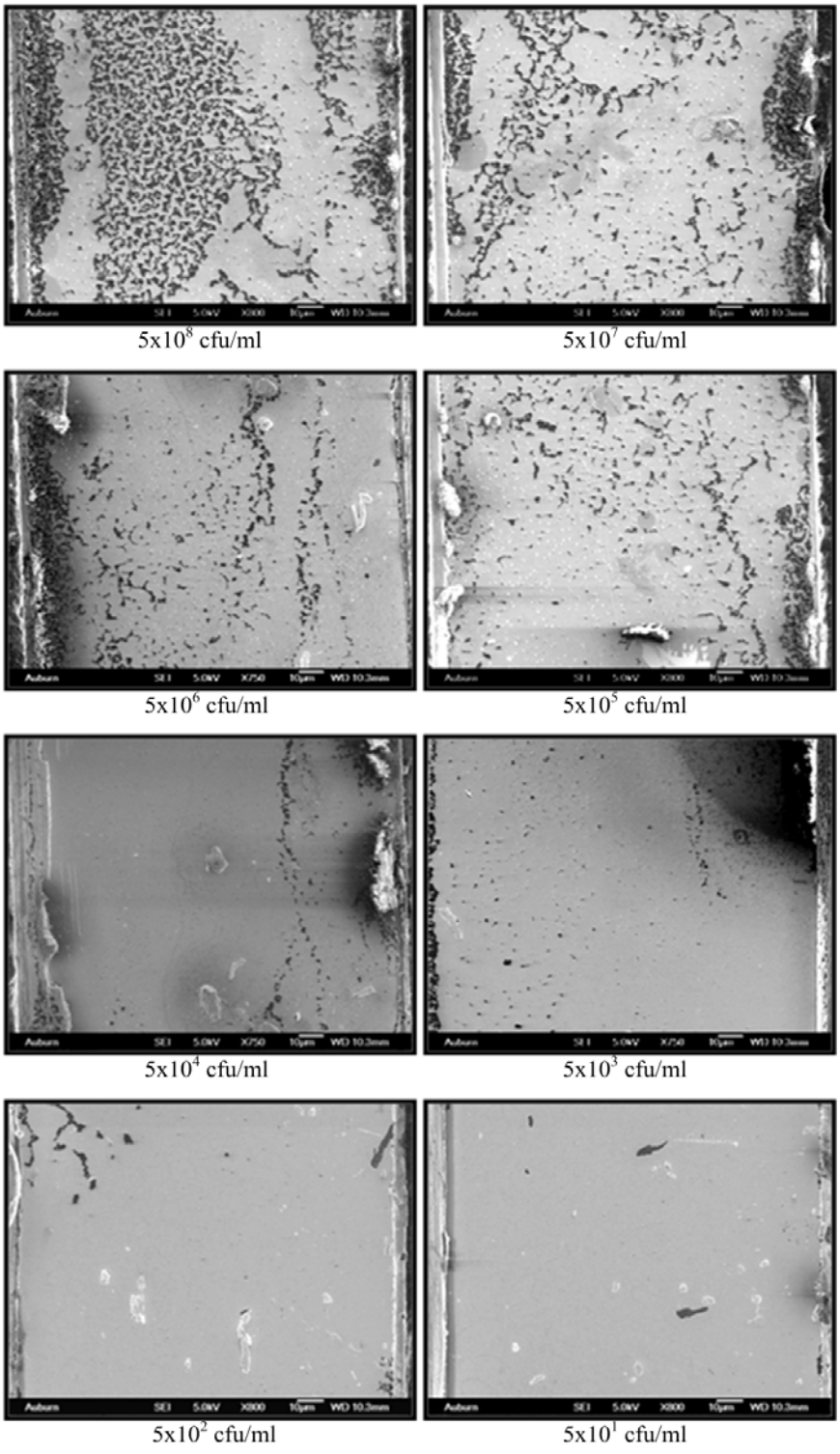

Figure 4.16 *Typical SEM images of the LOD experiments of S. aureus captured by ME biosensors. It is clear from the SEM images and LOD graph (figure 4.15) that the SEM micrographs correlate explicitly to the frequency shift data in the figure 4.15.*

Furthermore, it is also clear that at very low concentration of S. aureus bacteria the frequency shift is also very small which indicates the limit of detection deduced mathematically is a valid assessment.

4.7 Masking Bacteria Experiments

To investigate the masking effect of other bacteria on the performance of the phage immobilized sensors, the sensors were exposed to the three sets of suspensions, starting from a suspension with low concentration of *S. aureus* (5×10^1 cfu/mL) followed by successive increasing concentrations (5×10^2 cfu/mL through 5×10^8 cfu/mL). After the bacterial suspensions were prepared with three groups *S. aureus+ L. monocytogenes; S. aureus+ L. monocytogenes + E. coli; S. aureus+ L. monocytogenes+ E. coli+ S. typhimurium*, the phage immobilized sensor were exposed to the bacteria solutions. The resonant frequency difference of the sensors, before and after exposure to bacteria, was noted. Based on these frequency shifts a dose response curve was constructed and is as shown in **Figure 4.17**. It was observed that the sensor's response followed similar trends; however slightly lower frequency shifts were observed for the mixtures. Also there was no significant difference in response between the mixtures with one or two masking bacteria. The dose responses for all three mixtures were linear over the range of 5×10^3 cfu/mL to 5×10^8 cfu/mL. The sensitivity (measured as the slope of the linear range on the dose response plot) of the suspension in the absence of other masking bacteria was LOD 110 ± 30 cfu/mL with 277 Hz/decade sensitivity. In the presence of one masking bacteria (*E. coli*), two masking bacteria (*E. coli* and *L. monocytogenes*) and three masking bacteria (*E. coli*, *L. monocytogenes* and *S. typhimurium)* in the mixture the sensitivity was ~220 Hz/decade, ~ 190 Hz/decade and ~151 Hz/decade, respectively.

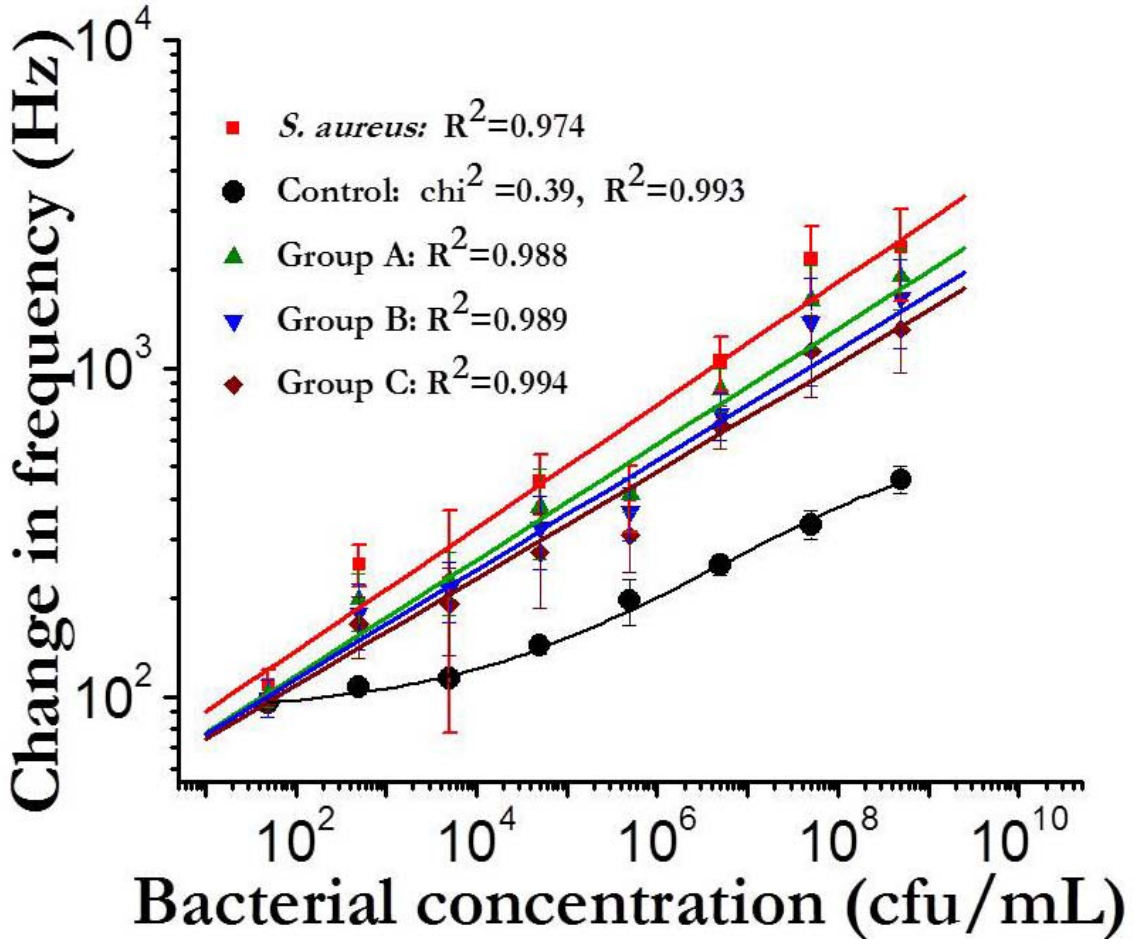

Figure 4.17 *Shows the masking bacteria experiments. (S. aureus only) is measurement sensors data with S. aureus* bacteria captures only. *(Control) is control sensors data devoid of phage on the sensors, Group A (S. aureus+ L. monocytogenes), Group B (S. aureus+ L. monocytogenes + E. coli); and Group C (S. aureus+ L. monocytogenes+ E. coli+ S. typhimurium). The data of all the three groups are not much different compared to the S. aureus data only. This indicates the stability of the sensors in the presence of high concentration of masking bacteria. The sensitivity of group A, B and C was measured to be ~220 Hz/decade, ~190 Hz/decade and ~ 151 Hz/decade, respectively. The equations of lines of S. aureus, Group A, Group B and Group C are* $y=58.21x^{0.187}$

R^2=0.974, $y=51.5x^{0.167}$ R^2=0.988, $y=51.88x^{0.167}$ R^2=0.989, and $y=50.11x^{0.163}$ R^2=0.994 respectively. Furthermore χ^2= 0.39 and R^2=0.993 for control sensors.

The control sensor was devoid of immobilized biomolecular-recognition probe. The control sensor showed a minimal response (≈ 450 Hz) even at a concentration of 5 × 10^8 cfu/mL, indicating negligible non-specific binding. The lower sensitivity for the masking bacteria experiments for the mixtures can be attributed to the presence of the other bacteria that are competing to bind on the sensor. **Figure 4.18** shows the typical SEM images of the masking bacteria experiments. It is clear from the SEM images in **Figure 4.18** that the bacteriophage 12600 is specific to the S. aureus even in the presence of high concentration of masking bacteria. The rod shaped cells are *L. monocytogenes*, slightly oval shaped are *S. typhimurium*, oval shaped and bit elongated cells are *E. coli* and spherical in nature are *S. aureus*.

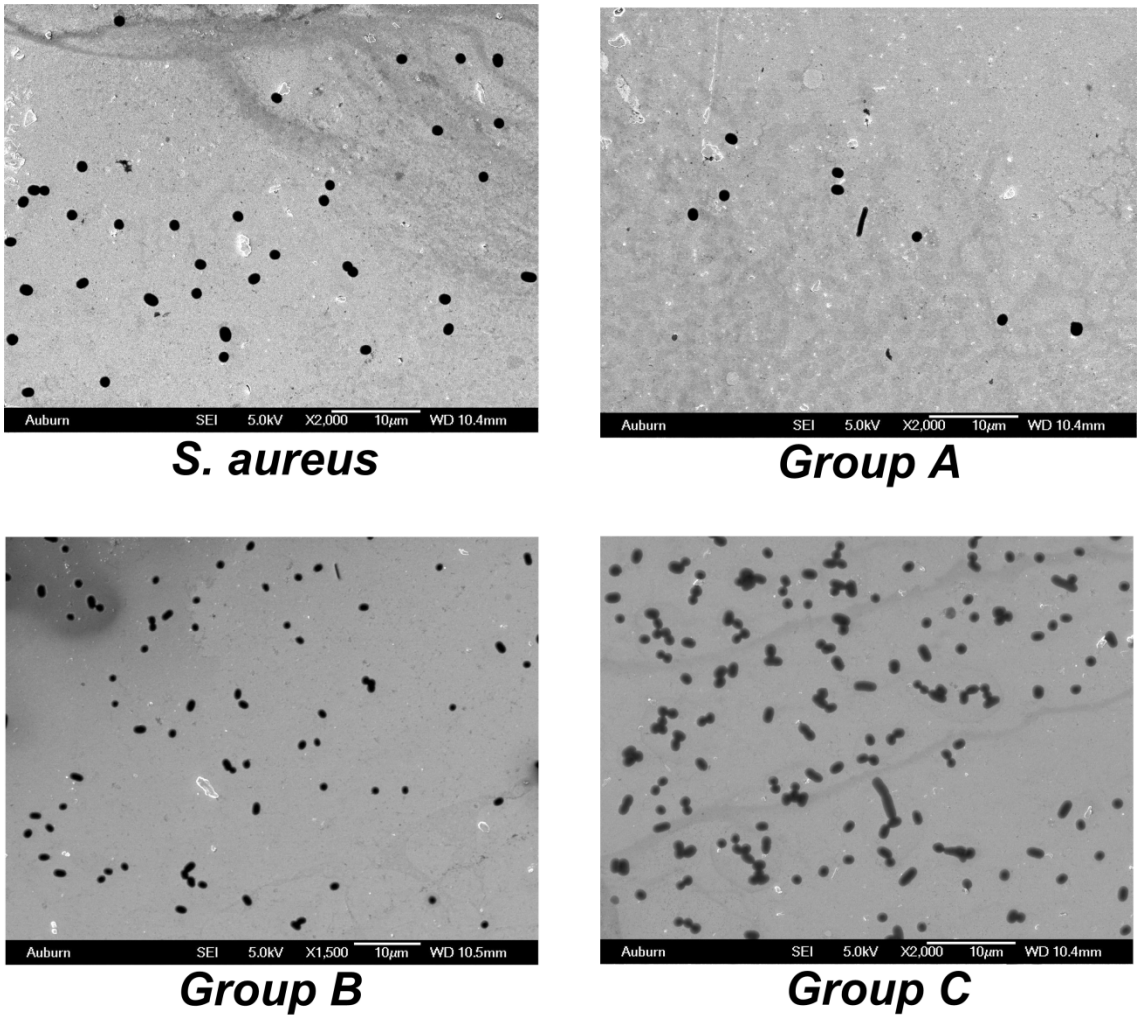

Figure 4.18 *Typical SEM images of Masking bacteria experiments. In group A, B and C it is clear that L. monocytogenes, L. monocytogenes+ E. coli, L. monocytogenes+ E. coli+ S. typhimurium respectively are bound to the sensor's surface. However, the specificity of the phage towards S. aureus is high making the sensors highly sensitive.*

CHAPTER 5

CONCLUSIONS

5.1 Phage-Characterization

A procedure for the immobilization of the highly specific lytic bacteriophage 12600 was studied. The phage was immobilized on ME resonator surfaces by physical adsorption. SEM analysis was carried out to determine the time-concentration conditions leading to maximum surface density of phage binding. In addition, MFL between successive bound phages was calculated for the biosensors that were found to have the highest uniform density of phage binding. These MFL measurements were then compared with the size of the target bacterium (0.8 – 1 μm), to estimate and correlate efficient capture of *S. aureus*. Experiments were conducted to confirm maximum *S. aureus* capture between the two, C4-T2 and C5-T2 conditions. Maximum *S. aureus* capture was achieved with 10^{11} pfu/mL concentration (C4), 30 min (T2) immobilization time, phage immobilized sensors with MFL ≈ 0.9 μm.

5.2 Specificity

Specificity experiments were conducted to determine the specificity of bacteriophage 12600 towards *S. aureus* by exposing phage immobilized biosensors to various bacteria such as *E. coli, L. monocytogenes* and *S. typhimurium* individually. It

was observed that the bacteriophage 12600 was highly specific to *S. aureus*. This confirmation was observed by SEM imaging of the biosensors.

5.3 Limit of Detection

Furthermore, the limit of detection and masking bacteria experiments were conducted in order to see the performance of the biosensor. The limit of detection was found to be 110 ± 30 cfu of bacteria which means that the biosensor performance is reasonably good. Masking bacteria experiments were also conducted to analyze biosensor performance in the real-type simulated environment (i.e. presence of other bacteria in high concentration other than the target bacteria in the medium, such as liquid). Masking bacteria experimental results demonstrated that the biosensor was able to detect the *S. aureus* even in the presence of high concentration of other bacteria and could be used in reality.

CHAPTER 6

FUTURE WORK

Characterization of highly specific biomolecular-recognition element on the sensor for different analyte detection system is necessary for increasing the efficiency of the biosensor. It would be interesting to study and characterize the ME biosensor with different biorecognition elements, such as phage, antibodies, enzymes for different analytes. It would also be interesting to understand the binding force between the phage and sensor surface, phage and the bacteria captured on the sensor surface. By finding the binding force the reliability factor of the sensor can be improved by improving the binding nature of the phage to the sensor surface.

REFERENCES

Alarie JP V-DT. 1996. Polycyclic Aromat Compd 8 45–52.

Anzai J, Kobayashi Y, Hoshi T, Saiki H. 1999. A layer-by-layer deposition of Concanavalin A and native glucose oxidase to form multilayer thin films for biosensor applications. Chemistry Letters(4):365.

Arbuthnott JP, Coleman, D.C., Deazavedo, J.S. 1990. . Staphylococcal toxins in human-disease. J. Appl. Bacteriol 69:S101–S107.

Balasubramanian S, Sorokulova IB, Vodyanoy VJ, Simonian AL. 2007. Lytic phage as a specific and selective probe for detection of< i> Staphylococcus aureus</i>—A surface plasmon resonance spectroscopic study. Biosensors and Bioelectronics 22(6):948-955.

Bardea A, Patolsky F, Dagan A, Willner I. 1999. Sensing and amplification of oligonucleotide-DNA interactions by means of impedance spectroscopy: a route to a Tay–Sachs sensor. Chem. Commun.(1):21-22.

Barie PS. 1998. Antibiotic-resistant gram-positive cocci: implications for surgical practice. World journal of surgery 22(2):118-126.

Barker SLR, Kopelman R, Meyer TE, Cusanovich MA. 1998. Fiber-optic nitric oxide-selective biosensors and nanosensors. Analytical chemistry 70(5):971-976.

Barker SLR, Zhao Y, Marletta MA, Kopelman R. 1999. Cellular applications of a sensitive and selective fiber-optic nitric oxide biosensor based on a dye-labeled

heme domain of soluble guanylate cyclase. Analytical chemistry 71(11):2071-2075.

Blake RC, Pavlov AR, Blake DA. 1999. Automated kinetic exclusion assays to quantify protein binding interactions in homogeneous solution. Analytical biochemistry 272(2):123-134.

Boncheva M, Duschl C, Beck W, Jung G, Vogel H. 1996. Formation and characterization of lipopeptide layers at interfaces for the molecular recognition of antibodies. Langmuir 12(23):5636-5642.

Broughan J, Anderson R, Anderson AS. 2011. Strategies for and advances in the development of Staphylococcus aureus prophylactic vaccines. Expert review of vaccines 10(5):695-708.

Byun DE, Kim, S.H, Shin, J.H, Suh, S.P, and Ryang, D.W. 1997. Molecular epidemiologic analysis of Staphylococcus aureus isolated from clinical specimens. Journal of Korean Medical Science 12:190-198.

Campbell CN, de Lumley-Woodyear T, Heller A. 1999a. Towards immunoassay in whole blood: separationless sandwich-type electrochemical immunoassay based on in-situ generation of the substrate of the labeling enzyme. Fresenius' journal of analytical chemistry 364(1):165-169.

Campbell T, Hodgson A, Wallace G. 1999b. Incorporation of erythrocytes into polypyrrole to form the basis of a biosensor to screen for Rhesus (D) blood groups and rhesus (D) antibodies. Electroanalysis 11(4):215-222.

CDC. 2011. http://www.cdc.gov/Features/dsFoodborneEstimates/.

CDC. 2012a. http://www.cdc.gov/listeria/index.html.

CDC. 2012b. http://www.cdc.gov/ncidod/dbmd/diseaseinfo/staphylococcus_food_g.htm.

CDC. 2012c. http://www.cdc.gov/salmonella/index.html.

Chakraborty SP, KarMahapatra S, Bal M, Roy S. 2011. Isolation and identification of Vancomycin Resistant Staphylococcus aureus from post operative pus sample. Al Ameen Journal of Medical Sciences 4(2):152-168.

Charych D, Cheng Q, Reichert A, Kuziemko G, Stroh M, Nagy JO, Spevak W, Stevens RC. 1996. A 'litmus test'for molecular recognition using artificial membranes. Chemistry & Biology 3(2):113-120.

Cornell BA, Braach-Maksvytis V, King L, Osman P, Raguse B, Wieczorek L, Pace R. 1997. A biosensor that uses ion-channel switches. Nature 387(6633):580.

Cosnier S, Senillou A, Grätzel M, Comte P, Vlachopoulos N, Jaffrezic Renault N, Martelet C. 1999. A glucose biosensor based on enzyme entrapment within polypyrrole films electrodeposited on mesoporous titanium dioxide. Journal of Electroanalytical Chemistry 469(2):176-181.

Costello R, Peterson I, Heptinstall J, Byrne N, Miller L. 1998. A robust gel–bilayer channel biosensor. Advanced Materials for Optics and Electronics 8(2):47-52.

Costello R, Peterson I, Heptinstall J, Walton D. 1999. Improved gel-protected bilayers. Biosensors and Bioelectronics 14(3):265-271.

Cotton GJ, Ayers B, Xu R, Muir TW. 1999. Insertion of a synthetic peptide into a recombinant protein framework: a protein biosensor. Journal of the American Chemical Society 121(5):1100-1101.

Cullum BM, Griffin GD, Miller GH, Vo-Dinh T. 2000. Intracellular measurements in mammary carcinoma cells using fiber-optic nanosensors. Analytical Biochemistry 277(1):25-32.

D D. 1998. Chemical and Biological Sensors. In: D D, editor. New York Wiley.

Duan LS, Lei HB, Huang E, Yi GM, Fan W. 2011. Drug resistance of staphylococcus aureus from lower respiratory tract. Zhonghua Yiyuanganranxue Zazhi 21(8):1667-1668.

Durgaryan AA, Dmitrenko, O.A., Metevosyan, M.M., and Galoyan, A.A. 2010. Infections induced by methicillin-resistant staphylococcus aureus. Zekuytsner - Hayastani Gitut'yunneri Azgayin Akademia 110:384-389.

Erdem A, Kerman K, Meric B, Akarca US, Ozsoz M. 1999. DNA electrochemical biosensor for the detection of short DNA sequences related to the hepatitis B virus. Electroanalysis 11(8):586-587.

Franchina JG, Lackowski WM, Dermody DL, Crooks RM, Bergbreiter DE, Sirkar K, Russell RJ, Pishko MV. 1999. Electrostatic immobilization of glucose oxidase in a weak acid, polyelectrolyte hyperbranched ultrathin film on gold: fabrication, characterization, and enzymatic activity. Analytical chemistry 71(15):3133-3139.

Garjonyte R, Malinauskas A. 1999. Amperometric glucose biosensor based on glucose oxidase immobilized in poly (< i> o</i>-phenylenediamine) layer. Sensors and Actuators B: Chemical 56(1):85-92.

Giamarellou H, Papapetropoulou M, Daikos GK. 1981. ‘Methicillin resistant’Staphylococcus aureus infections during 1978–79: clinical and bacteriologic observations. Journal of Antimicrobial Chemotherapy 7(6):649-655.

Girard-Egrot A, Morélis R, Coulet P. 1998. Direct bioelectrochemical monitoring of choline oxidase kinetic behaviour in Langmuir–Blodgett nanostructures. Bioelectrochemistry and bioenergetics 46(1):39-44.

Gooding JJ HD. 1999. Trac-Trend Anal Chem 18:525–533.

Gooding JJ, Situmorang M, Erokhin P, Hibbert DB. 1999. An assay for the determination of the amount of glucose oxidase immobilised in an enzyme electrode. Analytical Communications 36(6):225-228.

Göpel W, Heiduschka P. 1995. Interface analysis in biosensor design. Biosensors and bioelectronics 10(9):853-883.

Grate JW, S.J. Martin, and R.M. White. 1993. Acoustic-Wave Microsensors .1. Anal. Chem 65(21):p. A940.

Griffin GD, D.N. Stratis-Cullum, and S. Moselio. 2009. Biosensors, in Encyclopedia of Microbiology. Oxford: Academic Press. p p. 88-103.

Guntupalli R, Sorokulova I, Krumnow A, Pustovyy O, Olsen E, Vodyanoy V. 2008. Real-time optical detection of methicillin-resistant< i> Staphylococcus aureus</i> using lytic phage probes. Biosensors and Bioelectronics 24(1):151-154.

Hall EAH, Gooding JJ, Hall CE, Martens N. 1999. Acrylate polymer immobilisation of enzymes. Fresenius' journal of analytical chemistry 364(1):58-65.

Hara-Kuge S, Ohkura T, Seko A, Yamashita K. 1999. Vesicular-integral membrane protein, VIP36, recognizes high-mannose type glycans containing α1→ 2 mannosyl residues in MDCK cells. Glycobiology 9(8):833-839.

Heim S, Schnieder I, Binz D, Vogel A, Bilitewski U. 1999. Development of an automated microbial sensor system. Biosensors and Bioelectronics 14(2):187-193.

Houshmand H, Fröman G, Magnusson G. 1999. Use of bacteriophage T7 displayed peptides for determination of monoclonal antibody specificity and biosensor analysis of the binding reaction. Analytical biochemistry 268(2):363-370.

Hu T, Zhang XE, Zhang ZP. 1999. Disposable screen-printed enzyme sensor for simultaneous determination of starch and glucose. Biotechnology techniques 13(6):359-362.

Huang T, Warsinke A, Koroljova-Skorobogatko OV, Makower A, Kuwana T, Scheller FW. 1999. A Bienzyme Carbon Paste Electrode for the Sensitive Detection of NADPH and the Measurement of Glucose-6-phosphate Dehydrogenase. Electroanalysis 11(5):295-300.

Isola NR, Stokes DL, Vo-Dinh T. 1998. Surface-enhanced Raman gene probe for HIV detection. Analytical chemistry 70(7):1352-1356.

James E, Schmeltzer K, Ligler F. 1996. Detection of endotoxin using an evanescent wave fiber-optic biosensor. Applied biochemistry and biotechnology 60(3):189-202.

Jarraud S, Peyrat MA, Lim A, Tristan A, Bes M, Mougel C, Etienne J, Vandenesch F, Bonneville M, Lina G. 2001. egc, a highly prevalent operon of enterotoxin gene, forms a putative nursery of superantigens in Staphylococcus aureus. The Journal of Immunology 166(1):669-677.

Kim H, Hyun M, Chang I, Kim BH. 1999. A microbial fuel cell type lactate biosensor using a metal-reducing bacterium, Shewanella putrefaciens. J. Microbiol. Biotechnol 9(3):365-367.

Knopf HJ. 1997. Nosocomial infections caused by multiresistant pathogens. Clinical management exemplified by multiresistant Staphylococcus aureus. Der Urologe. Ausg. A 36:248-254.

Kriz D, Kempe M, Mosbach K. 1996. Introduction of molecularly imprinted polymers as recognition elements in conductometric chemical sensors. Sensors and Actuators B: Chemical 33(1):178-181.

Kriz D, Mosbach K. 1995. Competitive amperometric morphine sensor based on an agarose immobilised molecularly imprinted polymer. Analytica chimica acta 300(1):71-75.

Kröger D, Liley M, Schiweck W, Skerra A, Vogel H. 1999. Immobilization of histidine-tagged proteins on gold surfaces using chelator thioalkanes. Biosensors and Bioelectronics 14(2):155-161.

Landau L, Lifshitz E. 1975. Elasticity theory.

Lazcka O, F.J.D. Campo, and F.X. Muñoz,. 2007. Pathogen detection: A perspective of traditional methods and biosensors. Biosensors and Bioelectronics 22(7):p. 1205-1217.

Lebrón JA, Bjorkman PJ. 1999. The transferrin receptor binding site on HFE, the class I MHC-related protein mutated in hereditary hemochromatosis. Journal of molecular biology 289(4):1109.

Lee YC, Huh MH. 2007. Development of a biosensor with immobilized L-aminoacid oxidase for determination of L-aminoacids. Journal of food biochemistry 23(2):173-185.

Li P, Wen Y, Liu P, Li X, Jia C. 2010. A magnetoelectric energy harvester and management circuit for wireless sensor network. Sensors and actuators A: Physical 157(1):100-106.

Liang C, Morshed S, Prorok BC. 2007. Correction for longitudinal mode vibration in thin slender beams. Applied physics letters 90(22):221912-221912-3.

Lina G, Gillet Y, Vandenesch F, Jones ME, Floret D, Etienne J. 1997. Toxin involvement in staphylococcal scalded skin syndrome. Clinical infectious diseases 25(6):1369-1373.

Marrazza G, Chianella I, Mascini M. 1999. Disposable DNA electrochemical sensor for hybridization detection. Biosensors and Bioelectronics 14(1):43-51.

Mayes AG, Blyth J, Kyröläinen-Reay M, Millington RB, Lowe CR. 1999. A holographic alcohol sensor. Analytical Chemistry 71(16):3390-3396.

Mello LD, Kubota LT. 2002. Review of the use of biosensors as analytical tools in the food and drink industries. Food chemistry 77(2):237-256.

Nelson RW, Jarvik JW, Taillon BE, Tubbs KA. 1999. BIA/MS of epitope-tagged peptides directly from E. coli lysate: multiplex detection and protein identification at low-femtomole to subfemtomole levels. Analytical chemistry 71(14):2858-2865.

Niemeyer CM, Boldt L, Ceyhan B, Blohm D. 1999. DNA-directed immobilization: efficient, reversible, and site-selective surface binding of proteins by means of covalent DNA–streptavidin conjugates. Analytical biochemistry 268(1):54-63.

Pancrazio JJ, Bey Jr PP, Cuttino DS, Kusel JK, Borkholder DA, Shaffer KM, Kovacs GTA, Stenger DA. 1998. Portable cell-based biosensor system for toxin detection. Sensors and Actuators B: Chemical 53(3):179-185.

Patolsky F, Zayats M, Katz E, Willner I. 1999. Precipitation of an insoluble product on enzyme monolayer electrodes for biosensor applications: characterization by faradaic impedance spectroscopy, cyclic voltammetry, and microgravimetric quartz crystal microbalance analyses. Analytical chemistry 71(15):3171-3180.

Pemberton R, Hart J, Stoddard P, Foulkes J. 1999. A comparison of 1-naphthyl phosphate and 4 aminophenyl phosphate as enzyme substrates for use with a screen-printed amperometric immunosensor for progesterone in cows' milk. Biosensors and Bioelectronics 14(5):495-503.

Piehler J, Brecht A, Gauglitz G, Zerlin M, Maul C, Thiericke R, Grabley S. 1997. Label-free monitoring of DNA–Ligand interactions. Analytical biochemistry 249(1):94-102.

Piehler J, Brecht A, Hehl K, Gauglitz G. 1999. Protein interactions in covalently attached dextran layers. Colloids and Surfaces B: Biointerfaces 13(6):325-336.

Piervincenzi RT, Reichert WM, Hellinga HW. 1998. Genetic engineering of a single-chain antibody fragment for surface immobilization in an optical biosensor. Biosensors and Bioelectronics 13(3):305-312.

Polster J, Prestel G, Wollenweber M, Kraus G, Gauglitz G. 1995. Simultaneous determination of penicillin and ampicillin by spectral fibre-optical enzyme optodes and multivariate data analysis based on transient signals obtained by flow injection analysis. Talanta 42(12):2065-2072.

Ramasamy M. 2010. Resonance Behavior of Magnetostrictive Sensor in Longitudinal Vibration mode for Biological Agent Detection: Auburn University.

Ramsden J. 1998. Biomimetic protein immobilization using lipid bilayers. Biosensors and Bioelectronics 13(6):593-598.

Ramström O, Ansell RJ. 1998. Molecular imprinting technology: challenges and prospects for the future. Chirality 10(3):195-209.

Roos H, Karlsson R, Nilshans H, Persson A. 1999. Thermodynamic analysis of protein interactions with biosensor technology. Journal of Molecular Recognition 11(1-6):204-210.

Rosenzweig Z, Kopelman R. 1996. Analytical properties and sensor size effects of a micrometer-sized optical fiber glucose biosensor. Analytical chemistry 68(8):1408-1413.

Sawata S, Kai E, Ikebukuro K, Iida T, Honda T, Karube I. 1999. Application of peptide nucleic acid to the direct detection of deoxyribonucleic acid amplified by polymerase chain reaction. Biosensors and Bioelectronics 14(4):397-404.

Sergeyeva T, Soldatkin A, Rachkov A, Tereschenko M, Piletsky S, Elskaya A. 1999. β-Lactamase label-based potentiometric biosensor for α-2 interferon detection. Analytica chimica acta 390(1):73-81.

Serra B, Reviejo A, Parrado C, Pingarron J. 1999. Graphite-Teflon composite bienzyme electrodes for the determination of L-lactate: Application to food samples. Biosensors and Bioelectronics 14(5):505-513.

Shih YT, Huang HJ. 1999. A creatinine deiminase modified polyaniline electrode for creatinine analysis. Analytica chimica acta 392(2):143-150.

Shittu AO, Okon K, Adesida S, Oyedara O, Witte W, Strommenger B, Layer F, Nübel U. 2011. Antibiotic resistance and molecular epidemiology of Staphylococcus aureus in Nigeria. BMC microbiology 11(1):92.

Situmorang M, Gooding JJ, Hibbert DB. 1999. Immobilisation of enzyme throughout a polytyramine matrix: a versatile procedure for fabricating biosensors. Analytica chimica acta 394(2):211-223.

Skuridin SG, Yevdokimov YM, Efimov VS, Hall JM, Turner APF. 1996. A new approach for creating double-stranded DNA biosensors. Biosensors and Bioelectronics 11(9):903-911.

Song X, Swanson BI. 1999. Direct, ultrasensitive, and selective optical detection of protein toxins using multivalent interactions. Analytical chemistry 71(11):2097-2107.

SS H, J L, D C. 1999. Anal Sci 15:585–588

T V-D, CD G, MJ S, Wolfbeis OS. 1991. Fiber optic chemical sensors and biosensors: CRC press Boca Raton, FL.

Vo-Dinh T CB, Alarie JP, Griffin GD. J Nanoparticle Res.

Vo-Dinh T GG, Ambrose KR. 1986. Appl Spectrosc 40:696–670.

Vo-Dinh T, Houck K, Stokes D. 1994. Surface-enhanced Raman gene probes. Analytical chemistry 66(20):3379-3383.

Vo-Dinh T, Isola N, Alarie J, Landis D, Griffin G, Allison S. 1998. Development of a multiarray biosensor for DNA diagnostics. Instrumentation science & technology 26(5):503-514.

Vo-Dinh T, Tromberg B, Griffin G, Ambrose K, Sepaniak M, Gardenhire E. 1987. Antibody-based fiberoptics biosensor for the carcinogen benzo (a) pyrene. Applied spectroscopy 41(5):735-738.

Wang J, Rivas G, Fernandes JR, Jiang M, Paz JLL, Waymire R, Nielsen TW, Getts RC. 1998. Adsorption and detection of DNA dendrimers at carbon electrodes. Electroanalysis 10(8):553-556.

Wollenberger U, Neumann B, Scheller F. 1998. Development of a biomimetic alkane sensor. Electrochimica acta 43(23):3581-3585.

Yano K, Karube I. 1999. Molecularly imprinted polymers for biosensor applications. TrAC Trends in Analytical Chemistry 18(3):199-204.

YS W, GR L, CY L, ZY W, CX L. 1999. Prog Biochem Biophys 26:144–146.

Zhang W, Canziani G, Plugariu C, Wyatt R, Sodroski J, Sweet R, Kwong P, Hendrickson W, Chaiken I. 1999. Conformational changes of gp120 in epitopes near the CCR5 binding site are induced by CD4 and a CD4 miniprotein mimetic. Biochemistry 38(29):9405-9416.

Zhang YQ, Zhu J, Gu RA. 1998. Improved biosensor for glucose based on glucose oxidase-immobilized silk fibroin membrane. Applied biochemistry and biotechnology 75(2):215-233.

Zhao YB, Wen ML, Liu SQ, Liu ZH, Zhang WD, Yao Y, Wang CY. 1998. Microbial sensor for determination of tannic acid. Microchemical journal 60(3):201-209.

Appendix

A. Typical SEM images of phage distribution on the sensor surface

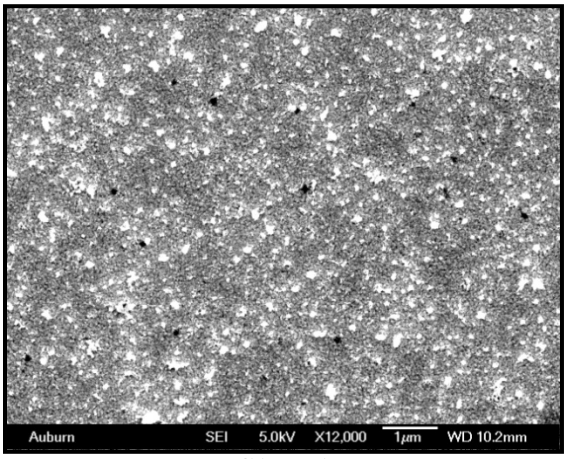

C1 – T1

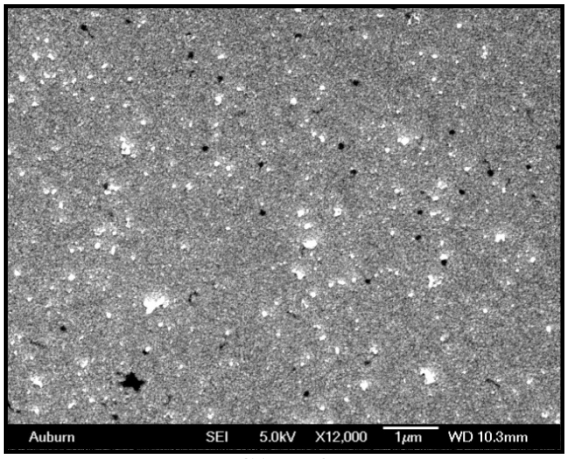

C1 – T2

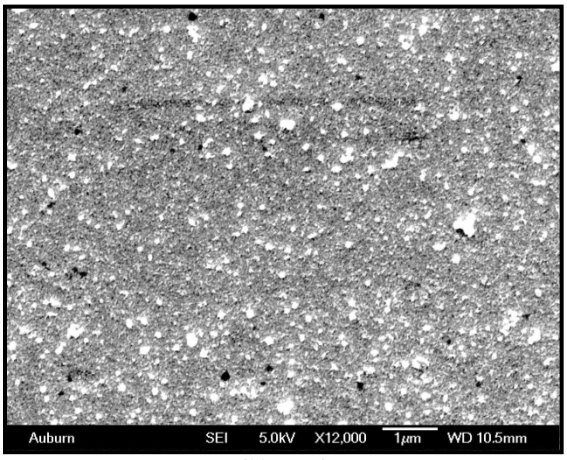

C1 – T3

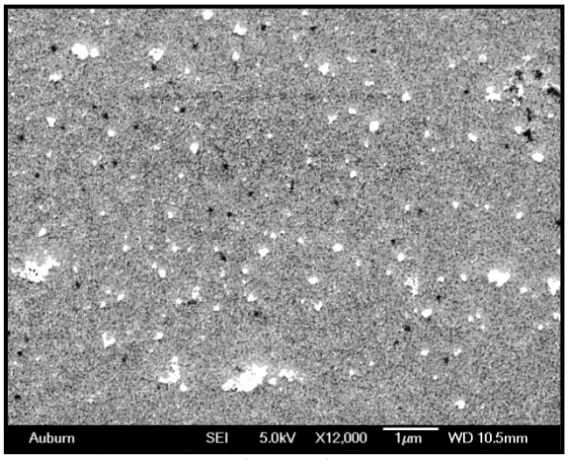

C1 – T4

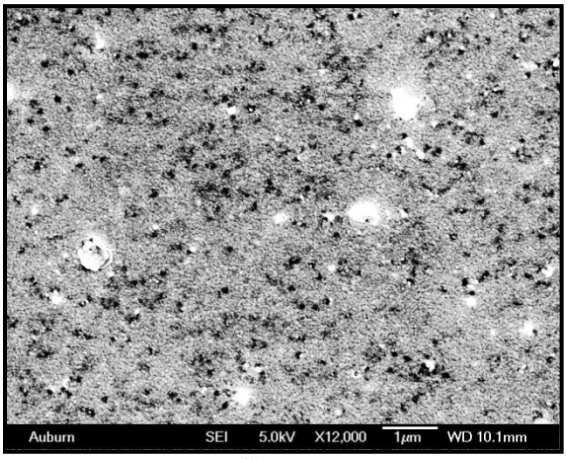

C1 – T5

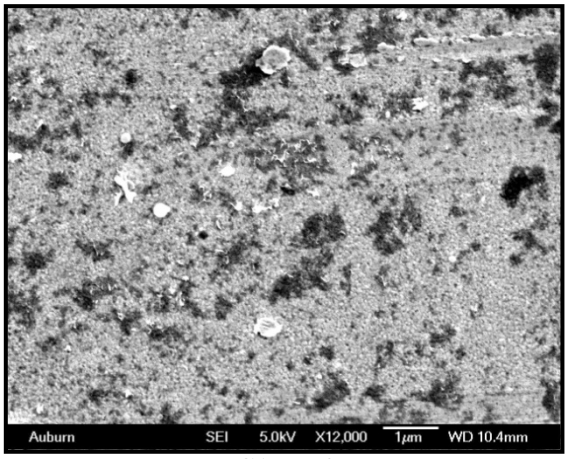

C1 – T6

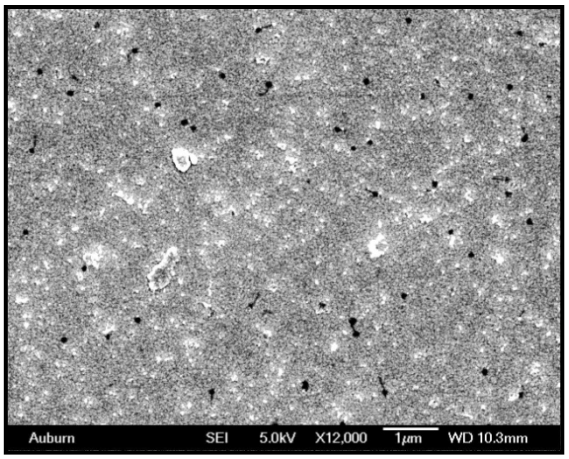

C2 – T1

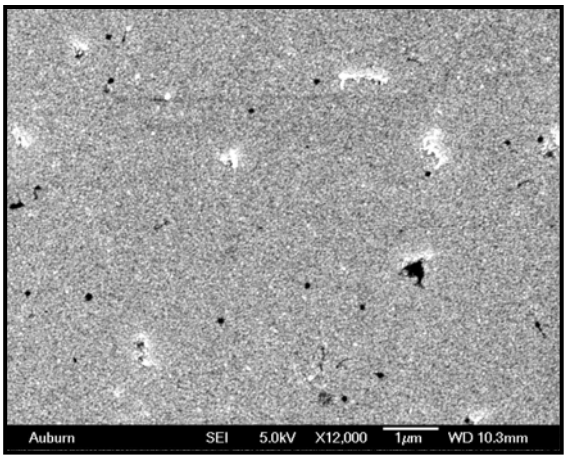

C2 – T2

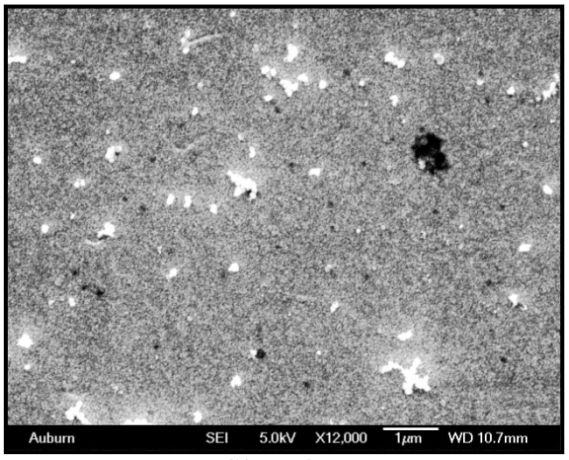

C2 – T3

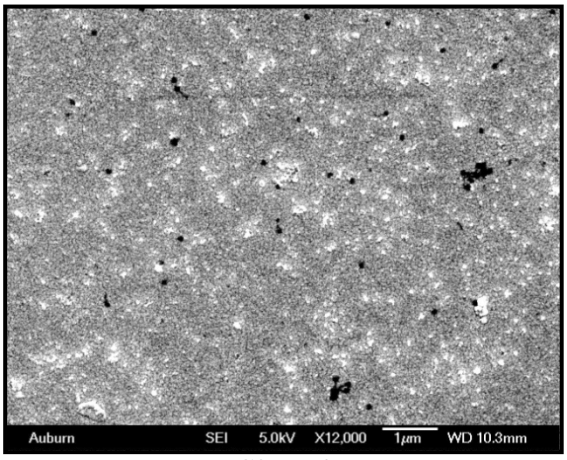

C2 – T4

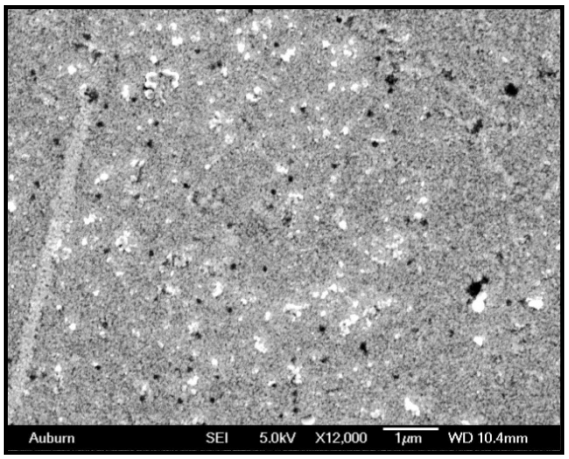

C2 – T5

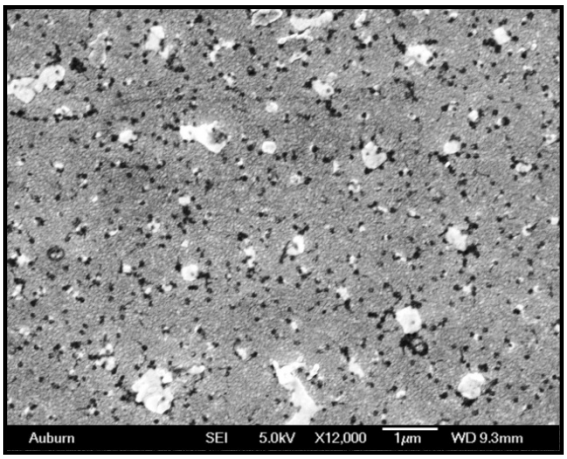

C2 – T6

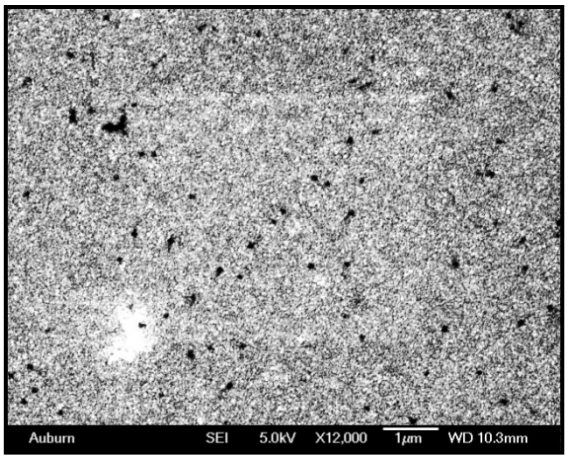

C3 – T1

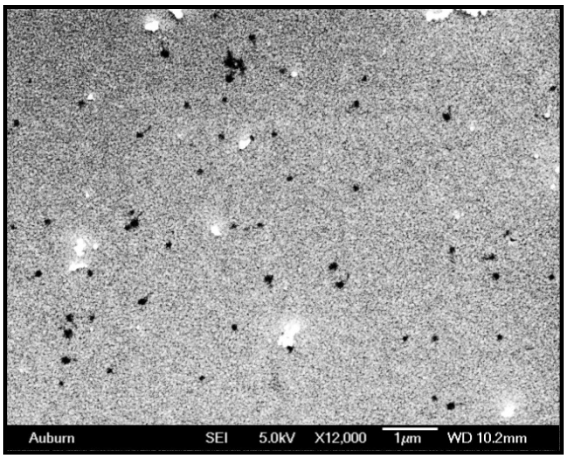

C3 – T2

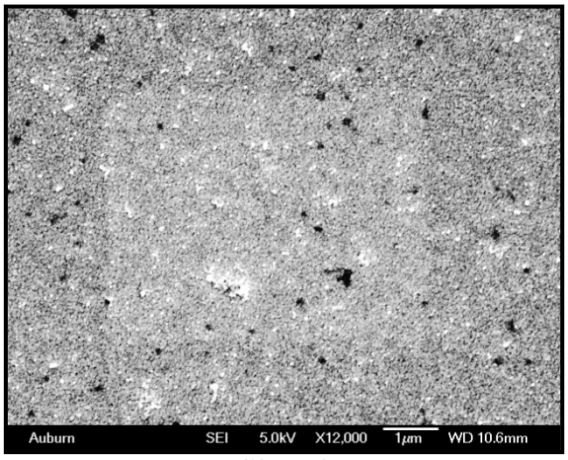

C3 – T3

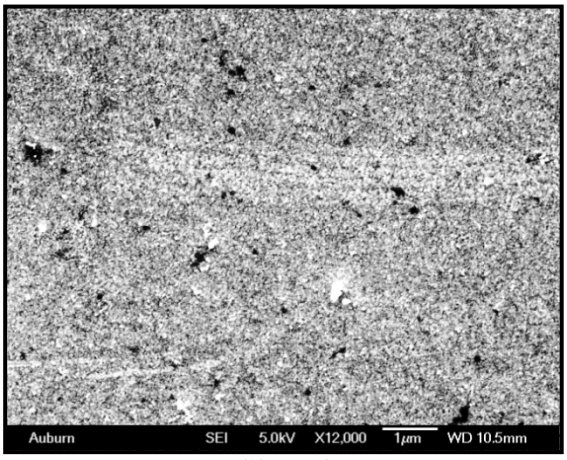

C3 – T4

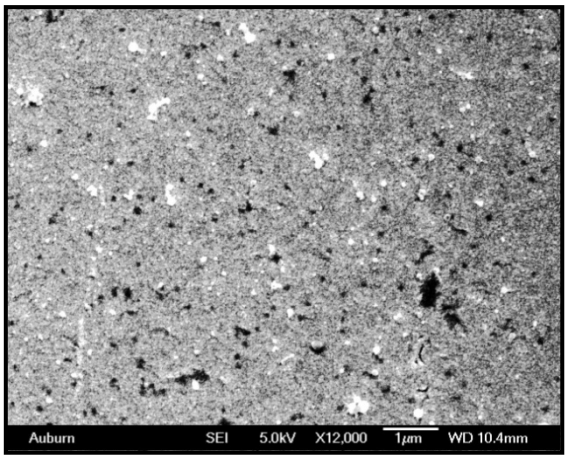

C3 – T5

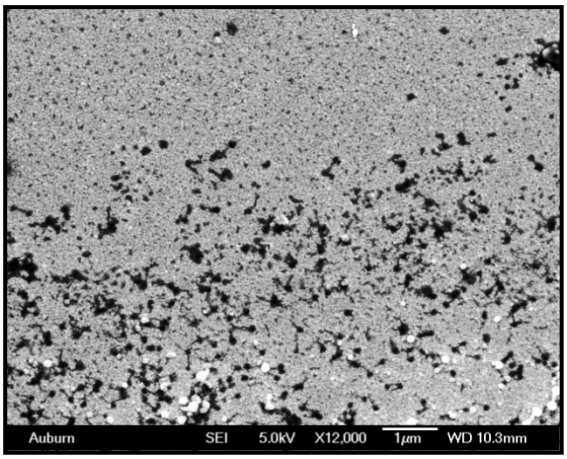

C3 – T6

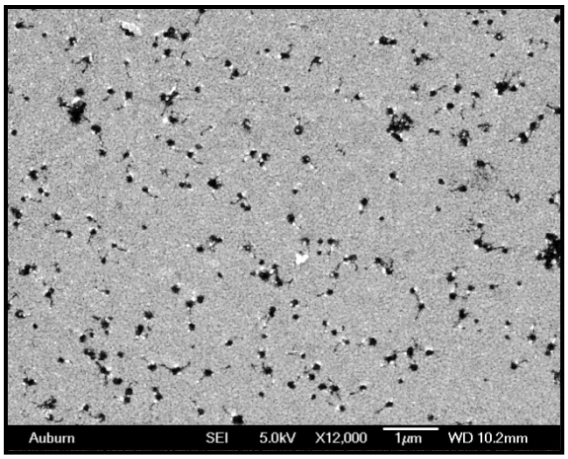

C4 – T1

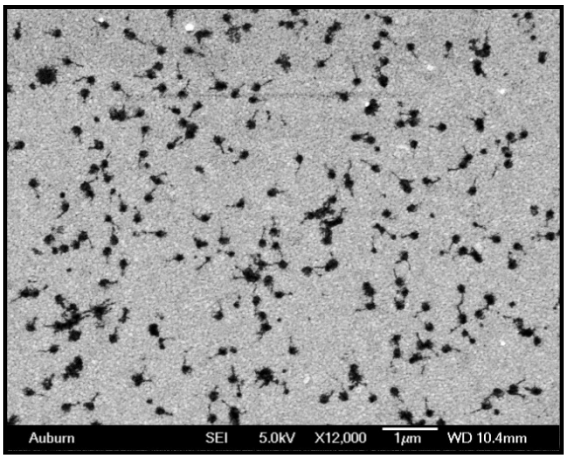

C4 – T2

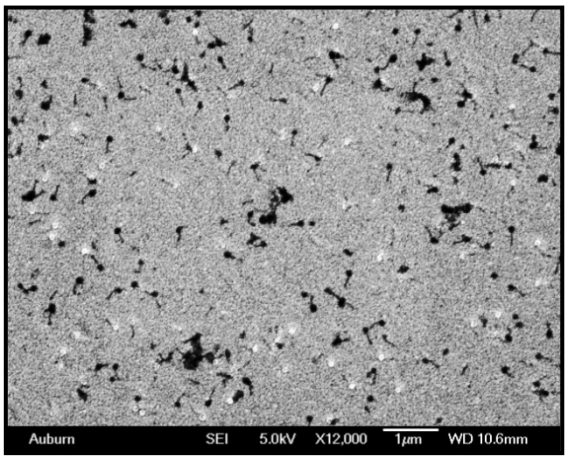

C4 – T3

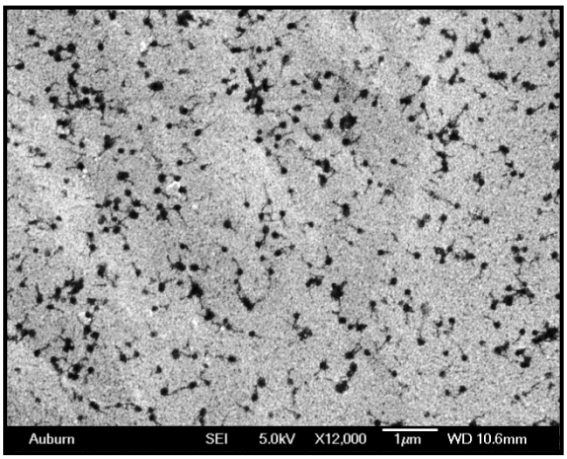

C4 – T4

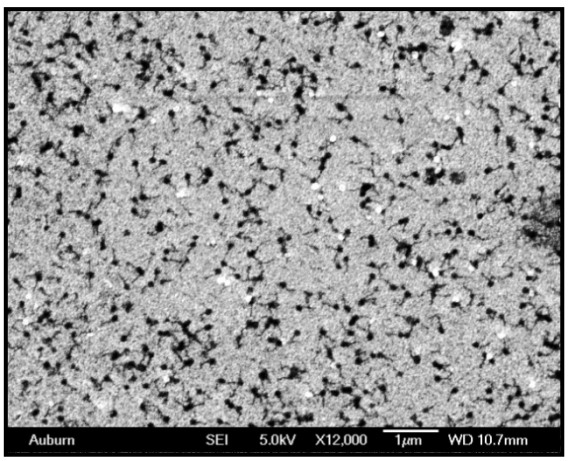

C4 – T5

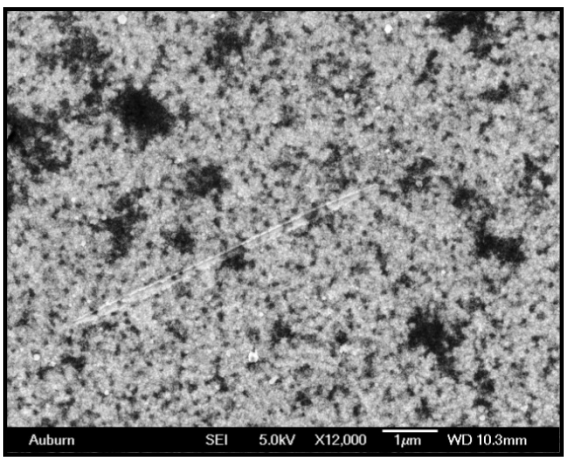

C4 – T6

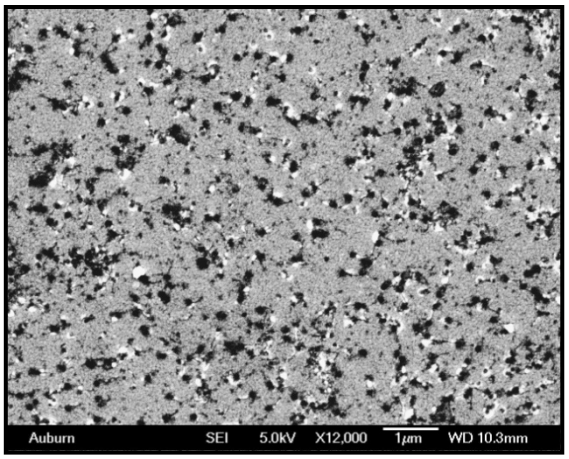

C5 – T1

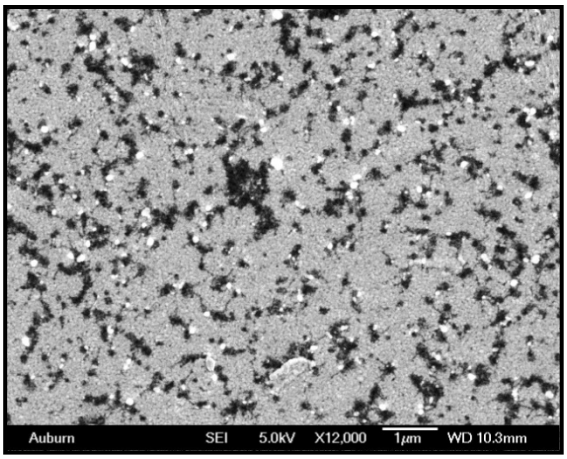

C5 – T2

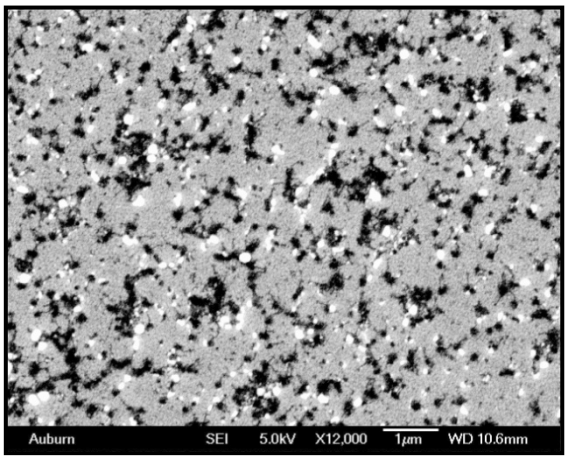

C5 – T3

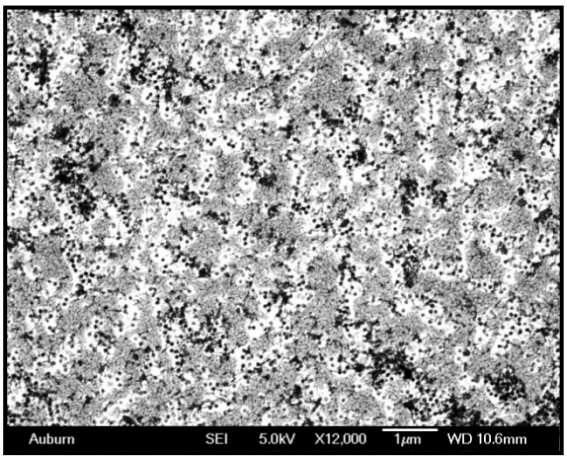

C5 – T4

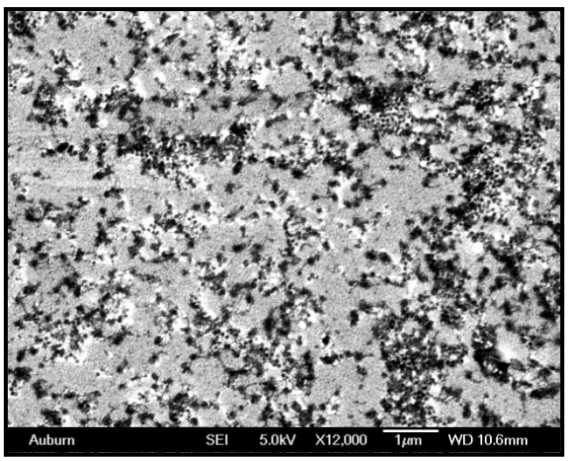

C5 – T5

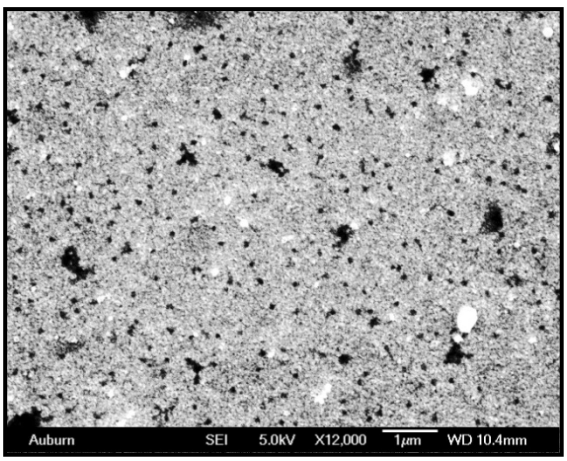

C5 – T6